การสังเคราะห์ซิลิคอนไนไตรด์จากเส้นใยขนาดนาโนของซิลิกา/คาร์บอนคอมพอสิตจากการปั่น

ด้วยไฟฟ้าสถิต

นาย รุ่งโรจน์ ชาญชัยฤกษ์
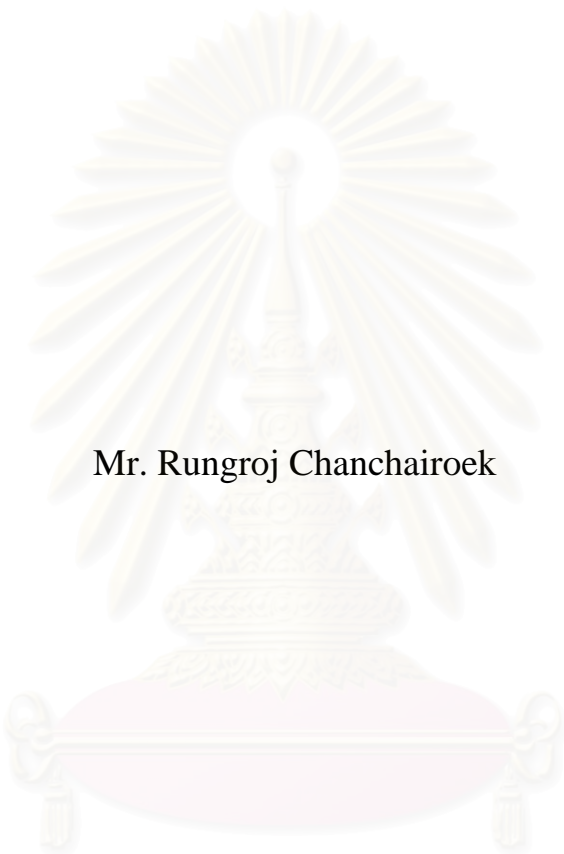
SILICON NITRIDE SYNTHESIS FROM ELECTROSPUN
SILICA/CARBON COMPOSITE NANOFIBERS

Mr. Rungroj Chanchairoek

A Thesis Submitted in Partial Fulfillment of the Requirements

for the Degree of Master of Engineering Program in Chemical Engineering

Department of Chemical Engineering

Faculty of Engineering

Chulalongkorn University

Academic Year 2005

Thesis Title   SILICON NITRIDE SYNTHESIS FROM ELECTROSPUN
                  SILICA/CARBON COMPOSITE NANOFIBERS
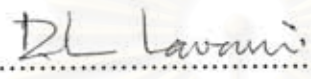
By   Mr. Rungroj Chanchairoek

Field of study   Chemical Engineering

Thesis Advisor   Assistant Professor Varong Pavarajarn, Ph.D.

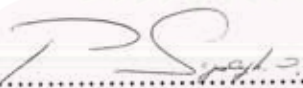Thesis Co-Advisor Associate Professor Pitt Supaphol, Ph.D.

Accepted by the Faculty of Engineering, Chulalongkorn University in Partial Fulfillment of the Requirements for the Master's Degree

.... Dean of the Faculty of Engineering

(Professor Direk Lavansiri, Ph.D.)

THESIS COMMITTEE

.... Chairman

(Associate Professor Tawatchai Charinpanitkul, Ph.D.)

.... Thesis Advisor

(Assistant Professor Varong Pavarajarn, Ph.D)

.... Thesis Co-Advisor

(Associate Professor Pitt Supaphol, Ph.D.)

.... Member

(Assistant Professor Sarawut Rimdusit, Ph:D.)

.... Member

(Assistant Professor Joongjai Panpranot, Ph.D.)

รุ่งโรจน์   ชาญชัยฤกษ์ : การสังเคราะห์ซิลิคอนไนไตรด์จากเส้นใยขนาดนาโนของซิลิกา/คาร์บอนคอมพอสิตจากการปั่นด้วยไฟฟ้าสถิต. (SILICON NITRIDE SYNTHESIS FROM ELECTROSPUN SILICA/CARBON COMPOSITE NANOFIBERS. อ.ที่ปรึกษา: ผศ.ดร.วรงค์ ปวราจารย์, อ.ปรึกษาร่วม: รศ.ดร.พิชญ์ ศุภผล 85 หน้า. ISBN 974-17-3993-1.

การสังเคราะห์ซิลิคอนไนไตรด์ซึ่งเป็นวัสดุโครงสร้างสำหรับการใช้งานที่มีความเครียดทางกลสูงภายใต้อุณหภูมิสูงจากซิลิกา/คาร์บอนคอมพอสิตซึ่งใช้พอลิเมอร์ที่ถูกเผาในบรรยากาศเฉื่อยหรือคาร์บอนแบล็คเป็นแหล่งของคาร์บอนได้ถูกศึกษาโดยลักษณะรูปร่างของสารตั้งต้นที่ศึกษานั้นอยู่ในรูปของเจลและเส้นใยที่ได้จากการเตรียมด้วยวิธี โซล-เจลและการปั่นด้วยไฟฟ้าสถิต ซิลิกา/คาร์บอนคอมพอสิตจะถูกเปลี่ยนให้เป็นซิลิคอนไนไตรด์ด้วยกระบวนการคาร์โบเทอร์มอลรีดักชั่นและไนไตรเดชั่น ในส่วนของการสังเคราะห์ซิลิคอนไนไตรด์จากซิลิกา/พอลิเมอร์คอมพอสิตที่ถูกเผาในบรรยากาศเฉื่อยนั้นพบว่า 3-อะมิโนโพรพิลไตรเมททอกซีไซเลนและพอลิไวนิลไพโรลิโดนที่มีมวลโมเลกุลต่ำ เป็นสารตั้งต้นที่เหมาะสมของซิลิกาและคาร์บอนตามลำดับ นอกจากนั้นยังพบว่าเวลาที่ตั้งทิ้งไว้และลักษณะรูปร่าง (เจล และ เส้นใย) ของคอมพอสิตเริ่มต้นเป็นปัจจัยสำคัญที่ส่งผลต่อการเกิดปฏิกิริยาไนไตรเดชั่นต่อไป โดยพบว่าลักษณะรูปร่างที่เป็นเส้นใยนั้นไม่เหมาะสมในการเปลี่ยนให้เป็นซิลิคอนไนไตรด์เนื่องจากปริมาณคาร์บอนอิสระไม่เพียงพอ ในส่วนของการใช้ซิลิกา/คาร์บอนแบล็คคอมพอสิตนั้น สามารถสังเคราะห์ซิลิคอนไนไตรด์/ซิลิคอนคาร์ไบด์คอมพอสิตในรูปของเส้นใยได้ โดยผลิตภัณฑ์ที่ได้ยังคงมีลักษณะรูปร่างเหมือนกับเส้นใยซิลิกา/คาร์บอนแบล็คคอมพอสิตตั้งต้น โดยมีขนาดเฉลี่ยของเส้นใยอยู่ระหว่าง 0.4-0.65 ไมโครเมตร และจากการศึกษาพบว่า เวลาที่ตั้งทิ้งไว้และสัดส่วนระหว่างคาร์บอนกับซิลิกาของคอมพอสิตตั้งต้นเป็นปัจจัยหลักที่มีผลต่อกลไกของกระบวนการคาร์โบเทอร์มอลรีดักชั่นและไนไตรเดชั่น

ภาควิชา..........วิศวกรรมเคมี.......................... ลายมือชื่อนิสิต..

สาขาวิชา..........วิศวกรรมเคมี.......................... ลายมือชื่ออาจารย์ที่ปรึกษา...............................

ปีการศึกษา........2548........................... ลายมือชื่ออาจารย์ที่ปรึกษาร่วม...........................

RUNGROJ CHANCHAIROEK: SILICON NITRIDE SYNTHESIS FROM ELECTROSPUN SILICA/CARBON COMPOSITE NANOFIBERS. THESIS ADVISOR: ASST. PROF. VARONG PAVARAJARN, Ph.D., THESIS CO-ADVISOR: ASSOC. PROF. PITT SUPAPHOL, Ph.D. 85 pp. ISBN 974-17-3993-1.

The synthesis of silicon nitride, one of the most promising structural materials for high-temperature and high mechanical-stress applications, from electrospun silica/carbon composite, whereas source of carbon including either pyrolyzed polymer or carbon black is investigated. Morphology of the starting materials is in form of gel and fibers, which are prepared by combining sol-gel and electrospinning method. Silica/carbon composite is converted into silicon nitride via the carbothermal reduction and nitridation. For preparation of silicon nitride from pyrolyzed silica/polymer composite, 3-Amino propyl trimethoxysilane and low-molecular weight PVP are found to be the suitable precursors for silica and carbon, respectively. It is also found that aging time and morphology of the starting materials (e.g. gel and fibers) are important factors affecting the subsequent nitridation. The silica/polymer composite in form of fibers is not appropriate for converting to silicon nitride because of inadequate free carbon content. For the use of silica/carbon black composite, silicon nitride/silicon carbide composite can be prepared in form of fibers. The obtained products also remain the same morphology as the as-spun silica/carbon black composite fibers and have the average size in the range of 0.4-0.65 μm. Carbon-to-silica ratio and aging time of the starting material are the major factor affecting mechanism of the carbothermal reduction and nitridation.

Department...Chemical Engineering..... Student's signature.....Rungroj Chanchairoek...
Field of study...Chemical Engineering...Advisor's signature.......
Academic year ....2005...............Co-advisor's signature....

ACKNOWLEDGEMENTS

CONTENTS

LIST OF TABLES

LIST OF FIGURES

Figure   **page**

Figure   **page**

Figure **page**

CHAPTER I

INTRODUCTION

Silicon nitride (Si_3N_4) is one of the most promising structural materials for high-temperature and high mechanical stress applications because of its excellent properties such as high strength retention at elevated temperature, low thermal expansion coefficient and good thermal shock resistance. It has much higher creep resistance than metals and its thermal shock resistance is much better than other ceramics. Moreover, silicon nitride is inert to many chemicals. Thus, another benefit of silicon nitride is its corrosion resistance. For these good properties, technology of silicon nitride materials has been studied intensively for more than 40 years in order to use silicon nitride instead of stainless steel or nickel-based alloy which is inferior in both properties and life-time.

Applications of silicon nitride depend upon its high temperature strength, good thermal shock resistance and chemical inertness. Reports on the use of silicon nitride as a refractory material appeared in the early 1950s. At that time, silicon nitride was produced by either the carbothermal reduction of silica (SiO_2) in the presence of nitrogen or by the direct nitridation of silicon. Silicon nitride has also been used as high temperature and unlubricated rollers and ball bearing for various applications, such as in oil drilling, sterilizable and unlubricated dental drills, and vacuum pumps, because of its high wear-resistance, low friction and high stiffness [Datton. et al., 1986].

In the past 30 years, during which most of the considerable developments on silicon nitride has been conducted primarily in the ceramics and electronics communities, many different aspects have been explored. Current development concerns further introduction of silicon nitride components to diesel and spark-ignited engines in the location where low mass and improved wear resistance are required. Examples of such components are exhaust valves, valve spring retainers, bucket tappets, stator blades, valve springs and rocker arm pads [Wotting et al., 1996].

There are three typical processes for producing silicon nitride powder [Alcala et al., 2001]. Each process is discussed in the next section. One of the common method used process is carbothermal reduction and nitridation of silica. However, the product from this process has purity problem from residual carbon. The overall reaction of the carbothermal reduction and nitridation of silica is as follow [Li et al., 1991; Wang et al., 1996]:

$$3 \, SiO_2 \, (s) + 6 \, C \, (s) + 2 \, N_2 \, (g) \quad \leftrightarrow \quad Si_3N_4 \, (s) + 6 \, CO \, (g) \qquad (1.1)$$
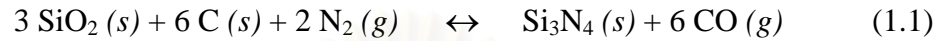
The silicon nitride obtained from this process can be in the form of powder, fibers or needle-like particles. The shape of the silicon nitride particles is the result of a nucleation mechanism. Reaction (1.1) is endothermic, with the heat of reaction approximately 1,268 kJ/mol Si_3N_4 at 1,427°C [Weimer et al., 1997]. Kinetically, reaction (1.1) is reported to be slow, requiring many hours to complete. Moreover, this process requires high reactivity and good distribution of raw materials, i.e. silica and carbon, to achieve satisfactory extent of the reaction.

Sol-gel process is a common technique for producing glass or ceramic material. Generally, sol-gel process involves the transition of a system from liquid *sol* (or colloidal suspension) to a solid *gel* through series of chemical reactions. The starting materials for the preparation of the *sol* are usually metal organic compounds such as metal alkoxides. The precursor is hydrolyzed to form *sol* and partially condensed to form a three-dimensional network *gel*. Important characteristics of the sol-gel preparation are ability to maintain high purity, ability to prepare sample at low temperature, ability to vary compositional homogeneity at a molecular level and ability to produce samples in different physical forms. In addition, processing of *sol* enables the production of ceramic materials in different forms such as thin film by spin-coating [Tongpool et al., 2005] or dip-coating on substrate [Konjhodzic et al., 2005] and fibers by extrusion [Chandradass et al., 2005] or *electrospinning*.

Electrospinning is a straightforward method to produce polymer nanofibers. When electrical force at the surface of a polymer solution or polymer melt overcomes the surface tension, a charged jet is ejected. The jet extends in a straight line for a certain distance, then bends following a looping and spiraling path. The electrical

force elongates the jet thousands or even millions of times and the jet becomes very thin. Ultimately the solvent evaporates, or the melt solidifies, resulting in very long fibers, often in the form of a non-woven fabric.

The electrospinning process produces fibers with diameter in the range of one or two orders of magnitude smaller than those of conventional textile fibers. The small diameter provides large surface area-to-mass ratio, in the range from 10 m^2/g (when the diameter is around 500 nm) to 1000 m^2/g (when the fiber diameter is around 50 nm). The small diameter also provides high surface area-to-volume ratio and high length-to-diameter ratio. These characteristics are useful in several applications such as reinforcing materials [Bergshoef et al., 1999], filters [Bognitzki et al., 2001] and templates for preparation of nanotubes [Bognitzki et al., 2001]. Moreover, the equipment required for electrospinning is simple and only a small amount of polymer sample is needed to produce nanofibers.

In this research, the main purpose is to synthesize silicon nitride from electrospun silica/poly vinylpyrolidone and silica/carbon black composite nanofibers via the carbothermal reduction and nitridation process. Effects of various factors, such as type of silica precursor, composition and aging time of silica in the composite, as well as conditions for the carbothermal reduction and nitridation, on yield of silicon nitride are also investigated. The scopes of this study are as following:

1 Silicon nitride is synthesized by carbothermal reduction and nitridation of silica/carbon composite, whereas source of carbon is either pyrolyzed polymer or carbon black. Morphology of the starting material is in form of gel and fibers, which are prepared by combining sol-gel and electrospinning method.

2 The study is divided into two parts, i.e. preparation of silica/carbon composite gel or electrospun fibers and the reaction to convert the composite into silicon nitride. The following parameters are investigated:

- For the preparation of silica/carbon composite, effects of silica-to-carbon ratio, source of carbon, precursor for silica synthesis and aging time are investigated.

- For the reaction to convert the composite into silicon nitride, the investigated parameter is composition and flow rate of reactant gas mixture, i.e. nitrogen and hydrogen, respectively.

This thesis is divided into five parts. The first three parts describe general information about the study, while the following two parts emphasize on the results and discussion from the present study. The background and scope of the study are presented in Chapter I. Chapter II consists of the theory and literature survey, while the experimental systems and procedures used in this study are shown in Chapter III. The experimental results, including an expanded discussion, are given in Chapter IV. Finally, in the last chapter, the overall conclusion from the results and some recommendations for future work are presented.

CHAPTER II

THEORY AND LITERATURE SURVEY

2.1 Sol-gel Processing

Sol is colloidal suspension of solid particles in liquid. *Aerosol* is a colloidal suspension of particles in gas and *emulsion* is a suspension of liquid droplets in another liquid. All of these types of colloids can be used to generate polymers or network of particles from which ceramic materials can be subsequently synthesized. In the sol-gel process, the *precursors* for preparation of the colloidal suspension consist of a metal or metalloid element surrounded by various *ligands* (appendages not including another metal or metalloid atom). For example, an *alkoxy* is a ligand formed by removing a proton from the hydroxyl group on an alcohol, as in *methoxy* (OCH_3) or *ethoxy* (OC_2H_5).

Metal alkoxides are member of the family of metal organic compounds, which have an organic ligand attached to a metal or metalloid atom. One of the most thoroughly studied metal alkoxides is silicon tetraethoxide (or tetraethoxysilane, tetraethyl orthosilicate, TEOS), $Si(OC_2H_5)_4$. On the other hand, organometallic compound is defined as a compound having direct metal-carbon bonds, not metal-oxygen-carbon linkages as in metal alkoxides. Thus, alkoxides are not organometallic compounds, although that usage turns frequently in the literature. Metal alkoxides are popular precursors for sol-gel process because they react readily with water. The reaction is called hydrolysis, because the hydroxyl ion become attached to the metal atom, as in the following reaction

$$Si(OR)_4 \; + \; H_2O \quad \rightarrow \quad HO\text{-}Si(OR)_3 \; + \; ROH \qquad (2.1)$$

In the reaction (2.1), R represents a proton or other ligand (if R is an alkyl, then OR is an alkoxy group), and ROH is alcohol. Depending on the amount of water and catalyst present, hydrolysis may go to completion (so that all of the OR groups are replaced by OH), or stop while the metal is only partially *hydrolyzed*, $Si(OR)_{4\text{-}}$

$_n(OH)_n$. Moreover, The molar ratio of H_2O: $Si(OR)_4$ in the sol should be at least 2:1 to approach complete hydrolysis of the alkoxide [Nicolaon et al., 1968].

Following the hydrolysis, two partially hydrolyzed molecules can link together in a *condensation reaction*, such as

$$(OR)_3Si\text{-}OH \ + \ HO\text{-}Si(OR)_3 \quad \rightarrow \quad (OR)_3Si\text{-}O\text{-}Si(OR)_3 \ + H_2O \quad (2.2)$$

or

$$(OR)_3Si\text{-}OR \ + \ HO\text{-}Si(OR)_3 \quad \rightarrow \quad (OR)_3Si\text{-}O\text{-}Si(OR)_3 \ + \ ROH \quad (2.3)$$
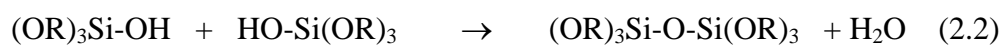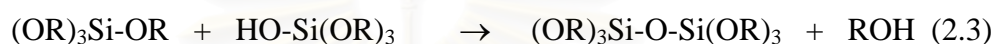
Further extent of the condensation of the sol results in the formation of gel. There are many parameters which affect gel properties such as temperature, pH, type of precursor and solvent. Varying the temperature is most effective when it can alter the relative rate of competing reactions. Solvent can change the nature of an alkoxide precursor through solvent exchange or affect the condensation reaction directly. It is also possible to prepare gel without solvent as long as another mean, such as ultrasound irradiation, is used to homogenize an otherwise immiscible alkoxide/water mixture. Furthermore, pH of the solution, which can be changed by the addition of either acid or base catalyst, is the most important parameter in obtaining gel because the rate and content of the hydrolysis reaction are influenced by the change in pH [Aelion et al., 1950].

For all the sol-gel parameters discussed so far, they have effect on gel properties which can often be observed by an experimental parameter known as gelation time. Gelation time is defined as the time that the solution undergoes rapid rise in viscosity which is corresponding to the transition from viscous fluid to elastic gel. At the gel point, the solid phase forms a continuous structure that reflects the formation and branching of particles under specific growth condition. This particular phase is important because it is the genesis of structural evolution that takes place in all subsequent processing steps [Ertl et al., 1999].

For hydrolysis reaction performed with a catalyst, three procedures are proposed: acid catalysis, base catalysis and two-step catalysis [Tamon et al., 1998; Rao et al., 2004]. Acid catalysis is performed with HCl, H_2SO_4, HNO_3, HF, oxalic acid, formic acid or acetic acid. It is generally agreed that, under acid catalyst, entangled linear and randomly branched chains are formed in silica sols. For base catalysis, it is easy to form a network of uniform particles in the sol because, under base catalysis, kinetics of the condensation is faster than hydrolysis kinetics [Dieudonné et al., 2000]. In typical procedure, tetraethoxysilane (TEOS), methanol, water and HCl are mixed and NH_3 is added as a second catalyst to the sol at different TEOS/HCl and TEOS/NH_3 ratio [Tamon et al., 1998]. The gelation time decreases with increasing concentration of either HCl or NH_3 because of increasing rate of hydrolysis and condensation reactions, respectively. Furthermore, two-step sol-gel process for silica aerogel synthesis has been more studied by using oxalic acid as hydrolysis catalyst and NH_4OH as condensation catalyst [Rao et al., 2004]. It was found that gelation time decreases with an increase in oxalic acid and NH_4OH concentration. Moreover, some properties of the obtained product, such as density, volume shrinkage and optical transmission are also found to be improved.

2.2 Electrospinning Technique

Electrospinning technique is a simple and versatile method for fabricating nanofibers. In the electrospinning process, polymer solution held by its surface tension at the end of a capillary tube is subjected to an electric field. Charge is induced to the liquid surface by an electronic field. As the intensity of electric field is increased, the hemispherical surface of the solution at the tip of the capillary tube elongates to form a conical shape known as the Taylor cone. When the electric field reaches a critical value at which the repulsive electric force overcomes the surface tension force, a charged jet of the solution is ejected from the tip of the Taylor cone. Since this jet is charged, its trajectory can be controlled by the electric field. As the jet travels in air, the solvent evaporates, leaving a charged polymer fiber behind which lays itself randomly on a collecting metal screen. Thus, continuous fibers are laid to form a non-woven fabric [Jayesh et al., 1995].

Polymer nanofibers are being used, or finding uses, in filtration, protective clothing, and biomedical applications including wound dressings and drug delivery systems. Other possible uses include solar sails, light sails, and mirrors for using in space. Nanofibers offer advantages for the application of pesticides to plants, as structural elements in artificial organs, as supports for enzymes or catalysts that can promote chemical reactions, and in reinforced composites. Ceramic or carbon nanofibers made from polymeric precursors extend nanofiber applications to uses involving high temperature and high modulus. The electrospinning process can incorporate particles such as pigments or carbon black particles into nanofibers. Flexible fibers are needed on a scale commensurate with micro or nano-electrical mechanical and optical systems. The use of electrical forces may lead to new ways to fabricate micro or nano scale devices.

Electrospinning process involves polymer science, applied physics, fluid mechanics, electrical engineering, mechanical engineering, chemical engineering, material engineering and rheology. Many parameters, including the electric field, solution viscosity, resistivity, surface tension, charge carried by the jet and relaxation time can affect the process. A comprehensive mathematical model of this process was developed by Reneker et al. [Reneker et al., 2000].

The electrospinning process consists of three stages: (1) jet initiation and the extension of the jet along a straight line; (2) the growth of bending instability and the further elongation of the jet, which allows the jet to become very long and thin while it follows a looping and spiraling path; (3) solidification of the jet into nanofibers. A schematic drawing of the electrospinning process is shown in Figure 2.1.
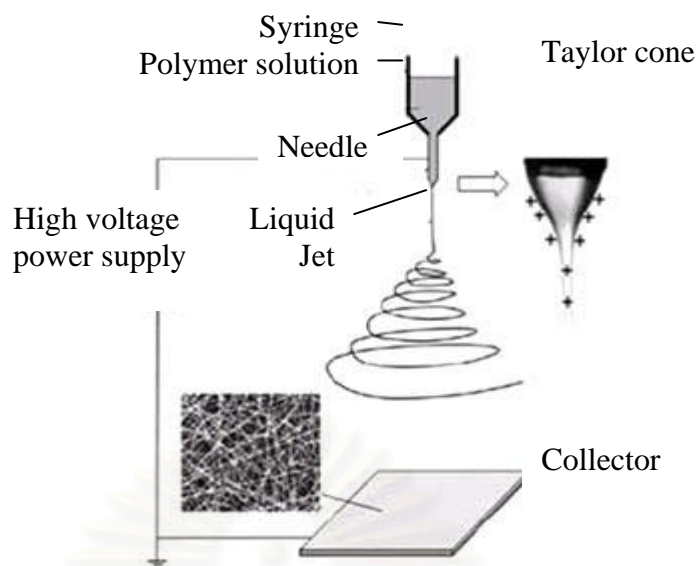
Figure 2.1 Schematic representation of the electrospinning process.

2.2.1 Jet initiation and diameter of a single jet

In a typical experiment, a pendent droplet of polymer solution is supported by surface tension at the tip of the spinneret. When the electrical potential difference between the spinneret and the grounded collector is increased, the motion of ions through the liquid charges the surface of the liquid. If the electrical forces at the surface overcome the forces associated with surface tension, a liquid jet emerges from a conical protrusion that formed on the surface of the pendant droplet. The jet is electrically charged. It carries away the ions that are attracted to the surface when the potential is applied. Increasing the potential increases both the charge density on the jet and the flow rate of the jet.

The jet diameter decreases with the distance from the orifice. Higher electric fields and a lower surface tension coefficient favor the formation of a thicker jet. Addition of salt (NaCl) to the solution, with other parameters held constant, reduces the diameter of the jet. Increasing the viscosity of the solution does not always increase the diameter. The largest jet diameter occurs when the solution viscosity is in a medium range. Both higher and lower viscosity favors a thinner jet.

2.2.2 Bending instability and elongation of the jet

After initiation, path of the jet is straight for a certain distance. Then, an electrically driven bending instability grows at the bottom end of the straight segment. The bending allows large elongation to occur in small region of space. The electrically driven bending instability occurs in self-similar cycles. Each cycle has three steps and it is smaller in scale than the preceding cycle.

The three steps in each cycle are:

Step 1. A smooth segment that is straight or slightly curved suddenly develops an array of bends.

Step 2. As the segment of the jet in each bend elongates, the linear array of bends becomes a series of spiraling loops with growing diameters.

Step 3. As the perimeter of each loop increases, the cross-sectional diameter of the jet forming the loop gets smaller, and the conditions for Step 1 are established everywhere along the loop.

After the first cycle, the axis of a particular segment might lies in any direction. The continuous elongation of each segment is most strongly influenced by the repulsion between the charges carried by adjacent segment of the jet. The externally applied field, acting on the charged jet, causes the entire jet to drift toward the collector, which is maintained at an attractive potential.

There are several parameters affecting the electrospinning process [Deitzel et al., 2001; Frenot et al., 2003; Li et al., 2004], i.e. (1) system parameters such as molecular weight, molecular weight distribution and architecture of the polymer (branched, linear, etc.) as well as properties of polymer solution (viscosity, conductivity, dielectric constant and surface tension); (2) process parameters such as electrical potential, flow rate and distance between the capillary and collected screen; and (3) ambient parameters (temperature, humidity and air velocity in the chamber). For instance, the polymer solution must have concentration high enough to cause

polymer entanglements but not so high that the viscosity prevents motion of polymer induced by the electric field. The solution must also have surface tension low enough, charge density high enough, and viscosity high enough to prevent the jet from collapsing into droplets (or beads) before the solvent has evaporated. Morphological changes can occur upon decreasing the distance between the syringe needle and the collector. Increasing or decreasing the electrical field decreases the bead density, regardless of the concentration of the polymer in the solution.

In recent years, electrospinning technique has been adopted for the synthesize of ceramic nanofibers. Organic-inorganic composite nanofibers with diameter in range of 200 to 400 nm have been prepared from poly (vinyl) alcohol (PVA)/silica composite precursors, using tetraethoxysilane (TEOS) as a source for silicon. The obtained fibers give a new state and some special properties of the organic-inorganic composite materials different from the state of film and gel [Shao et al., 2003]. Furthermore, ultrafine fibers of amorphous silica could also be electrospun directly from silica sol without the aid of polymer or gelator. Most silica fibers electrospun under the electrical field of 12-16 kV has diameter in range of 200-600 nm [Choi et al., 2003]. In addition, the electrospun silica fibers without gelator have been prepared and coated with thermal management materials like aluminium nitride using traditional physical vapor deposition technique for potential space-based applications [Zhang et al., 2004].

2.3 Silicon Nitride Synthesis from Silica

The carbothermal reduction of silica powder under nitrogen was the earliest method used for silicon nitride production [Riley 2000]. It produces silicon nitride according to the following overall reaction [Segal 1985]:

$$3 \, SiO_2 \, (s) \, + \, 6 \, C \, (s) \, + \, 2 \, N_2 \, (g) \, \leftrightarrow \, Si_3N_4 \, (s) \, + \, 6 \, CO \, (g) \qquad (2.4)$$
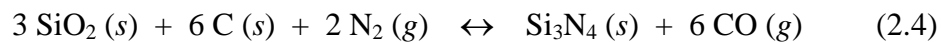
This reaction also occurs via a gas-solid mechanism. The mechanism of reaction (2.4) is believed to involve multiple steps, where silicon monoxide acts as an intermediate [Arik 2003]. It is proposed that silicon monoxide is produced by reduction of silica by either carbon or carbon monoxide.

$$SiO_2 \, (s) \, + \, C \, (s) \quad \leftrightarrow \, SiO \, (g) \, + \, CO \, (g) \qquad (2.5)$$
$$SiO_2 \, (s) \, + \, CO \, (g) \, \leftrightarrow \, SiO \, (g) \, + \, CO_2 \, (g) \qquad (2.6)$$
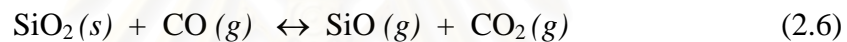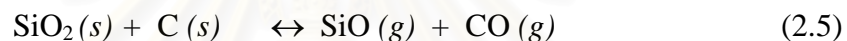
Carbon dioxide generated from reaction (2.6) can further react with carbon to produce more carbon monoxide :

$$CO_2 \, (g) \, + \, C \, (s) \quad \leftrightarrow \, 2 \, CO \, (g) \qquad (2.7)$$
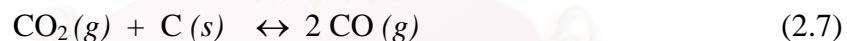
Silicon nitride is then produced by reaction of silicon monoxide, nitrogen gas and either solid carbon or carbon monoxide. It is believe that nucleation of silicon nitride takes place via heterogeneous reaction (2.8) while the growth occurs by a gas phase process according to reaction (2.9) [Weimer et al., 1997].

$$3 \, SiO \, (g) \, + \, 3 \, C \, (s) \, + \, 2 \, N_2 \, (g) \quad \leftrightarrow \, Si_3N_4 \, (s) \, + \, 3 \, CO \, (g) \qquad (2.8)$$
$$3 \, SiO \, (g) \, + \, 3 \, CO \, (g) \, + \, 2 \, N_2 \, (g) \, \leftrightarrow \, Si_3N_4 \, (s) + \, 3 \, CO_2 \, (g) \qquad (2.9)$$
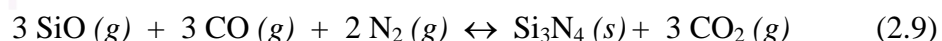
The problem of this method is associated with the formation of silicon carbide, because silicon carbide can also be produced by reaction of silicon monoxide with carbon.

$$SiO\,(g)\ +\ 2\,C\,(s)\ \leftrightarrow\ SiC\,(s)\ +\ CO\,(g) \tag{2.10}$$
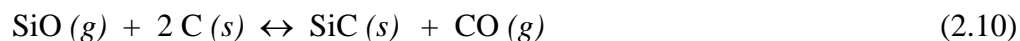
Furthermore, silicon nitride can be converted to silicon carbide in the presence of carbon as well, according to reaction (2.11):

$$Si_3N_4\,(s)\ +\ 3\,C\,(s)\ \leftrightarrow\ 3\,SiC\,(s)\ +\ 2\,N_2\,(g) \tag{2.11}$$
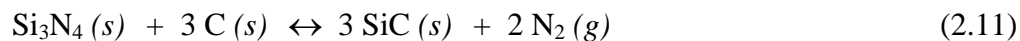
Therefore, the reaction conditions are particularly important in establishing which compound will be formed.

The carbothermal reduction and nitridation synthesis of α-silicon nitride is controlled by the nucleation of α-silicon nitride crystallites. α-Silicon nitride nuclei is formed through the formation of fine amorphous Si-O-C intermediate [Weimer et al., 1997]. Kinetically, overall reaction is reported to be slow, requiring many hours (up to 12 hours) to complete. The reaction (2.4) is usually performed at temperature in the range of 1200-1450°C, depending on the reactivity of raw materials. According to the proposed mechanism of the carbothemal reduction and nitridation process, physical contact between carbon and silica is essential for SiO vapor formation. Full conversion using silica and carbon in stoichiometric ratio (1:2) can occur only if there is perfect contact between carbon and silica particles. Hence, an excess amount of carbon is always required for full transformation of silica to silicon nitride, and free carbon can remain in silicon nitride powder. Although the remaining carbon can be removed by heat treatment in air, the silicon nitride would be oxidized as well. Consequently, the powder synthesized by this method often suffers from purity problem associated with residual carbon and oxygen content.

Considerable attention has been paid to the synthesis of ceramics from organosilica, which has been prepared by hydrolysis of organo-alkyoxysilanes [White et al., 1987; Kamiya et al., 1990]. Tetraalkoxysilanes (tetramethoxysilane and tetraethoxysilane (TEOS)), the usual precursors for the synthesis of silica in the sol-gel process, have only alkoxy groups attached to the central Si atom whereas organo-alkoxysilanes have organic groups in addition to the alkoxy groups. The organic groups are not hydrolyzable during the hydrolysis of the organo-alkoxysilanes, and

remain as carbon source in the resulting organo-silicas. Therefore, it is possible to obtain carbon- or nitrogen- containing ceramics by the heat treatment of organosilicas derived from organo-alkoxysilanes.

Recently, several researchers have synthesized spherical organo-silica powders prepared from phenyltrimethoxysilane-tetraethoxysilane (PTMS–TEOS) systems and obtained spherical SiC powders via the pyrolysis of the organo-silica powders under argon atmosphere [Hatakeyama et al., 1990; Soeg et al., 1993]. This result has shown that shape, size, and size distribution of the SiC powder could be controlled effectively in this process. After the pyrolysis, these organo-silica powders still retained the initial spherical shape. However, the powders derived from the PTMS system changed to a shiny black solid, which has also been observed in the pyrolysis of many ceramic-precursor polymers. It can be assumed that the characteristics of the polymers are critical in maintaining the initial particle shape through the pyrolysis.

Pyrolytic conversion of spherical organosilica powder to obtain silicon nitride has been studied from a mixture of PTMS and TEOS under nitrogen atmosphere at 1,400-1,550^{o}C [Choi et al., 1998]. During the pyrolysis at 500-670°C, the organo-silica powders decompose to a mixture of fine free carbon and silica particulates, with an increased surface area. This mixture is transformed to silicon nitride at 1,400 to 1,500^{o}C through carbothermal reduction and nitridation, but still retains the same spherical shape as the starting organo-silica powders.

Further synthesis of monodispersed spherical silicon nitride and silicon carbide nanocomposite powder has also been investigated [Choi et al., 1999]. The spherical product is synthesized by heating spherical organo-silica powders prepared by the same procedure as the previous study [Choi et al., 1998] under nitrogen atmosphere at 1,500^{o}C for 8 h and heat-treated again under argon atmosphere at 1,450^{o}C for 1, 2, 4 or 8 h. During the first heat treatment, the organo-silica powders are converted into a mixture of silica and free carbon and conducted to the formation of silicon nitride via the carbothermal reduction and nitridation reaction. In addition, silicon carbide particles are formed with in the silicon nitride and carbon mixture through the carbothermal reduction of silicon nitride during the second heat treatment

in order to produce silicon nitride and silicon carbide composite powders. Silicon carbide particles are homogeneously mixed with silicon nitride particles within the composite powders and still retain the spherical shape.

2.4 Mechanisms for Crystal Growth from Gas Phase

Two types of mechanism are often used to explain the crystal growth associated with gas phase, as shown in Figure 2.2 [Kawai et al., 1998]. In the vapor-solid (VS) mechanism, Figure 2.2(a), chemical species diffuse toward a substrate through an interfacial gas layer, and adsorbed on the surface of the substrate. The adsorbed species may be mobile on the surface. Subsequently, nucleation and crystal growth occur, accompanied by the elimination of any by-product. In VS mechanism, the diffusion of the chemical species in the gas phase and their surface migration on the substrate are fast. Therefore, high deposition rate will be obtained if a reaction between the chemical species is fast enough. On the other hand, there are few studies focusing on the use of the vapor-liquid-solid (VLS) mechanism. As shown in Figure 2.2(b), if liquid-phase exists on a substrate, chemical species must be first dissolved in the liquid phase for crystal growth. Next, they diffuse in liquid and adsorbed on the substrate. Finally, crystal growth occurs via nucleation in the liquid phase. The diffusion rate of the chemical species in the liquid phase is probably much slower than in gas phase. Therefore, the rate of the supplement of chemical species to nucleus for crystal growth is very small. This results in high nucleation density and the formation of the finer crystals than those through the VS mechanism.

Diffusion

Interfacial layer

Adsorption

Substrate

Migration and

Nucleation

Crystal

Growth

(a)

Dissolution

Diffusion

Liquid Phase

Adsorption

Substrate

Migration and

Nucleation

Crystal

Growth

(b)
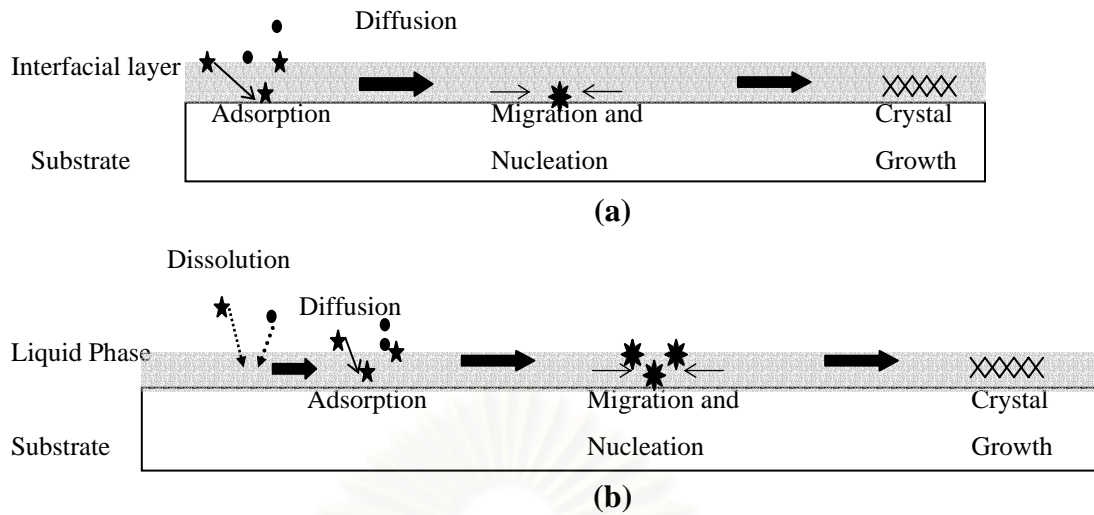
Figure 2.2 Mechanism of two types of gas phase process: (a) VS mechanism,

(b) VLS mechanism.

CHAPTER III

EXPERIMENTAL

This chapter describes the experimental systems and procedures used in this study. The chapter is divided into four sections. Section 3.1 is raw materials. Section 3.2 and 3.3 present preparation of silica/poly vinylpyrolidone composite and conversion of the composite into silicon nitride, respectively. Characterization of the products is presented in the last section.

3.1 Materials

Chemicals used in this study include are 3-amino propyl trimethoxysilane (APTMS), tetraethyl orthosilicate (TEOS), silatrane, poly vinylpyrolidone (PVP), poly (vinyl) alcohol (PVA), carbon black, ethyl alcohol, and hydrochloric acid (HCl).

3-Amino propyl trimethoxysilane (APTMS) 97%, tetraethyl orthosilicate (TEOS) 98%, poly vinylpyrolidone (PVP), $M_w \approx 1,300,000$ and 10,000, ethyl alcohol 98 % were purchased from Sigma-Aldrich Chemical Company and used as recieved.

Silatrane was synthesized according to procedures reported in literature [Chroenpinijkarn et al., 2001]

Poly (vinyl) alcohol 72,000 was purchased from Fluka Chemical company and used as received.

Carbon black (particle size ~ 29 nm.) were supplied by the East Asiatic Public and used as received.

 Hydrochloric Acid was purchased from Asia Pacific Specialty Chemicals Limited and used as received.

3.2 Preparation of Silica/PVP Composite

In a typical procedure, the solution was first prepared by mixing 5 g of APTMS, 0.05 ml of 37% by volume hydrochloric acid and 5 ml of distilled water at room temperature for 6 h. Then, 10 g of PVP solution in ethanol, at predetermined concentration of 30 % by weight, was dropped into the mixture and stirred for 12 h. It

should be noted that PVP used was a mixture of PVP with molecular weight of 1,300,000 and PVP with molecular weight of 10,000 in the ratio of 1:5 by mass. The solution was aged at room temperature for 0-5 days. The resulting product is referred to as the silica/PVP composite gel, although its appearance is still liquidous.

For preparation the silica/PVP composite fibers, the composite gel is employed as the electrospinning solution. The electrospinning apparatus is consisted of a high-voltage power supply (Gamma High Voltage Research ES30PN), a plastic syringe containing the electrospinning solution equipped with a 20-gauge stainless steel needle, and an aluminum foil used as a collective screen. The needle is connected to the negative electrode of the power supply, while the aluminum collector is attached with the grounding electrode placed 10 cm below the tip of the needle (referred as tip-to-target distance). The electrical potential and collection time were fixed at 8 kV and 30 minutes, respectively. The schematic of the electrospinning apparatus used in this work is shown in Figure 3.1
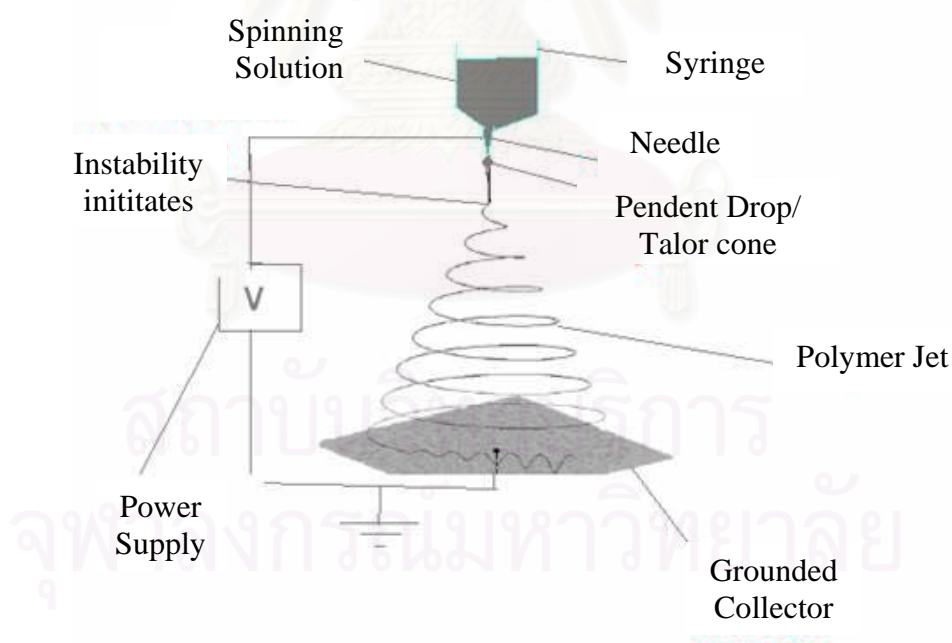
Figure 3.1 Experimental set up for electrospinning process.

3.3 Conversion of Silica/PVP Composite into Silicon Nitride

Silicon nitride synthesis consists of two steps: (1) pyrolysis and (2) carbothermal reduction and nitridation. Silica/PVP is converted to a mixture of silica and free carbon by pyrolysis. Then, silica and free carbon mixture are reacted to form silicon nitride by the carbothermal reduction and nitridation process.

For pyrolysis step, the composite gel and fibers were put into alumina trays (40 mm × 30 mm × 5 mm deep). Then, these trays were placed in the uniform temperature zone of a horizontal tubular reactor which is an alumina tube (50 mm inside diameter × 1.2 m long) placed inside a high temperature furnace (Carbolite-STF 15/--/180). Samples were heated at 600°C under heating rate of 10°C/min in argon atmosphere for 6 h. The flow rate of argon was fixed at 36 l/h (measured at room temperature). The schematic diagram of this system is shown in Figure 3.2

For carbothermal reduction and nitridation step, the pyrolyzed samples were put into alumina trays (25 mm × 15 mm × 5 mm deep) and placed in the uniform zone of the horizontal tubular flow reactor (Figure 3.2). The samples were heated up to desired temperature at 1,450^{o}C with constant heating rate of 10°C/min under constant flow of argon. After the system had reached the reaction temperature, the reactant gas mixture consisting of nitrogen and hydrogen was fed into the reactor at the flow rate in the range of 17-150 l/h.

3.4 Preparation of Silica/Carbon Black Composite

In a typical procedure, the solution was first prepared by mixing 5 g of APTMS, 0.05 ml of 37% by volume hydrochloric acid and 5 ml of distilled water at room temperature for 6 h. Then, 10 g of carbon black-PVP solution in ethanol, at predetermined carbon-to-silica ratio in the range of 2-6, was dropped into the mixture and stirred for 12 h. It should be noted that PVP used as the spinning aid was fixed at the amount of 1.2 g. The solution was aged at room temperature for 0-3 days. The resulting product is referred to as the silica/carbon black composite gel, although its appearance is still liquidous.

For preparation the silica/carbon black composite fibers, the composite gel is employed as the electrospinning solution. The electrospinning apparatus is consisted of a high-voltage power supply (Gamma High Voltage Research ES30PN), a plastic syringe containing the electrospinning solution equipped with a 20-gauge stainless steel needle, and an aluminum foil used as a collective screen. The needle is connected to the negative electrode of the power supply, while the aluminum collector is attached with the grounding electrode placed 10 cm below the tip of the needle (referred as tip-to-target distance). The electrical potential and collection time were fixed at 5.5 kV and 30 minutes, respectively. The schematic of the electrospinning apparatus used in this work is shown in Figure 3.1

3.5 Conversion of Silica/Carbon Black Composite into Silicon Nitride

For carbothermal reduction and nitridation step, the green composite samples were put into alumina trays (25 mm × 15 mm × 5 mm deep) and placed in the uniform zone of the horizontal tubular flow reactor (Figure 3.2). The samples were heated up to desired temperature at 1,450^{o}C with constant heating rate of 10°C/min under constant flow of argon. After the system had reached the reaction temperature, the reactant gas mixture consisting of nitrogen and hydrogen was fed into the reactor at the flow rate in the range of 30-70 l/h.
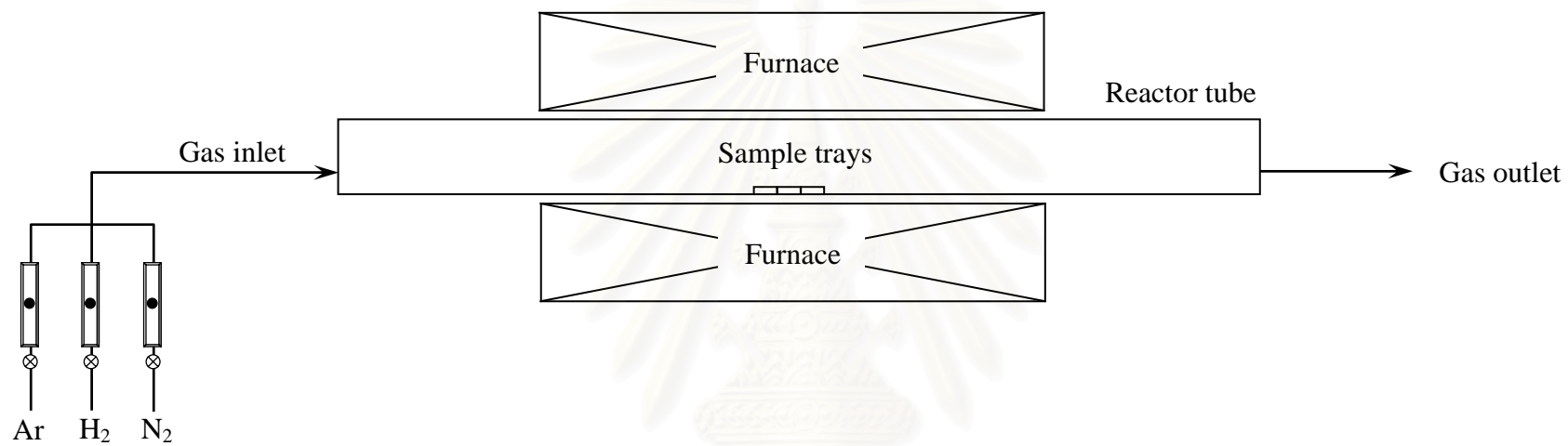
Figure 3.2   Schematic diagram of the tubular flow reactor system.

3.6 Characterization of the Products

The obtained products were characterized by using various techniques, as following:

3.6.1 X-ray Diffraction Analysis (XRD)

Crystalline phases of the product were determined from X-ray diffraction analysis, using a SIEMENS D5000 diffractometer with CuKα radiation. Each sample was scanned in the range of $2\theta = 10\text{-}50°$ with a step size of $2\theta = 0.02°$.

3.6.2 Fourier-Transform Infrared Spectroscopy (FT-IR)

The functional groups in the samples were determined by using a Nicolet Impact 400 infrared spectrometer. The sample was mixed with KBr by sample: KBr ratio of 1: 100 and formed into a thin pellet, before measurement. The spectra were recorded at wavenumber between 400 and 4000 cm^{-1}.

3.6.3 Thermogravimetric Analysis (TGA)

The free carbon, residual carbon content and thermal behaviors of the samples were determined by using TG/DTA analysis on a Diamond TG/DTA thermogravimetric instrument. The analysis was performed from temperature of 50 to 1,000^{o}C under a heating rate of 20°C/min in 200 ml/min flow of either oxygen or nitrogen.

3.6.4 Scanning Electron Microscopy (SEM)

Morphology of the electrospun product as well as the nitrided product was examined by using a scanning electron microscope (JSM-6400, JEOL Co., Ltd.) at the

Scientific and Technological Research Equipment Center (STREC), Chulalongkorn University.

3.6.5 Transmission Electron Microscope (TEM)

The morphology of an individual grain in the samples was observed on a JEOL JEM-2100 Analytical Transmission Electron Microscope, operated at 80-200 keV at the Scientific and Technological Research Equipment Center (STREC), Chulalongkorn University. The crystallographic information was also obtained from the selected area electron diffraction (SAED) analysis performed in the same instrument.

3.6.6 Surface Area Measurement

The single point BET surface area of as-spun and nitrided silica/carbon black composite fibers were measured by using nitrogen as the adsorbate. The operating conditions are as follows:

Sample weight   ~ 0.05 g

Degas temperature $200^{o}C$ for as-synthesized sample

CHAPTER IV

RESULTS AND DISCUSSION

4.1 Preliminary Experiments

In preliminary experiments, amorphous silica nanofibers with diameter in range of 200 to 400 nm were prepared by combined sol-gel and electrospinnning techniques according to procedures reported in literature [Shao et al., 2003]. The spinning solution was consisted mainly of poly (vinyl) alcohol (PVA) and tetraethoxysilane (TEOS), which was used as source for silicon. Effects of electrospinning conditions on fibers, i.e. PVA concentration and the applied voltage were investigated. Figure 4.1 shows SEM images of as-spun PVA/silica composite fibers, using various concentrations of PVA. The applied voltage and the tip-to-target distance were fixed at 8 kV and 10 cm, respectively

(a)   (b)   (c)
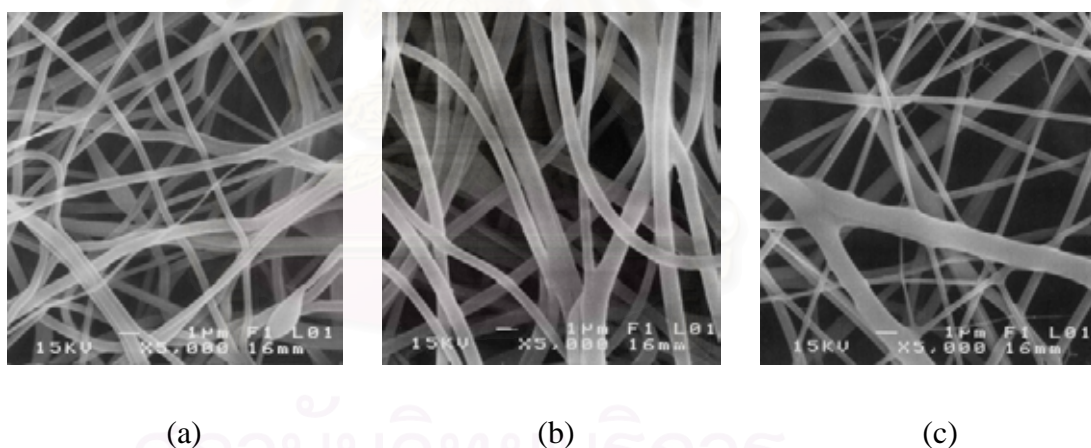
Figure 4.1 SEM micrographs of the as-spun PVA/silica composite fibers with

different PVA contents: (a) 12 wt.%, (b) 14 wt.% and (c) 16 wt.%

From this result, it can be seen that the obtained fibers generally have diameter in nanometer scale. The diameter of the as-spun composite fibers with 12 wt.% PVA ranges from 200 to 400 nm, while the size of the fibers with 16 wt.% PVA is in the range of 200 nm to 1 μm. The increase in PVA content in the spinning solution results in fibers with broader size distribution. This is in agreement with the findings in the previous report on titania/PVP composite fibers that the increased fraction of polymer

in the spinning solution results in changes in viscosity, which subsequently affects the morphology of the spun fibers [Watthanaarun et al., 2005].

The effect of applied voltage on the fiber structure is shown in Figure 4.2, whereas the concentration of PVA is kept at 12 wt.%. It was found that the fibers became less uniform in size, when the applied voltage was increased. More junction and bead formations were observed at applied voltage of 20 kV. This result is in contrast with the observation from the electrospinning of titania/PVP nanofibers [Watthanaarun et al., 2005]. It is suggested that the combined effect of the increasing applied voltage and the viscosity of the spinning solution may cause instability of the jet. Moreover, since water employed as solvent in this work is less volatile than ethanol used in the previous work, the spun fibers require longer time to solidify. Therefore, it is possible that the rearrangement and fusing of crossing fibers can take place, especially when diameter of the spun fiber is small.

(a)   (b)   (c)
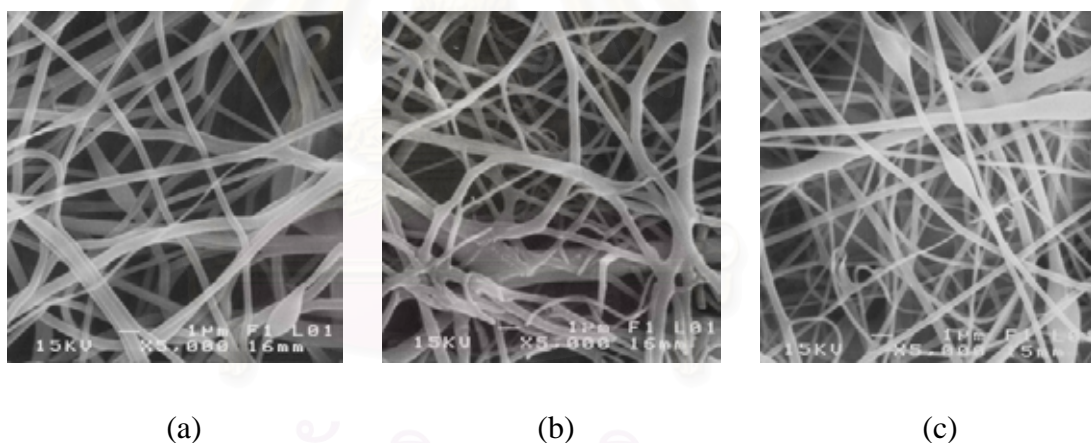
Figure 4.2 SEM micrographs of the as-spun silica/PVA composite fibers produced by different applied voltages: (a) 8 kV, (b) 12 kV and (c) 20 kV.

The FT-IR spectra of the as-spun silica/PVA fibers are shown in Figure 4.3. It is shown that the as-spun silica/PVA composite fibers have absorption bands at wave number of 1100 and 3400 cm^{-1}, which is corresponding to Si-O-Si and O-H bonding [Hajji et al., 1999], respectively. It is implied that TEOS in the composite fibers is hydrolyzed and condensed to form Si-O-Si bonding according to sol-gel process.
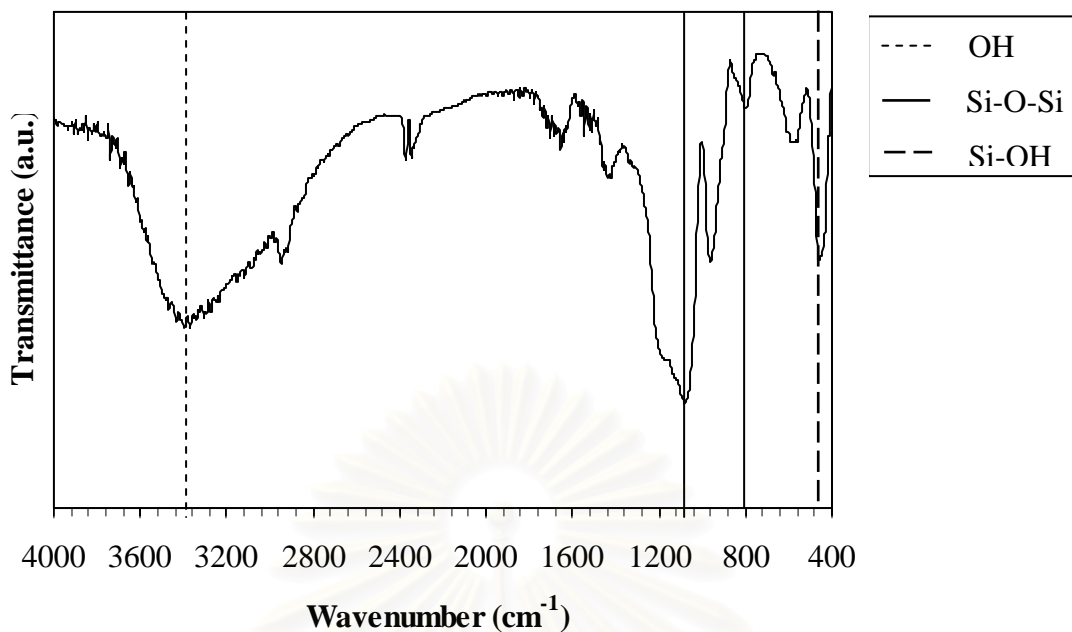
Figure 4.3 FT-IR spectra of as-spun silica/PVA composite fibers.

Further experiment was conducted by subjecting the silica/PVA composite to the carbothermal reduction and nitridation process under pure nitrogen atmosphere at 1,400°C for 8 h. The only crystalline phase in the obtained products was silica in cristobalite phase as evidenced in XRD pattern shown in Figure 4.4. The presence of broad peak at low angle of diffraction, when high content of PVA is used, should also be noted. This is an indirect indication of amorphous residue in the sample. From this result, it is suggested that free carbon content in the composite may not be enough for reducing silica and actuating the formation of silicon nitride because carbon is still in form of polymer chain in PVA, not free carbon.
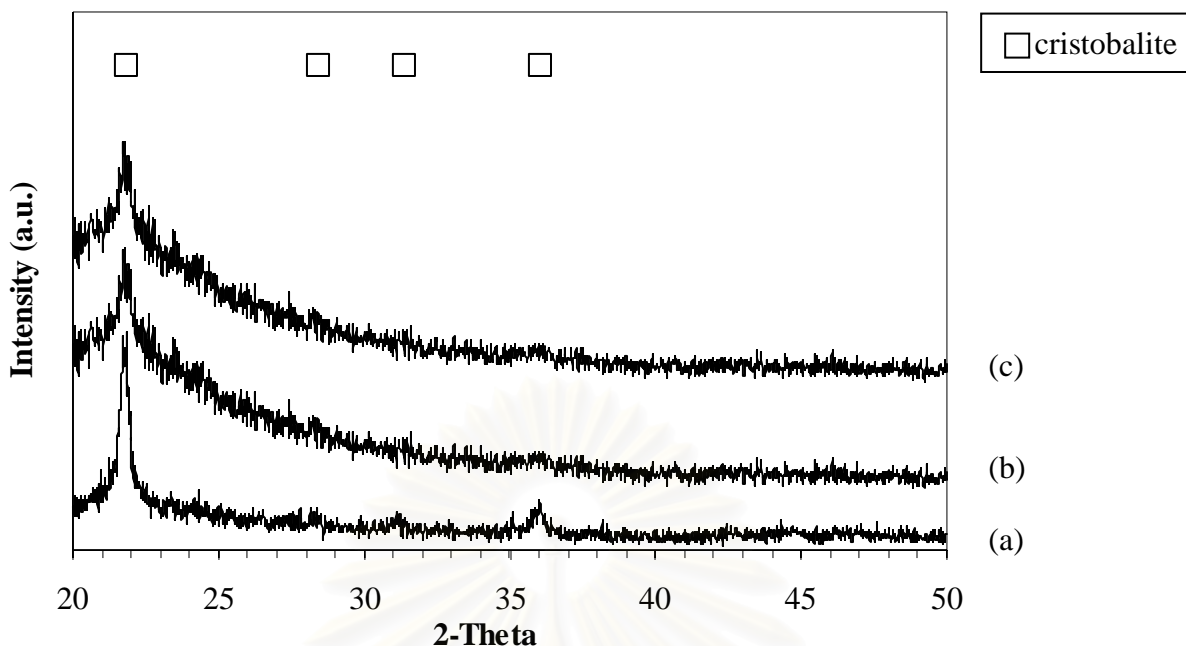
Figure 4.4 XRD patterns of products from the carbothermal reduction and nitridation
at 1,400°C for 8 h with different PVA concentrations as starting material:
(a) 5 wt.%, (b) 8 wt.% and (c) 10 wt.%.

Pyrolysis process is used in this work to break long hydrocarbon chains to become free carbon. The pyrolysis condition for silica/PVA composite was investigated at temperature in the range of 600-1,000°C under argon atmosphere for 3 h. The pyrolyzed products are amorphous, as observed from XRD analysis (Figure 4.5). Thermogravimetric analysis under flow of oxygen (Figure 4.6) reveals mass loss in the range of 1-15%, which suggests that main content of the sample is non-combustable. Since the product pyrolyzed at 600°C shows the highest mass loss in TGA analysis (assuming that the mass loss is corresponding to free carbon content in sample), it was further used in the reaction with nitrogen and hydrogen (in the ratio of 90:10) at 1,450°C for 6 h. The morphology of the as-spun, pyrolyzed and nitrided silica/PVA composite fibers is shown in Figure 4.7.
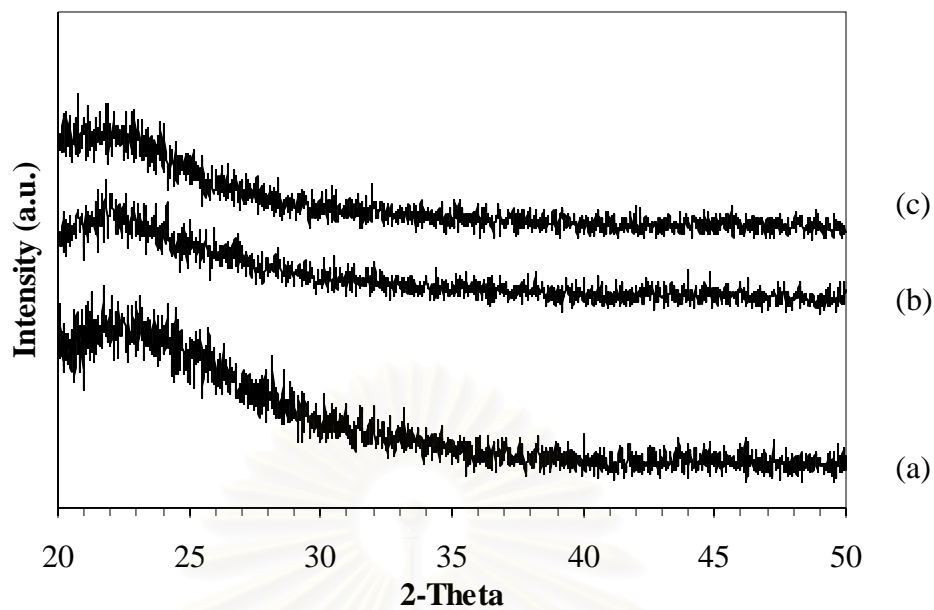
Figure 4.5 XRD patterns of products from pyrolysis at various temperatures:
(a) 600°C, (b) 800°C and (c) 1,000°C for 6h.
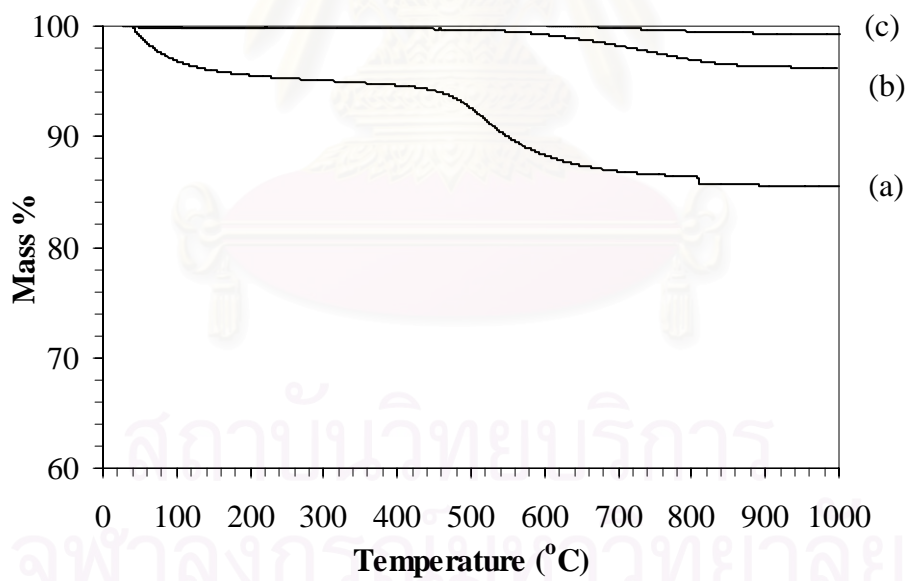
Figure 4.6 TGA analysis of products from pyrolysis at various temperatures:
(a) 600°C, (b) 800°C and (c) 1,000°C for 6h.

(a)   (b)   (c)
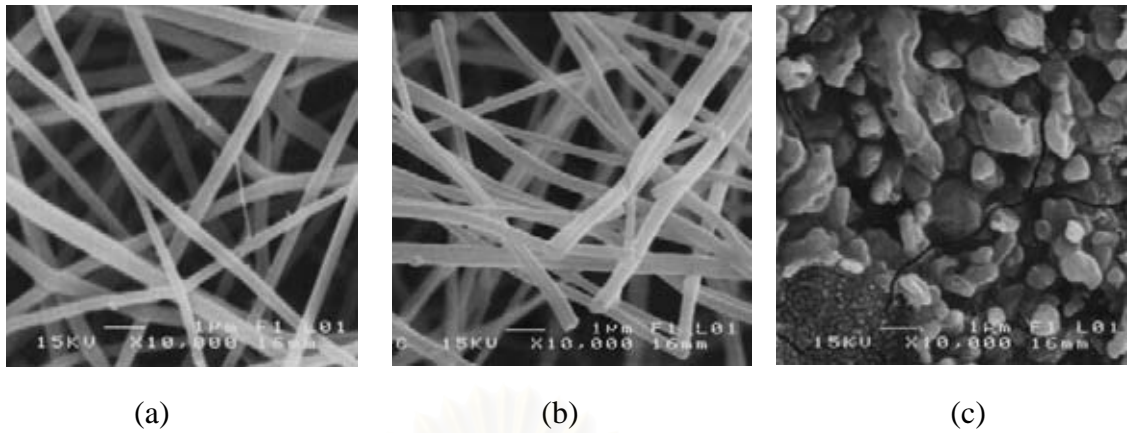
Figure 4.7 SEM micrographs of silica/PVA composite fibers: (a) as-spun, (b) after
         pyrolysis at 600°C for 6h and (c) after nitridation at $1,450^{\circ}$C for 6h.

From these results, it can be seen that morphology of the pyrolyzed product is
still in the form of fibers, but it becomes sheet with rough surface after nitridation. It
can be anticipated that silica/PVA composite in the form of fiber is closely packed
and easily fuse together via sintering. Moreover, free carbon content in the pyrolyzed
composite fibers may not be enough to ensure the separation of silica particles
consisted in the fiber to avoid sintering [Liou et al., 1995].
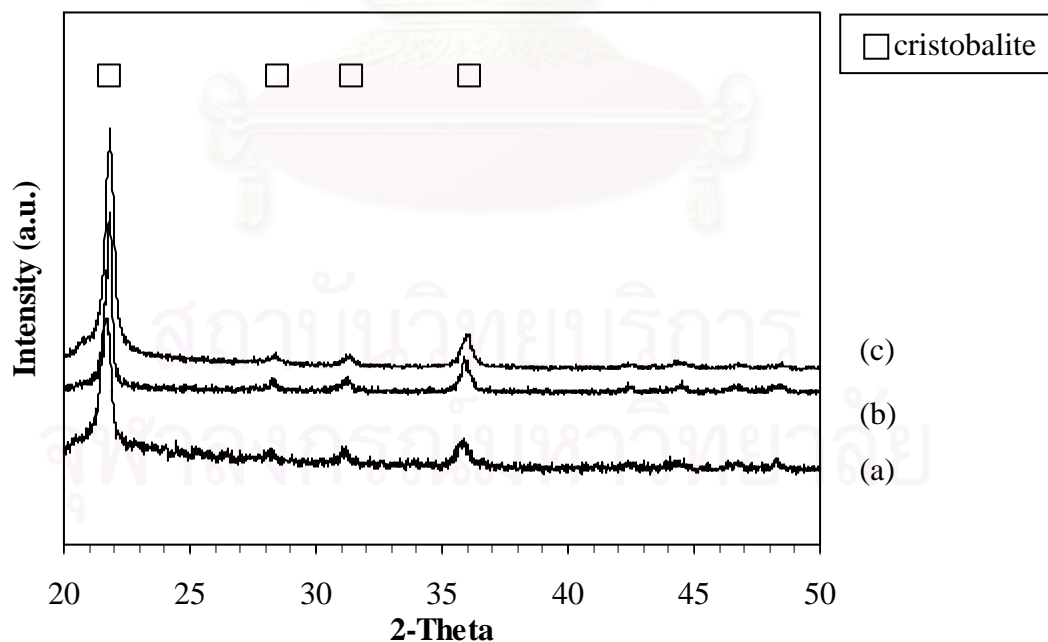
Figure 4.8 XRD patterns of products from the carbothemal reduction and nitridation
         at 1,450 $^{\circ}$C for 6 h with various PVA concentrations: (a) 10 wt.%,
         (b) 12 wt.% and (c) 16 wt.%.

Figure 4.8 shows XRD patterns of nitrided products with different PVA concentrations. Although the products from nitridation are well crystalline, they are still silica in cristobalite phase. No nitridation is taken place. Therefore, the use of TEOS as silicon source may not be appropriate because phase transformation from amorphous silica to cristobalite can take place at temperature in the range of 1,000-1,200°C [K. Kamiya 1990]. It has been generally accepted that cristobalite is the most chemically stable form of silica. Thus, once cristobalite is formed, silica in the composite can not be reduced to intermediate SiO, which is essential for the formation of silicon nitride during the carbothermal reduction and nitridation. Phase transformation from amorphous silica to cristobalite was confirmed by heating the same composite fibers, after pyrolyzed at 600°C, up to 1,450°C and instantly cooled them down to room temperature. It is found that the obtained product is silica in cristobalite phase as shown in Figure 4.9. This result implies that silica in the composite has already transformed from amorphous silica to cristobalite before the carbothermal reduction and nitridation is innitiated. In term of surface area, surface area of the nitrided product is dramatically decreased since silica/PVA composite in the form of fiber fuses together during heating up to 1,450°C. Thus, pyrolyzed silica/PVA composite fibers can not be transformed to silicon nitride via the carbothermal reduction and nitridation.
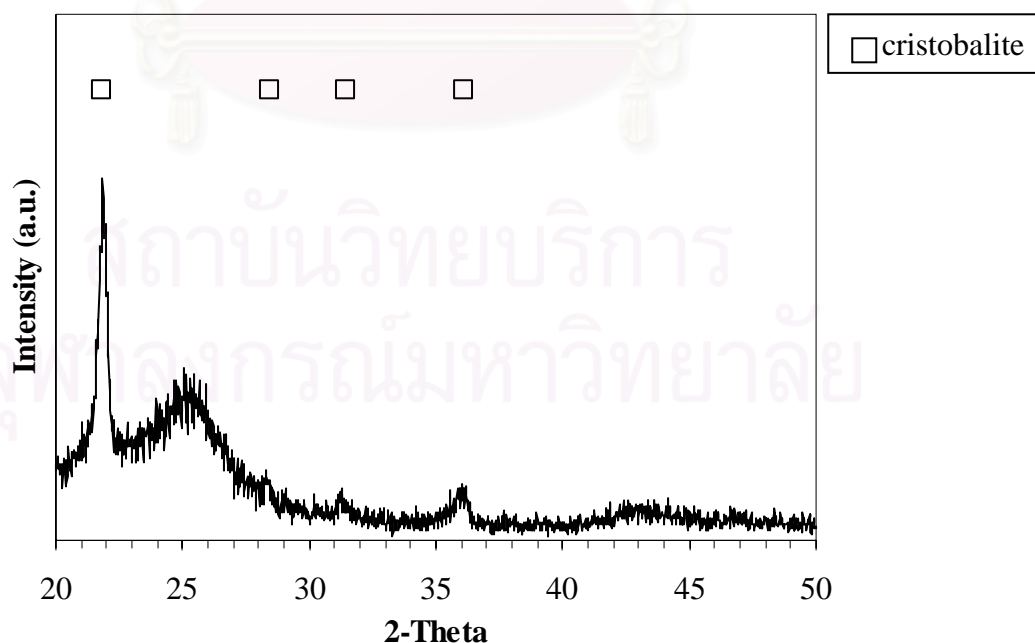
Figure 4.9 XRD pattern of pyrolyzed silica/PVA composite after heating up to 1,450°C (without nitridation).

4.2 Effect of Silica Precursor

From preliminary experiments, silica in the composite fibers obtained from TEOS can not transform to silicon nitride due to the presence of cristobalite before the carbothermal reduction and nitridation. Therefore, effect of type of silicon precursor, which directly relates to the formation of cristobalite, should be studied first. In this work, three silica precursors, i.e. silatrane, APTMS and TEOS are investigated. Silica/carbon composite powder was prepared by physically mixing the silica powder with carbon black (as source of free carbon) in the silica-to-carbon ratio of 1:4. It should be noted that silatrane, which is solid powder, was directly mixed with carbon black. For APTMS and TEOS, silica powder was prepared via sol-gel process. The obtained product was dried and ground before mixed with carbon black. After that, the silica/carbon composite powder was subjected to the carbothermal reduction and nitridation process under nitrogen and hydrogen (in the ratio of 90:10) at 1,450°C for 6 h (standard operating condition). The results from the x-ray diffraction analysis of the products after the nitridation are shown in Figure 4.10.
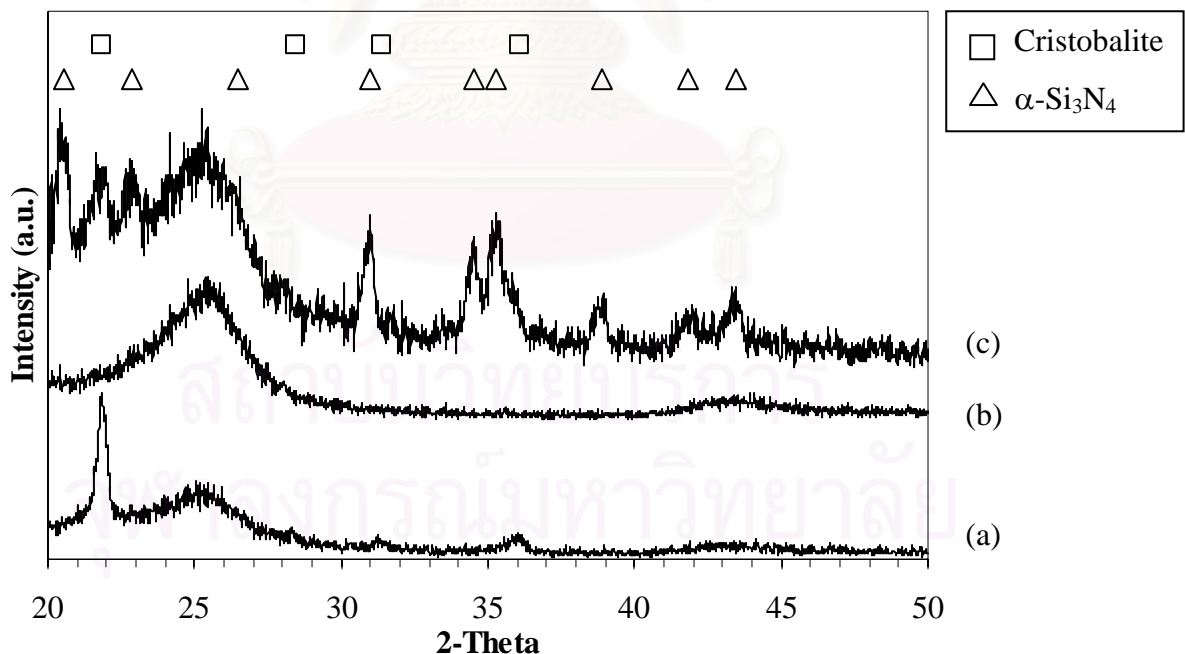
**Figure 4.10** XRD patterns of products from the carbothermal reduction and nitridation at 1,450°C for 6 h using different silca precursors: (a) TEOS, (b) silatrane and (c) APTMS.

From this result, it can be observed that α-silicon nitride can be synthesized only when APTMS is used as silica precursor. Nevertheless, the XRD analysis in Figure 4.10 (c) also shows a sign of broad diffraction pattern from amorphous phase. This amorphous peak comes from residual carbon after nitridation. On the other hand, the nitrided product using silatrane as the precursor reveals only amorphous curve (no crystalline peak can be observed). It is anticipated that APTMS has a suitable structure to form crosslinked Si-O-Si network during the sol-gel process, while silatrane has a complex structure as shown in Figure 4.11. With this structure, it is hard to break its bond to generate the intermediate SiO and react with carbon to form silicon nitride via the carbothermal reduction and nitridation. Moreover, Figure 4.12 shows FT-IR spectra of silica gel using APTMS as silica precursor. Anti-symmetric and symmetric stretching vibrations of Si-O-Si bonding (refering to silica) are found at 1,090 and 800 cm^{-1}, while silatrane does not show the similar spectra (see Table 4.1). This result indicates that silatrane does not have the appropriate bonding to react with carbon for silicon nitride synthesis via the carbothermal reduction and nitridation.

(a)   (b)
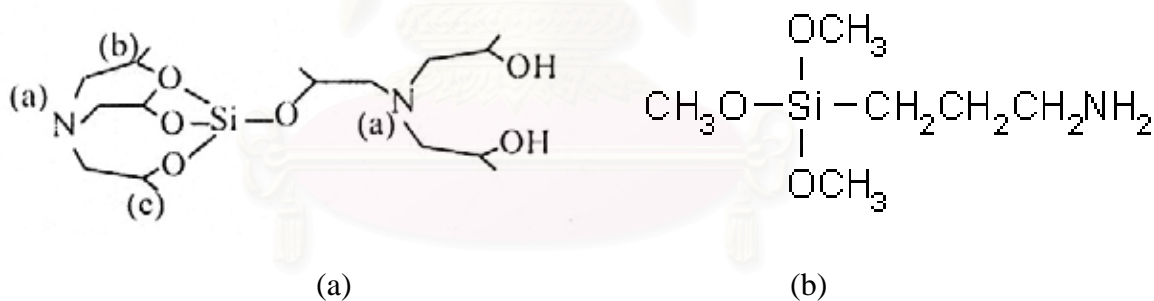
Figure 4.11 Structure of: (a) Silatrane and (b) APTMS.
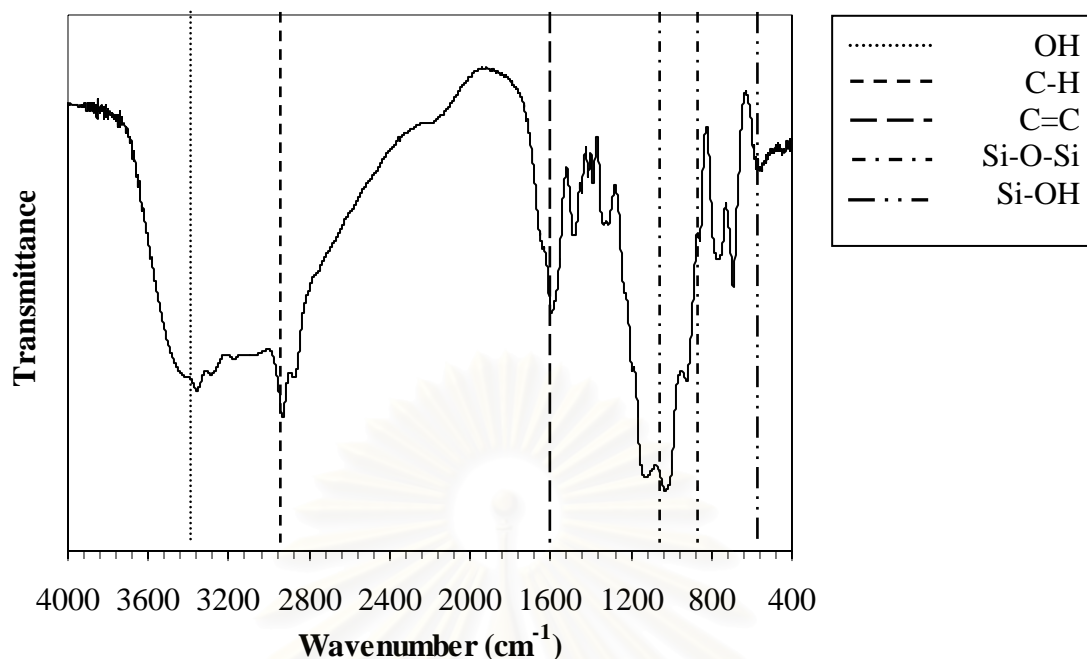
Figure 4.12 FT-IR spectra of silica gel using APTMS as silica precursor.

Table 4.1 Assignment of infrared spectra of silatrane [Charoenpinijkarn et al., 2001].

Table 1
Assignments of infrared spectra of the products

Characterization	Silatrane complexes
Si–N stretching[a]	560–590 cm^{-1}
Si–O–CH[b]	970,883 cm^{-1}
C–O[a]	1013–1070 cm^{-1}
Si–O–CH$_2$[b]	1015–1085 cm^{-1}
C–N[a]	1270 cm^{-1}
C–H bending[a]	1380–1460 cm^{-1}
C–H stretching[a]	2800–29760 cm^{-1}

[a] Silverstein et al., 1991 [17].
[b] Anderson D.R., 1974 [18].

After this section, the next studies are divided into two parts depend upon source of carbon, i.e. carbon black and pyrolyzed polymer. Source of carbon, silica-to-carbin ratio, aging time, morphology of the starting material (e.g. gel or fibers), reaction time and flow rate of reactant gas mixture for the carbothermal reduction and nitridation are investigated.

4.3 Preparation of Silicon Nitride from Pyrolyzed Silica/Polymer Composite

4.3.1 Effect of carbon source

After APTMS was chosen as the appropriate precursor, the type of carbon source for the carbothermal reduction and nitridation was investigated again. In this section, carbon black, h-PVP (PVP with molecular weight of 1,300,000), l-PVP (PVP with molecular weight of 10,000) and mixed-PVP (mixture of h-PVP and l-PVP in the ratio of 1:5 by weight) were used as carbon source. The mixed-PVP was used besides h-PVP and l-PVP (M_w 10,000) because silica/carbon composite using only l-PVP could not be spun by electrospinning. h-PVP was also added as the spinning aid. Nevertheless, it should be noted that no electrospinning was done in this part of the experiment. Silica containing gel, derived via sol-gel process using APTMS as the precursor, was mixed with PVP according to the procedure described earlier in Chapter III. Then, all green samples containing PVP, in form of gel, have to be pyrolyzed at $600^{\circ}C$ for 6 h to convert long hydrocarbon chains of polymer to free carbon before subjected into the nitridation. XRD patterns of the nitrided products using different carbon sources are shown in Figure 4.13.
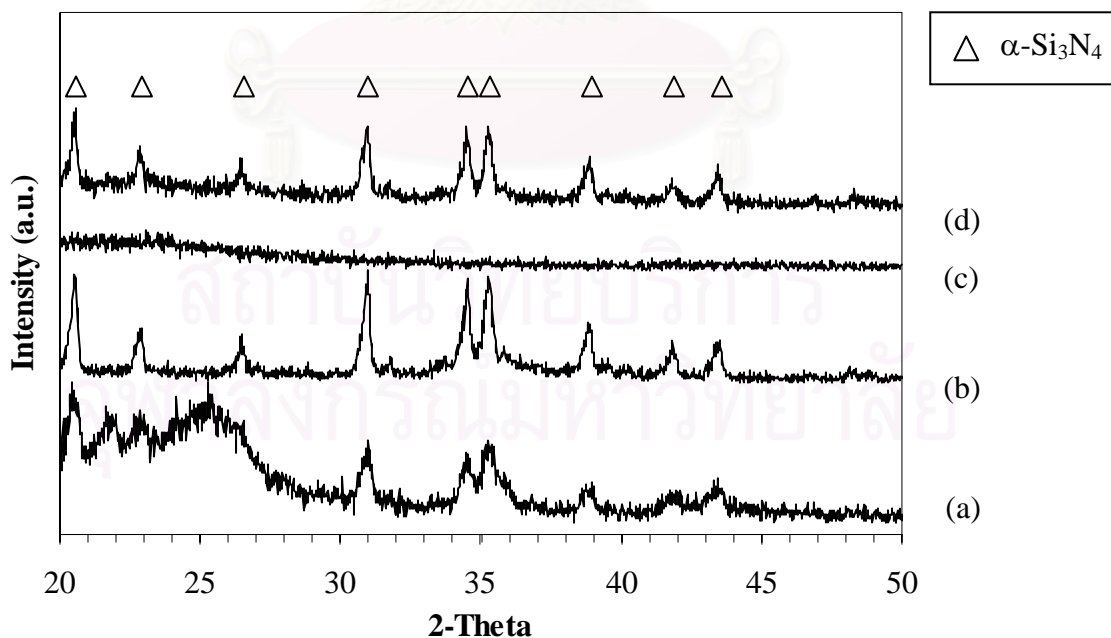

Figure 4.13 XRD patterns of products from the carbothermal reduction and nitridation using different carbon sources: (a) carbon black, (b) l-PVP, (c) h-PVP and (d) mixed-PVP (l-PVP and h-PVP in the ratio of 1:5).

From this result, silicon nitride was found in the product when carbon black, l-PVP and mixed-PVP were used as carbon source. When h-PVP was used, the XRD pattern showed amorphous curve. It is indicated that the polymer chain in l-PVP and h-PVP can be broken to free carbon during the pyrolysis. However, l-PVP provides higher content of free carbon than h-PVP, due to the fact that h-PVP has longer polymer chain than l-PVP. Breaking long polymer chain to free carbon is more difficult than the shorter chain. This anticipation is confirmed by TGA analysis as shown in Figure 4.14.
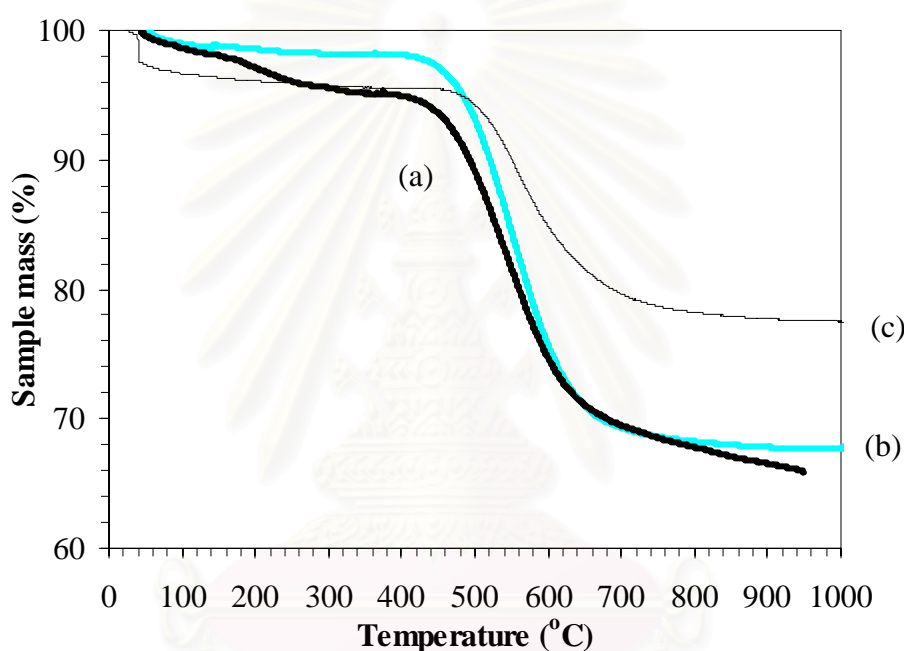
Figure 4.14 TGA analysis of products from pyrolysis using various kinds of PVP:
(a) l-PVP, (b) mixed-PVP and (c) h-PVP.

After pyrolysis, silica/PVP composite gel is converted to a mixture of silica and free carbon. The mass loss observed during TGA analysis (assuming that all mass loss is corresponding to free carbon) from the pyrolyzed products using either l-PVP and mixed-PVP as carbon source was approximately 35 wt.%, which is greater than that of the pyrolyzed products using h-PVP. So, the nitrided product when h-PVP was used as the carbon source was still amorphous because the free carbon content in a pyrolyzed mixture was not enough for the carbothermal reduction.

4.3.2 Effect of aging time

After finding the suitable silicon and carbon source, the next parameter which affects the silicon nitride production from silica/PVP composite is aging time. In this work, it was found that silica/mixed-PVP composite gel could be converted to silicon nitride via the carbothermal reduction and nitridation when the composite gel was aged for at least 3 days. No nitridation took place when the composite gel was used without aging. Figure 4.15 reveals the FT-IR spectra of pyrolyzed products with various aging times. It is found that the absorption peak at 3,440 cm^{-1} is attributed to stretching vibration of Si-OH in SiO$_2$ gel and O-H bond in water absorbed insample [Fu et al., 2003]. The absorption bands at 3,000-2,800 and 1,600 cm^{-1} are ascribed to C-H structure and C=C bond, respectively [Ercin et al., 2003]. Moreover, The bands at 1,090, 800 and 460 cm^{-1} are attributed to anti-symmetric and symmetric stretching vibrations of Si-O-Si and Si-OH bonding in silica gel [Martos et al., 2003]. This result confirms that APTMS in the all composite samples are hydrolyzed and condensed to form Si-O-Si bonding according to sol-gel process, regardless of the aging time. Figure 4.16 shows XRD patterns of the nitrided product when different aging time was applied. It is suggested that the prolonged aging time allows the condensation reaction to further form Si-O-Si network (refer to silica) in the sol-gel fashion. The greater number of silica consequently promotes the formation of silicon nitride during the carbothermal process.
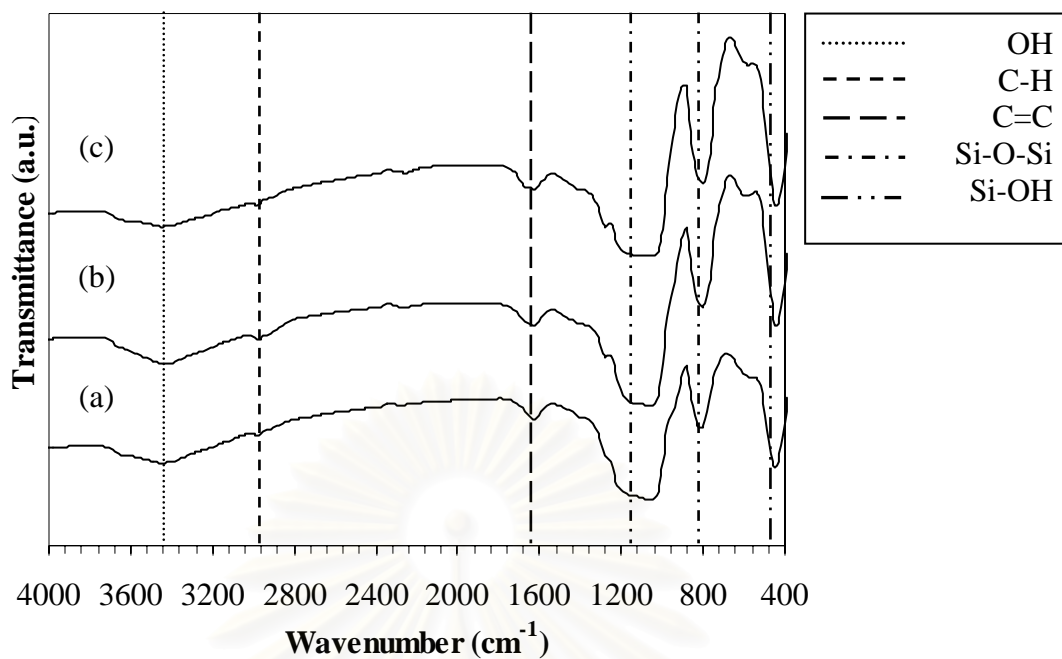
Figure 4.15 FT-IR spectra of products from 6 h pyrolysis at 600°C of silica/mixed PVP composite gel with different aging time: (a) no aging time, (b) 3 days and (c) 5 days.
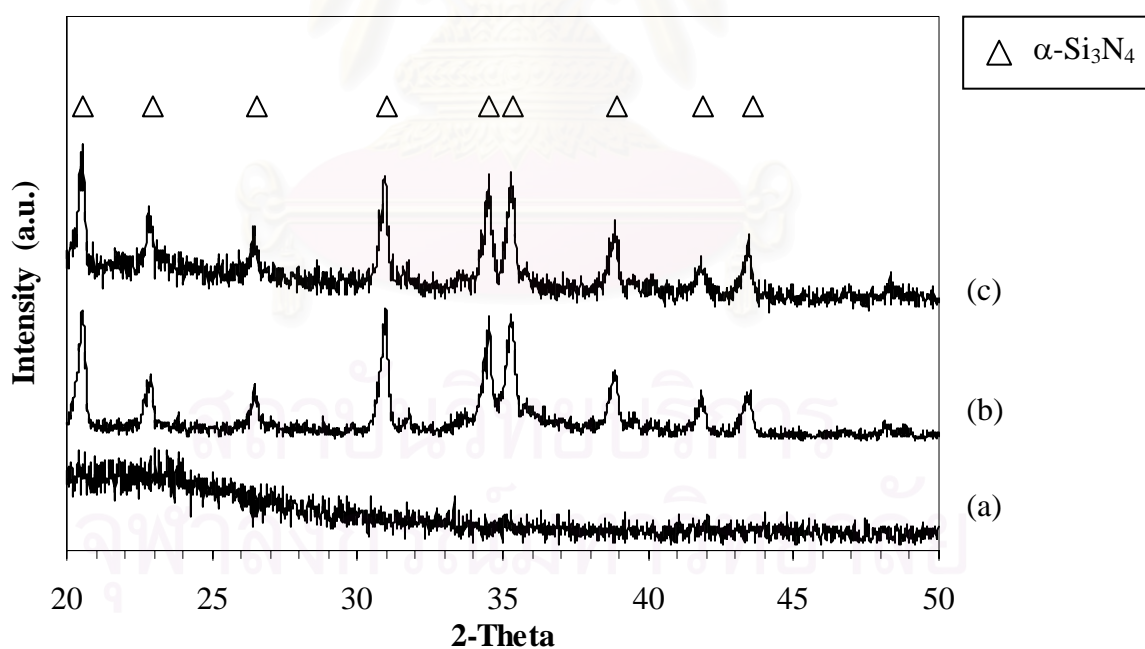
Figure 4.16 XRD patterns of products from the carbothermal reduction and nitridation using pyrolyzed silica/mixed-PVP composite gel with different aging time as the starting material: (a) no aging time, (b) 3 days and (c) 5 days.

FT-IR spectras of nitrided products with different aging time are shown in Figure 4.17. It can be observed that the nitrided product with 3-days aging shows absorption bands of silicon nitride, while the nitrided product without aging time does not reveal the same result. The bands at 1,090, 800 and 460 cm^{-1}, which are attributed to anti-symmetric and symmetric stretching vibrations of Si-O-Si and Si-OH bonding [Martos et al., 2003], are still clearly visible in the sample with no aging time This result confirms that aging time is essential for increasing physical contact between silica and carbon which is essential for silicon nitride formation [Durham et al., 1991]
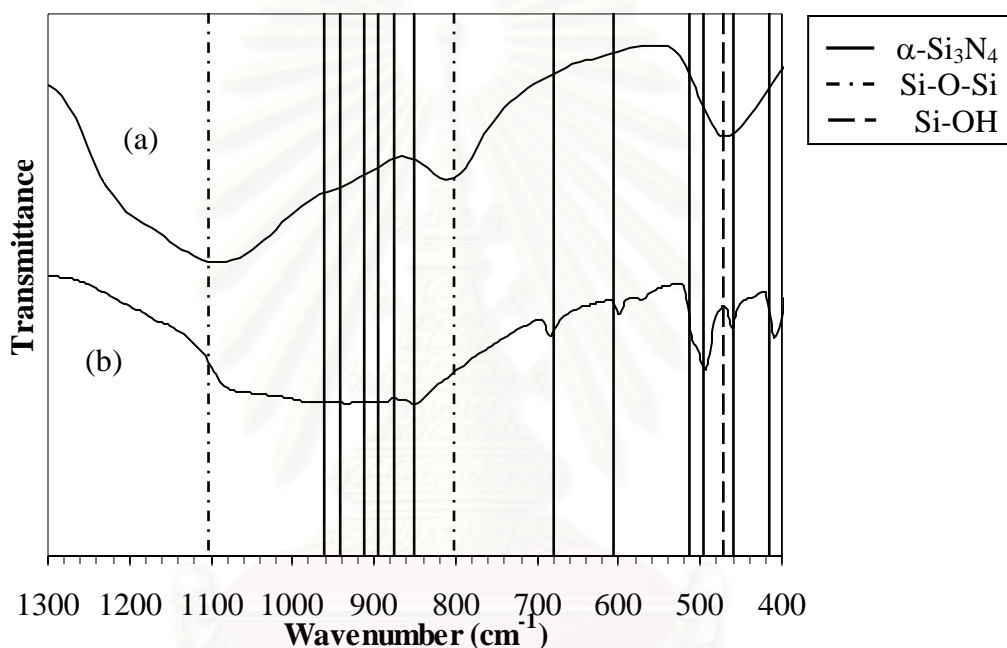
Figure 4.17 FT-IR spectra of product from the carbothermal reduction and nitridation of pyrolyzed silica/mixed PVP composite gel with different aging time: (a) no aging time, (b) 3 days.

4.3.3 Effect of sample morphology

In this section, effect of sample morphology, i.e. gel and fibers, was investigated. Silica/PVP composite gel was prepared according to the same procedures employed in the previous section, by using APTMS and mixed-PVP as sources for silica and carbon, respectively. The gel was aged for 3 days. Portion of the aged gel was pyrolyzed in the same manner as discussed in the last section. The rest

of aged gel was spun into fibers by the electrsospinning technique, before subjected to the same pyrolysis process. Both samples were then nitrided at 1,450°C for 6h.

Figure 4.18 reveals FT-IR spectra of pyrolyzed products with different morphology. It is found that the pyrolyzed products, in both fiber and gel forms, show the same absorption bands at 3,440, 3,000, 1,600, 1,090, 800 and 460 cm^{-1} as discussed in prior section. In the aspect of functional groups, it can be indicated that the pyrolyzed product in the form of fibers should be convertable to silicon nitride via the carbothermal reduction and nitridation, as well as the pyrolyzed product in the form of gel. However, according to Figure 4.19 and 4.20 which show XRD patterns and SEM images of nitrided products, only the sample in form of gel can be transformed to silicon nitride after the carbothermal reduction and nitridation. The fibers do not exhibit the same behavior.
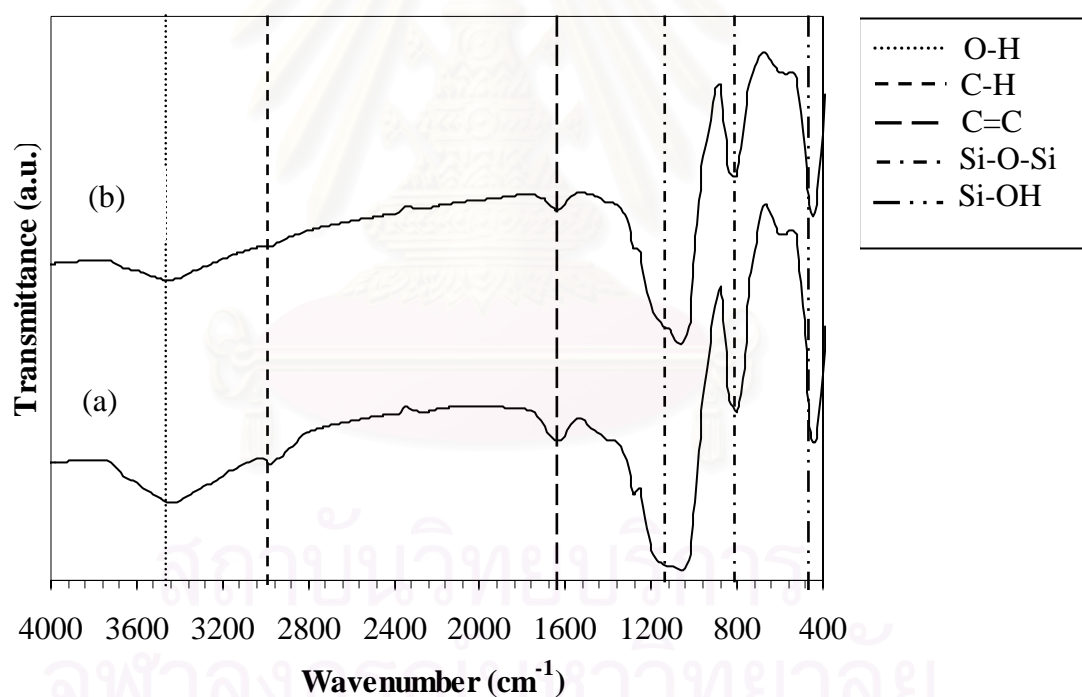
Figure 4.18 FT-IR spectra of product from pyrolysis of silica/mixed PVP composite gel in different forms: (a) fibers and (b) gel.
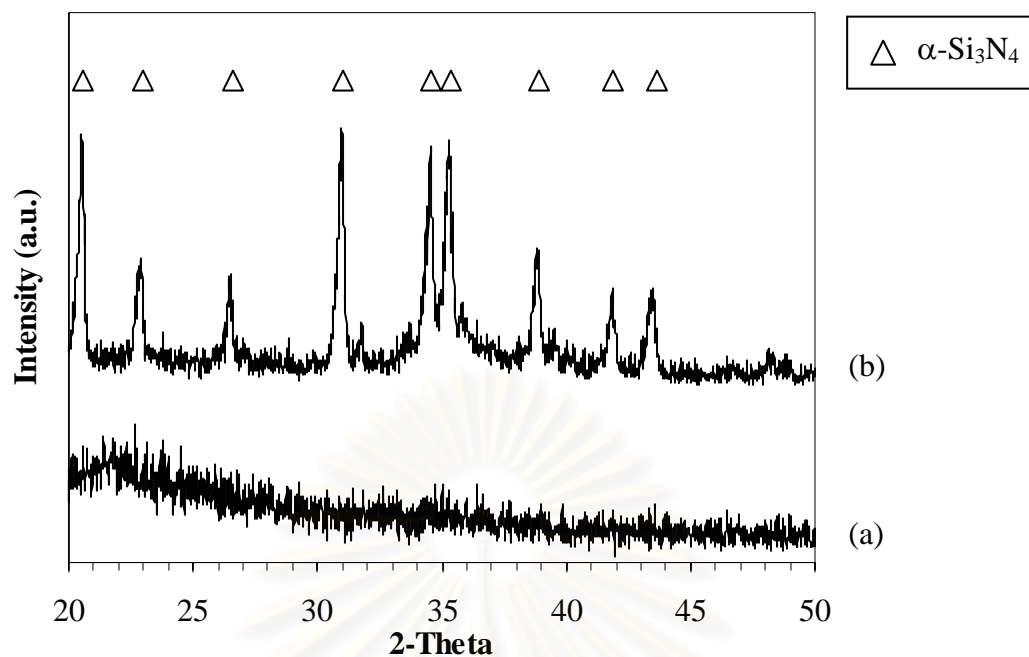
Figure 4.19 XRD patterns of products from the carbothermal reduction and
nitridation of pyrolyzed silica/PVP composite in different form:
(a) fibers and (b) gel.
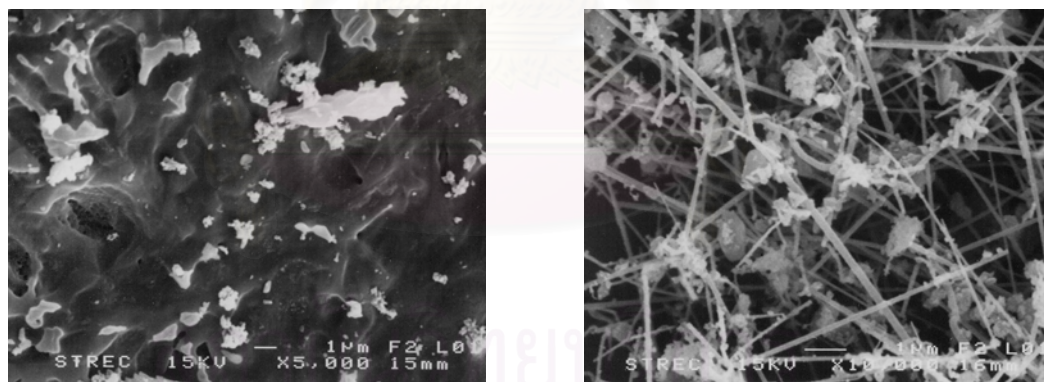
Figure 4.20 SEM micrographs of products from the carbothermal reduction and
nitridation of pyrolyzed silica/carbon composite in different forms:
(a) fibers and (b) gel.

From these results, it is indicated that although the starting materials are the same, morphology in form of fibers is not appropriate for converting to silicon nitride, because of two possible causes. Firstly, free carbon content in the pyrolyzed fibers may not enough for the carbothermal reduction and nitridation. According to the proposed mechanism for the carbothemal reduction and nitridation, full conversion using silica and carbon in stoichiometric ratio (1:2) can occur only when the contact between carbon and silica particles is perfect (i.e. carbon and silica are homogeneous mixed). In practice, an excess amount of carbon is always required for full transformation of silica to silicon nitride [Durham et al., 1991]. Furthermore, the excess carbon is also employed by the following reasons: (1) to reduce the moisture content in the silica, (2) to reduce the partial pressure of oxygen to suppress the formation of silicon oxynitride, (3) to ensure that the silica particles remain separated to avoid sintering, (4) to act as a reducing agent, which causes the initial formation of SiO, and (5) to act as a source of active sites at which silicon nitride can nucleate [Liou et al., 1995]. To verify the speculation about the content of free carbon in the samples, TGA experiments were conducted. The results are shown in Figure 4.21 and 4.22. Figure 4.21 shows the mass loss of sample mass during heating up to 600°C under inert atmosphere (N_2) and held at 600°C for 1h. This is the same condition as the pyrolysis process. Then, the pyrolyzed samples were heated up to $1,000^{o}$C under N_2 atmosphere in TGA equipment again. Mass of the sample was constantly monitored, as shown in Figure 4.22. This process simulates the heating up period before the carbothermal reduction and nitridation.
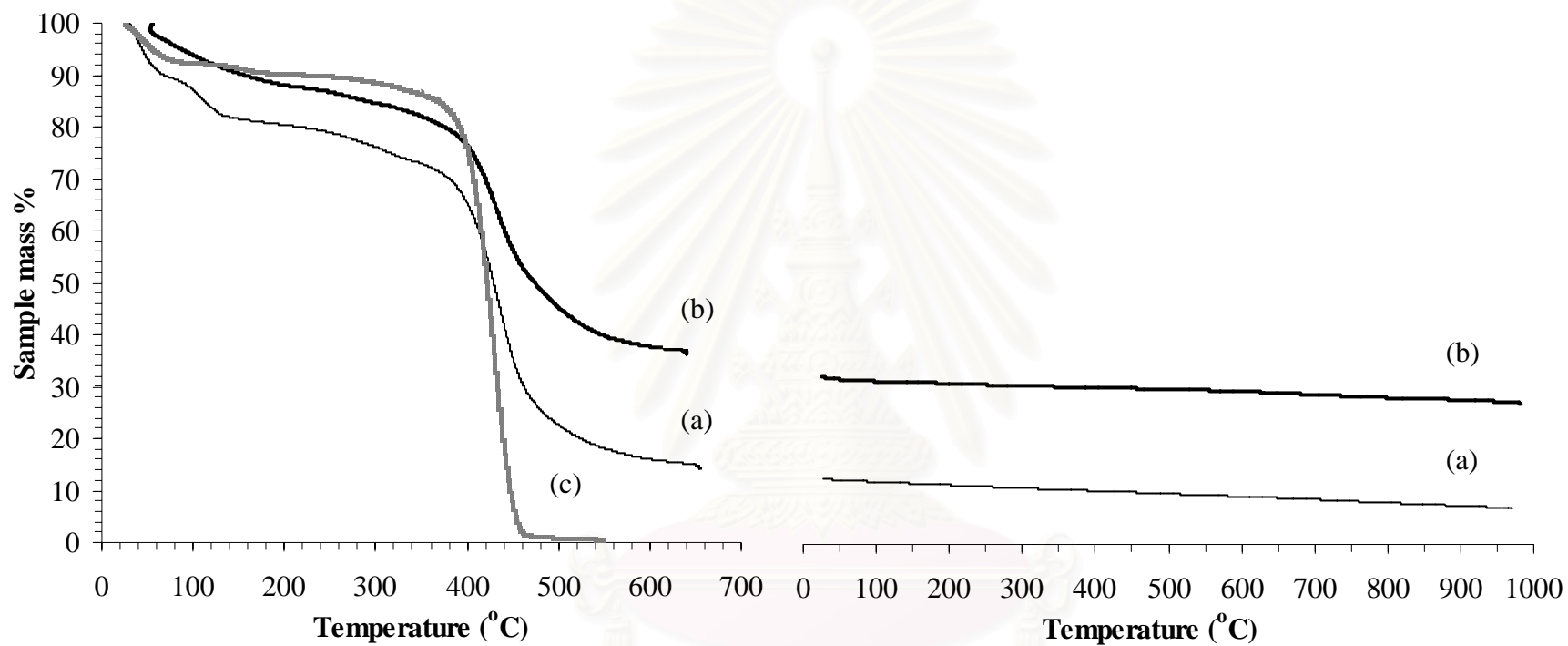
Figure 4.21 TGA analysis of products from silica/PVP composite at 600°C under N$_2$ atmosphere: (a) fibers and (b) gel and (c) pure mixed-PVP.

Figure 4.22 TGA analysis of products from heating up pyrolyzed composite to 1,000°C under N$_2$ atmosphere: (a) fibers and (b) gel.

The results shown in Figure 4.21 and 4.22 reveal that silica/carbon composite in the form of fibers has greater mass loss than in the form of gel. Mass loss from composite gel is approximately 70%, whereas mass loss from composite fibers is approximately 92%. Although this mass loss is partially accounted by the evaporation of physical absorption of moisture, significant mass loss occurs at temperature in the range of 400-450°C. This mass loss is associated with the decomposition of PVP [Barbosa-Coutinho et al., 2003], as witnessed from the TGA results of pure PVP (Figure 4.21c). It also implied as the mass loss of carbon from the sample. Therefore, these results suggest that the content of carbon left in the fibers after pyrolysis is too low and not enough for the carbothermal reduction and nitridation.

The other factor, which prohibits the nitridation of sample in fiber form, is the fact that silica in each fiber is sintered together because amount of carbon to ensure the separation of silica particles is not enough. The sintering of silica reduces its surface area and consequently limits the generation of SiO, which is essential for silicon nitride formation via the carbothermal reduction and nitridation.

4.3.4 Effect of flow rate of reactant gas mixture

In this section, in the attempt to produce silicon nitride from the silica/PVP composite fibers, the effect of overall flow rate of the reactant gas mixture, which was nitrogen mixed with 10% hydrogen. The ranges of the overall flow rate investigated are 17-150 l/h. These ranges are extreme conditions for investigating whether the flow rate of reactant gas mixture affects the silicon nitride formation. Normally, the increased flow rate reduces the gas film mass transfer resistance for the diffusion of SiO vapor to bulk gas stream which results in higher growth of silicon nitride according to vapor-solid (VS) mechanism. It should be note that SiO, which is generated by the reduction of silica (Eq. 2.5), is the key intermediate for the formation of silicon nitride. Moreover, since the vapor pressure of SiO vapor at temperature of system is very low, SiO vapor generated must be continuously removed by the flow of gas in the reactor, in order to sustain its production [Wotting et al., 1996]. Copious flow of reactant gas ensures adequate nitrogen gas for conversion to silicon nitride. The X-ray diffraction analysis of the products from the nitridation with different flow rates is shown in Figure 4.23.
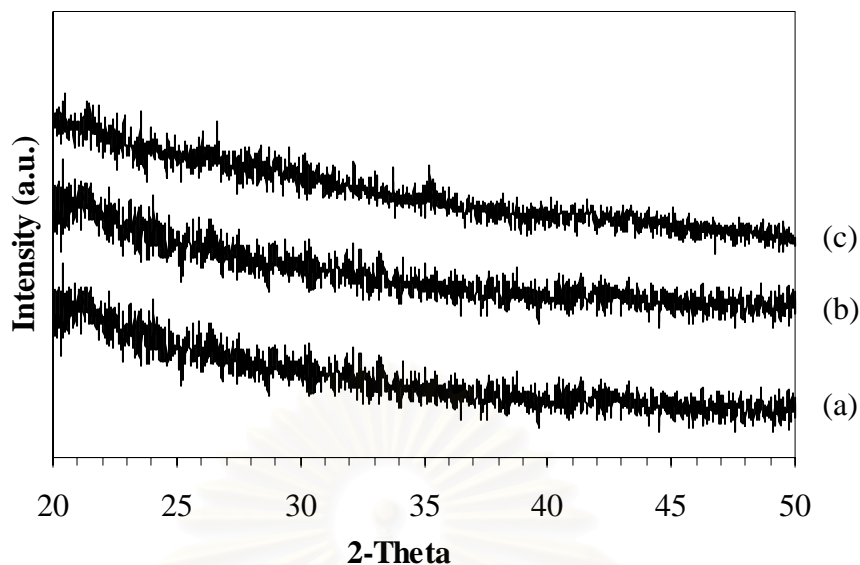
**Figure 4.23** XRD patterns of products from the carbothemal reduction and nitridation of pyrolyzed silica/PVP composite fibers with various flow rates of reactant gas: (a) 17 l/h, (b) 50 l/h and (c) 150 l/h.

From this result, it can be observed that all obtained products are still amorphous after nitridation, regardless of the flow rate used. No crystalline peak is detected. The increased flow rate of reactant gas should promote SiO formation as discussed in this section, but actual generation of SiO also depends upon the content of free carbon in the composite because silica is reduced by carbon to form SiO (Eq. 2.5). If free carbon in the composite is not enough for the reduction of silica, SiO will not occur. Hence, it indirectly implies that pyrolyzed silica/PVP fibers do not generate SiO mainly because the carbon content in the composite fibers is inadequate. This anticipation supports the TGA analysis (Figure 4.21) as discussed in the previous section.

4.4 Preparation of Silicon Nitride from Silica/Carbon Black Composite Fibers

According to discussion in prior sections, synthesis of silicon nitride from silica/PVP was failed mainly because of insufficient content of free carbon in the sample after pyrolysis. Moreover, the pyrolyzed PVP may not be the proper form of carbon for the carbothermal reduction and nitridation. In this section, carbon black was used as alternative carbon source in the electrospun composite fibers. Amount of carbon black used was equivalent to carbon content in PVP in the last section. It

should be noted that small amount of h-PVP was still added to the sample as the spinning aid and the mixture was spun without aging. No pyrolysis was conducted on the silica/carbon black composite fibers.

4.4.1 Effect of carbon-to-silica ratio

In this section, carbon-to-silica ratio, the influential parameter affecting the silicon nitride formation via the carbothermal reduction and nitridation, was investigated under fixed composite fibers preparation and nitridation conditions. Figure 4.24 shows SEM images of as-spun composite fibers with various carbon-to-silica ratios, in the range of 2:1 to 6:1. The applied voltage and the tip-to-target distance for fiber electrospinning were fixed at 10 kV and 10 cm, respectively. It can be seen that the obtained fibers generally have diameter in micrometered scale. The diameter of the as-spun composite fibers ranges from 0.65 to 1 μm. The increased content of carbon black in the spinning solution results in the fibers with broader distribution of fiber diameter as shown in Figure 4.25. The elevated fraction of carbon black in the spinning solution results in changes in viscosity, which subsequently affects the morphology of the fibers [Shao et al., 2003].

| (a) | (b) | (c) |
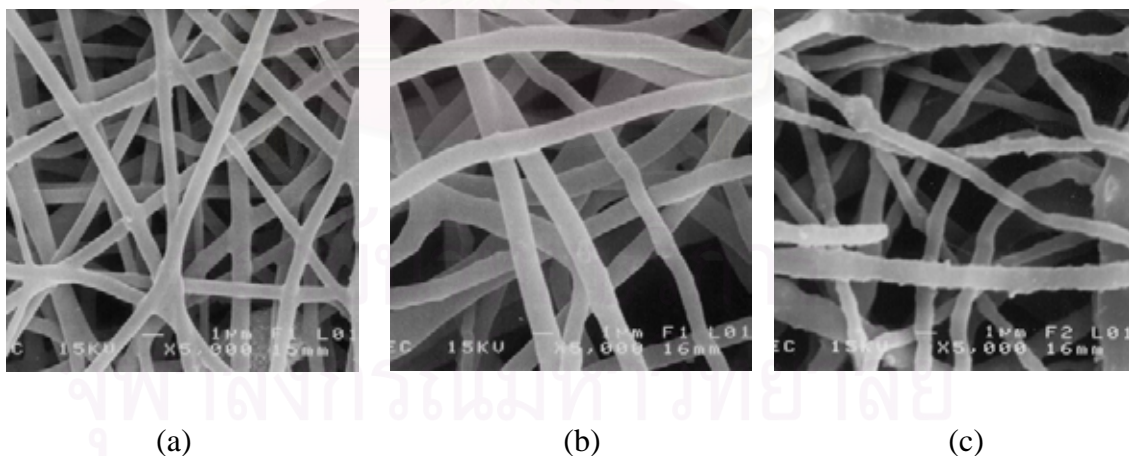
Figure 4.24 SEM micrographs of as-spun silica/carbon black composite fibers with
various carbon-to-silica ratio: (a) 2:1, (b) 4:1 and (c) 6:1.
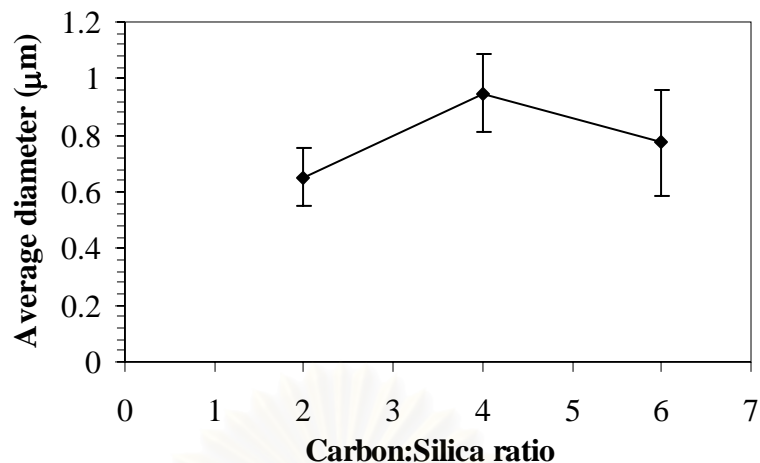
Figure 4.25 Average size and size distribution of as-spun silica/carbon composite fibers using various carbon-to-silica ratios.

Figure 4.26 shows XRD patterns of the obtained products after nitridation at 1,450^{o}C under nitrogen and hydrogen atmosphere for 6h, using the composite fibers with different carbon-to-silica ratio. It can be observed that the as-spun silica/carbon composite fibers with carbon-to-silica ratio of 2:1 and 4:1 are converted into silicon carbide, while those with carbon-to-silica ratio of 6:1 are silicon carbide/silicon nitride composite. These results suggest that silicon nitride can be formed only when carbon content is excessively large since the silicon nitride formation requires the high excess carbon used as a site for silicon nitride formation. Excess carbon also increases physical contact with silica particles and increases effectiveness in silica reduction to generate SiO, which subsequently actuates the formation of silicon nitride, according to Eq. (2.5) to (2.9) [Durham et al., 1991]. When carbon content is not high enough, formation of silicon carbide is favored. Formation of silicon carbide is prominent when the starting material is in form of fiber because silica and carbon in the nanofiber, which has high surface, can generate more CO than the other forms (e.g. powder or gel). High CO partial pressure has been reported to promote β-silicon carbide formation during the carbothermal reduction [Durham et al., 1991].
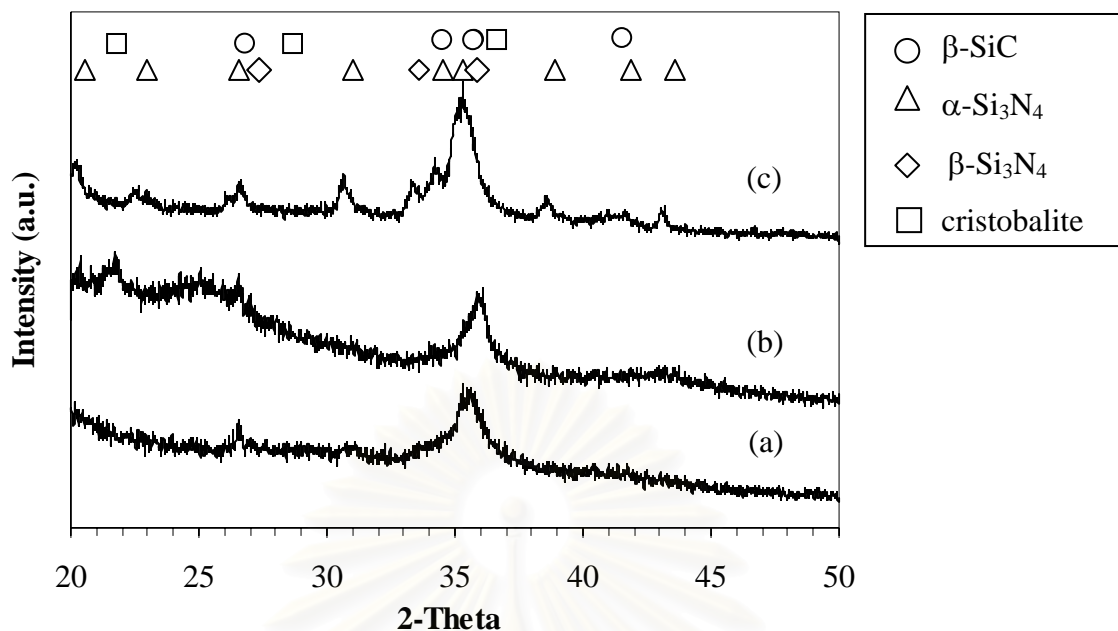
Figure 4.26 XRD patterns of products from the carbothermal reduction and nitridation of silica/carbon composite fibers with various carbon-to-silica ratios: (a) 2:1, (b) 4:1 and (c) 6:1

SEM micrographs from the nitrided products are shown in Figure 4.27. Silicon nitride and/or silicon carbide obtained from the carbothermal reduction and nitridation generally remains the same morphology as the as-spun silica/carbon composite fibers. It can be seen that, for carbon-to-silica ratio of 2:1, the nitrided product (Figure 4.27a) has similar structure as the as-spun silica/carbon composite fibers (Figure 4.24a). For carbon-to-silica ratio of 4:1 and 6:1, some parts of the nitrided fibers are broken off and become short fibers (Figure 4.27b,c) consisting of the number of aggregated primary particles with average size approximately 40 nm (see in Figure 4.27d). Figure 4.28 shows average size and size distribution of the nitrided products. It can be observed that the average size of the nitrided fibers is in the range of 0.7 to 0.8 μm. The nitrided fibers with carbon-to-silica ratio of 4:1 and 6:1 are smaller than the as-spun fibers, whereas the nitrided fibers with carbon-to-silica ratio of 2:1 show the contrary result. The increased carbon content results in the greater number of active sites at which silicon nitride can nucleate [Liou et al., 1995].

(a)

(b)

(c)

(d)
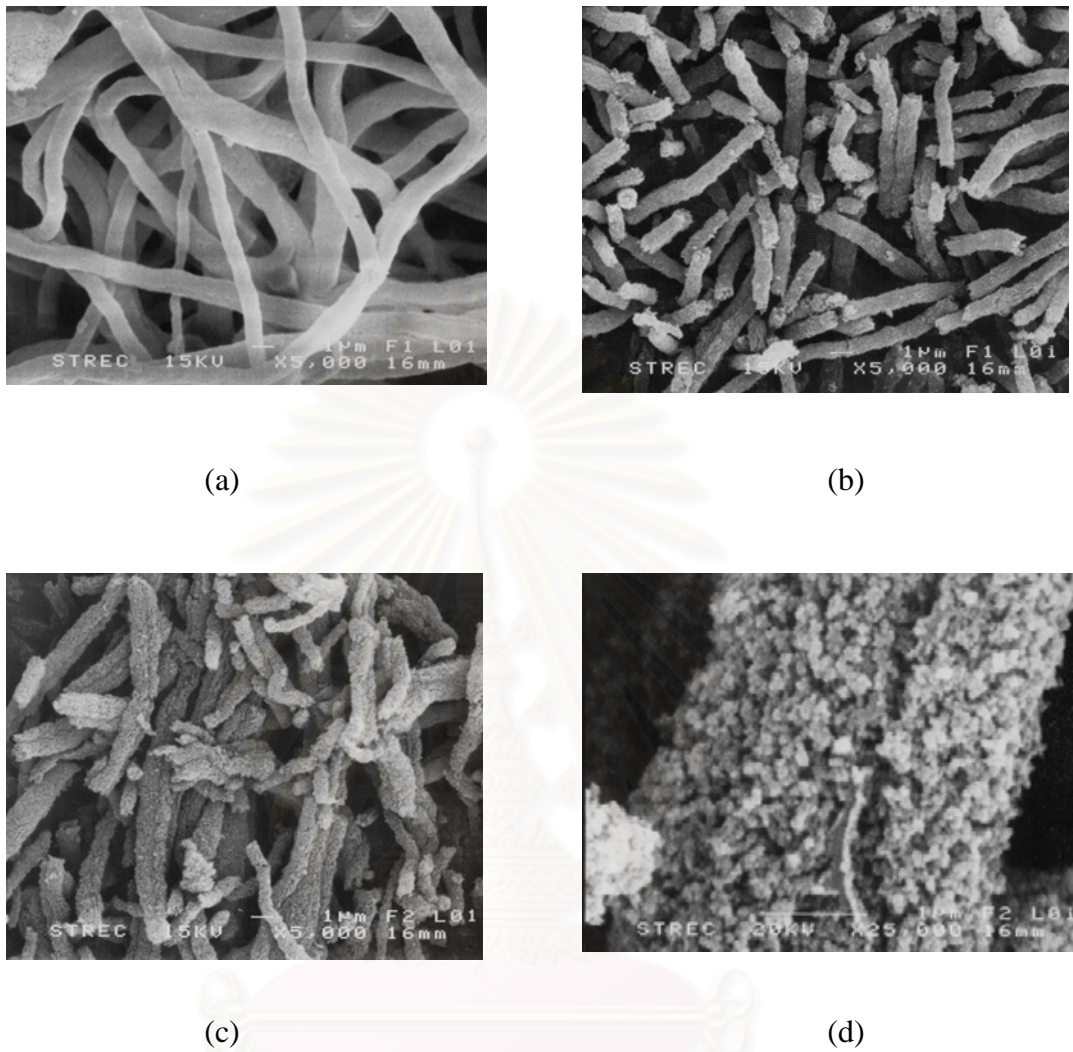
Figure 4.27 SEM micrographs of the products from the carbothermal reduction and nitridation of silica/carbon black composite fibers with various carbon-to-silica ratios: (a) 2:1, (b) 4:1, (c) 6:1 (low magnification) and (d) 6:1 (high magnification).
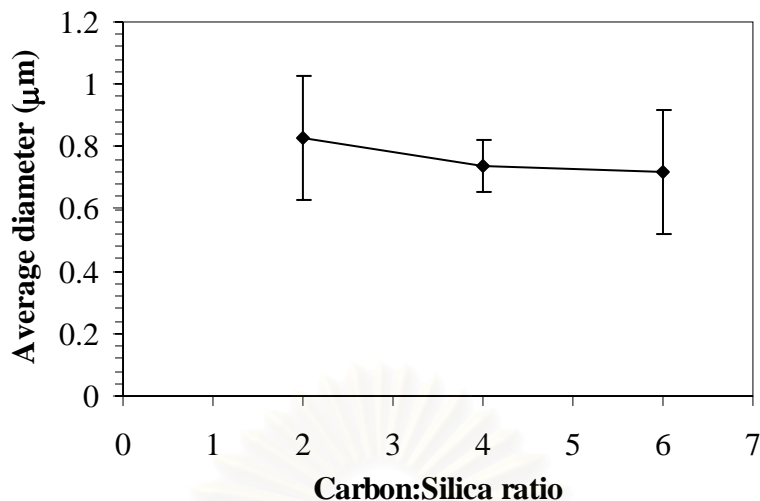
Figure 4.28 Average size and size distribution of products from the carbothermal reduction and nitridation of silica/carbon black composite fibers with various carbon-to-silica ratios.

(a)   (b)
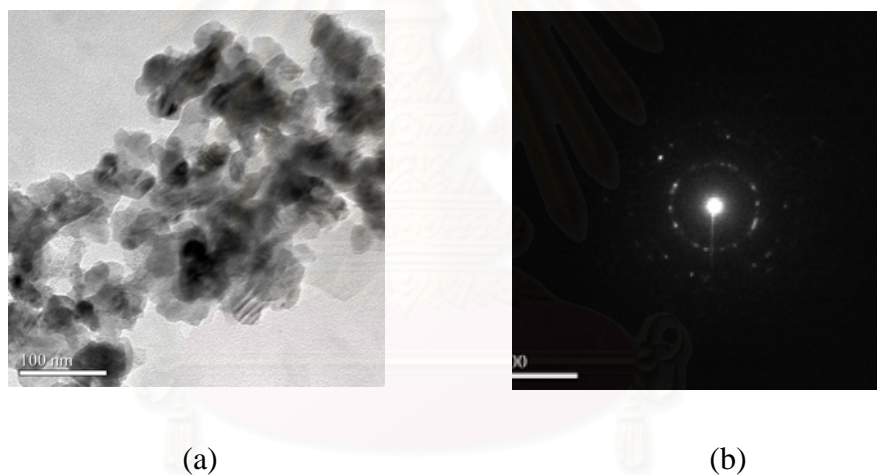
Figure 4.29 TEM micrographs of the product from the carbothermal reduction and nitridation of silica/carbon black composite fibers with carbon-to-silica ratio of 6:1 (a) TEM image and (b) SAED pattern.

Figure 4.29 reveals TEM image and the selected area electron diffraction pattern (SAED) of the nitrided product using carbon-to-silica ratio of 6:1. The TEM image clearly illustrates that the nitrided fiber is polycrystalline, consisting of silicon nitride and/or silicon carbide aggregated particles. Size of the primary particles forming into the fiber is about 40 nm. The sharp circular pattern in SAED image indicates that, although the fiber is polycrystalline, it has very high crystallinity. It is

suggested that each particle observed in TEM image is in fact single-crystal particle. This result supports the finding from SEM analyses and literature [Choi et al., 1999].

4.4.2 Effect of aging time

In this section, effect of aging time was also investigated in the same manner as previously discussed for silica/pyrolyzed PVP composite in section 4.3.2. The carbon-to-silica ratio in the composite fibers was kept at 2:1. During electrospinning, the applied voltage and the tip-to-target distance are fixed at 10 kV and 10 cm, respectively. Figure 4.30 shows SEM images of as-spun composite fibers with aging time of 0 and 3 days. It can be observed that the as-spun fibers generally have diameter in micrometered scale. The diameter of the as-spun composite fibers ranges from 0.6 to 0.7 μm, as shown in Table 4.2. The aging time slightly affects both size and size distribution of the as-spun fibers. The prolonged aging time in the spinning solution results in changes in viscosity, which subsequently affects the morphology of the fibers as discussed in prior section [Shao et al., 2003].

(a) (b)
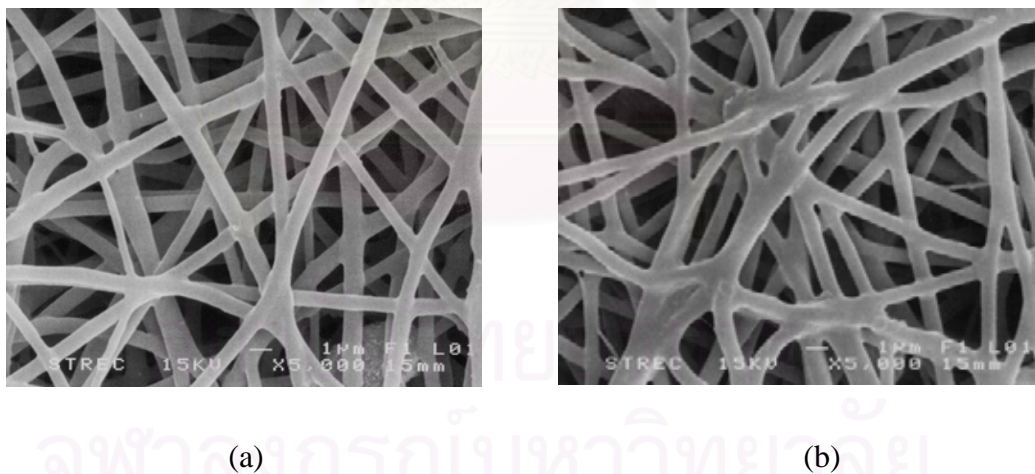
Figure 4.30 SEM micrographs of as-spun silica/carbon black composite fibers with various aging time: (a) no aging, (b) aging for 3 days.

Table 4.2 Average size and size distribution of as-spun silica/carbon black composite

fibers with various aging time.

Sample description	Average diameter (μm)	Standard deviation
No aging	0.636	0.117
Aging for 3 days	0.705	0.163

Figure 4.31 reveals the XRD patterns of nitrided products using silica/carbon

black composite fibers with different aging times as the starting materials. It can be

observed that aging time significantly affects the product. The obtained product with

3-day aging is predominantly silicon nitride, while the product without aging time is

silicon carbide. The prolonged aging time results in the increased extent of the

condensation reaction to form Si-O-Si bonding (refer to silica) according to sol-gel

process. This result is in agreement with the previous result obtained from

silica/pyrolyzed PVP composite section.
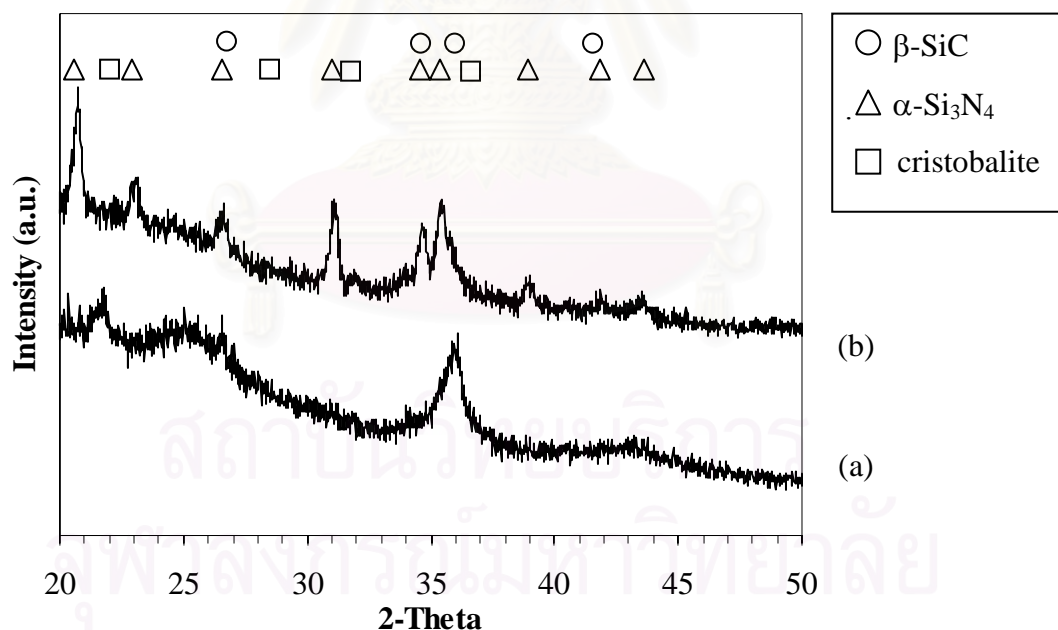
Figure 4.31 XRD patterns of products from the carbothermal reduction and

nitridation of silica/carbon black composite fibers with various

aging times: (a) no aging and (b) aging for 3 days.

Figure 4.32 reveals SEM micrographs from the nitrided products with different aging times. The nitridation of the composite fibers with 3-day aging time results in product with the same morphology as the nitrided product without aging time. However, the average diameter of the nitrided fibers with 3-day aging time is significantly smaller, as reported in Table 4.3. The SAED pattern (Figure 4.33b) shows that silicon nitride/silicon carbide fibers obtained from 3-day aging silica/carbon black composite is single crystalline, as clearly evidenced from the set of discrete dots in the pattern. No ringed diffraction pattern, which implies the polycrystalline nature of the sample, was observed.

(a)　　　　　　　　　　(b)　　　　　　　　　　(c)
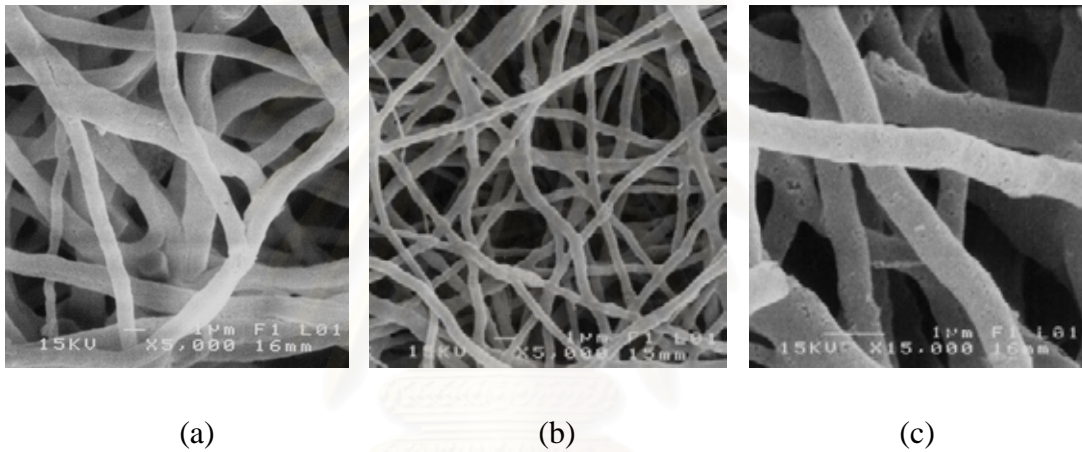
Figure 4.32 SEM micrographs of products from the carbothermal reduction and
　　　　　nitridation using carbon-to-silica ratio 2:1 with various aging time:
　　　　　(a) no aging, (b) aging for 3 days (low magnification) and
　　　　　(c) aging for 3 days (high magnification).

(a)   (b)

Figure 4.33 TEM micrographs of the product from the carbothermal reduction and nitridation of aged silica/carbon black composite fibers with carbon-to-silica ratio of 2:1 with 3-day aging time: (a) TEM image and (b) SAED pattern.

Table 4.3 Average size and size distribution of products from the carbothermal reduction and nitridation, carbon-to-silica ratio 2:1 with various aging time.

Sample description	Average diameter (μm)	Standard deviation
No aging	0.827	0.198
Aging for 3 days	0.419	0.073

For carbon-to-silica ratio of 4:1, it was found that aging time of the starting material had significant impact on the formation of silicon nitride as well. Figure 4.34 shows the XRD patterns of products from the nitridation of silica/carbon black composite fibers with different aging time. It is found that the obtained product with 3-day aging is silicon nitride/silicon carbide composite, while the product without aging time is silicon carbide. This result supports that the prolonged aging time bring about the formation of silicon nitride as discussed in prior section.

Figure 4.34 XRD patterns of products from the carbothermal reduction and
nitridation of silica/carbon black composite fibers, carbon-to-silica ratio
4:1 with various aging time: (a) no aging and (b) aging for 3 days.

(a) (b)

(c) (d)
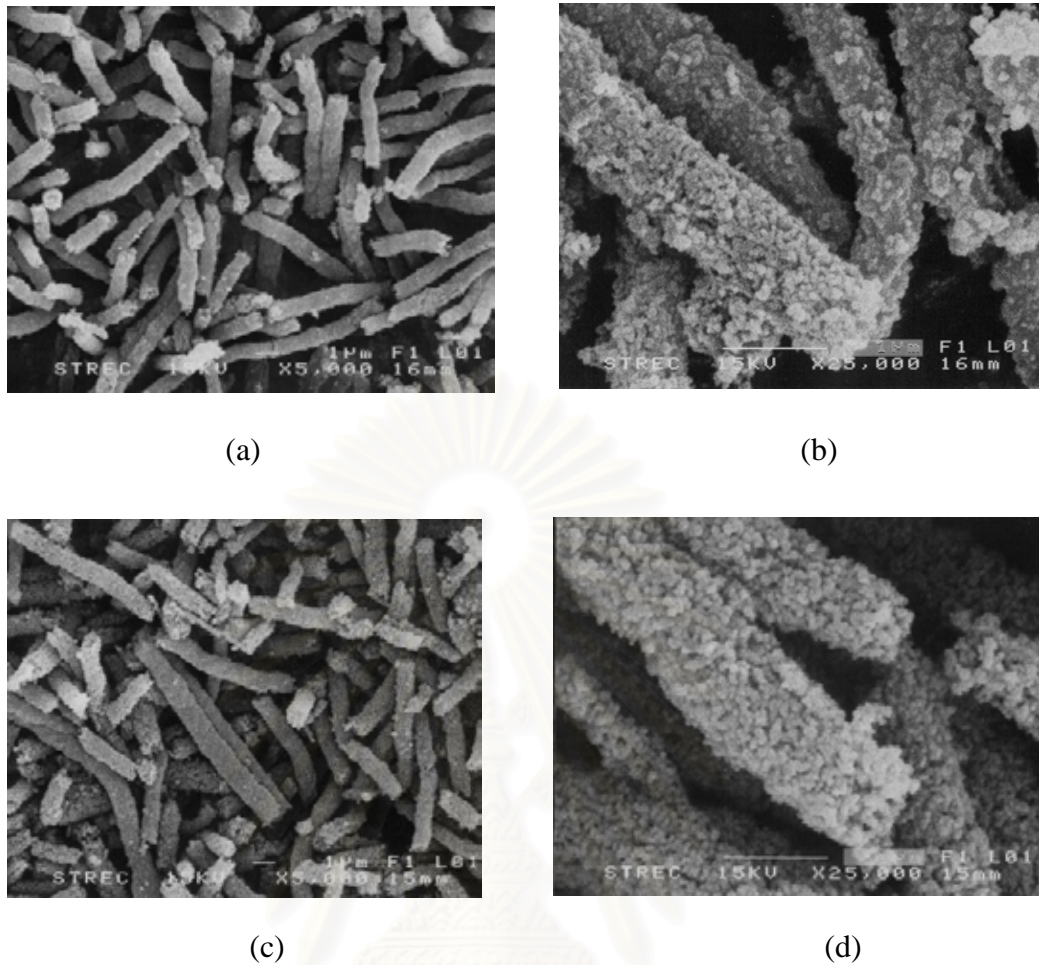
Figure 4.35 SEM micrographs of products from the carbothermal reduction and nitridation of silica/carbon black composite fibers with carbon-to-silica ratio 4:1 with various aging time: no aging ((a)-low magnification and (b)-high magnification) and aging for 3 days ((c)-low magnification and (d)-high magnification).

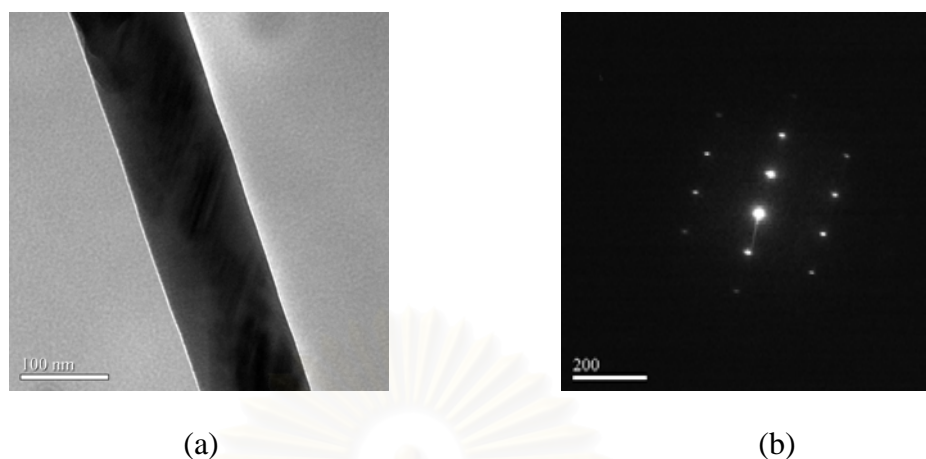Figure 4.35 reveals SEM micrographs of products from the carbothermal reduction and nitridation of silica/carbon black composite fibers with carbon-to-silica ratio of 4:1 using different aging time. The nitrided product of the composite fibers with 3-day aging time has the same morphology as the nitrided product without aging time. Some parts of fibers are broken off and become short fibers (Figure 4.35a,c), especially the nitrided fibers with 3-day aging time. Close investigation of SEM images reveals that the fibers are comprised of the number of aggregated primary particles (see in Figure 4.35d). Comparing with the nitrided product using the composite fibers with carbon-to-silica ratio of 2:1 and aged for 3 days (Figure 4.32b-

c), it is found that the nitridation of the fibers in this section (carbon-to-silica ratio of 4:1, 3-day aging) may occur via different mechanism, even though silicon nitride is formed in both cases. These results can be implied that the carbothermal reduction and nitridation mechanism also depends upon carbon-to-silica ratio. The change in the content of carbon, which acts as reducing agent for SiO production and as active sites for silicon nitride nucleation, obviously alters partial pressure of CO and SiO in the system as well as the growth of silicon nitride crystal. The effects of these factors have already been discussed in the previous sections.

Table 4.4 Average size and size distribution of products from the carbothermal reduction and nitridation of silica/carbon black composite fibers with carbon-to-silica ratio 4:1 using various aging time.

Sample description	Average diameter (µm)	Standard deviation
No aging	0.790	0.134
Aging for 3 days	0.660	0.108

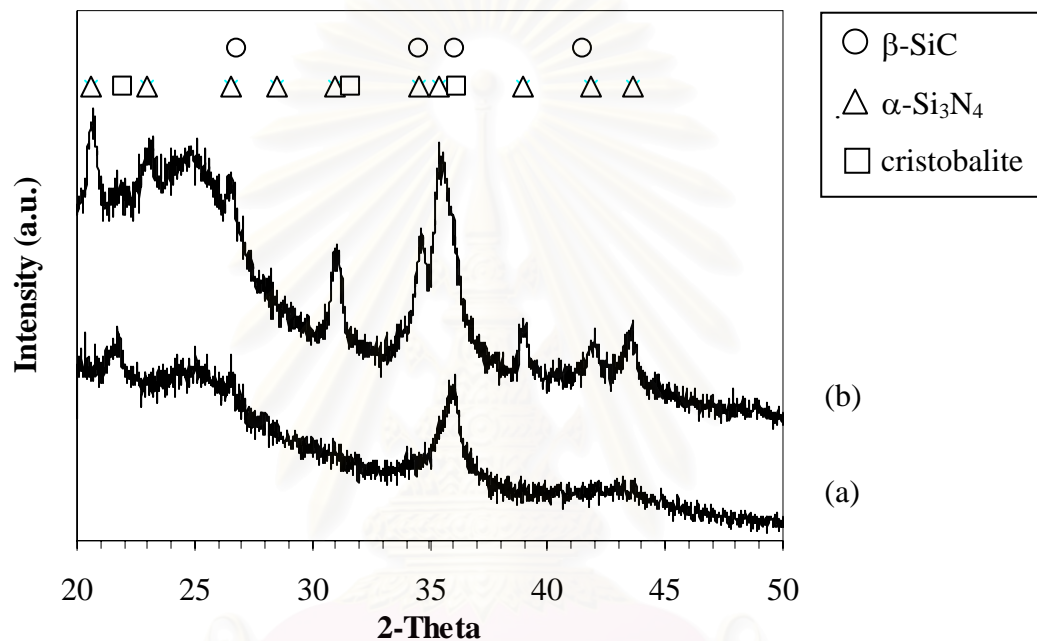Table 4.5 shows BET surface area of products from the carbothermal reduction and nitridation of silica/carbon black composite fibers with carbon-to-silica ratio 2:1 using different aging time. It is observed that the fibers after nitridation have much greater surface area than the as-spun fibers, because the nitrided fibers become porous due to the loss of reacted carbon (from the carbothermal reduction and nitridation) and the decomposition of PVP. Furthermore, in term of fiber size, the nitrided fibers with 3-days aging time are smaller in diameter than the nitrided fibers without aging time. Hence, they consequently have higher surface area. In addition, by comparing with the nitrided products using different carbon-to-silica ratio (Table 4.6), it can be found that the nitrided fibers using carbon-to-silica ratio of 4:1 have lower surface area than the ones using carbon-to-silica ratio of 2:1. This result is interesting since the fibers using carbon-to-silica ratio of 4:1 comprise of a number of aggregated primary particles, which seems to corresponding to a lot of surface area (see Figure 4.35d). However, in term of fiber size, the nitrided fibers using carbon-to-silica ratio of 4:1 have larger average diameter than the other (values are shown in Table 4.3-4.4. This result can be implied that the fiber size (refer to average diameter

of fiber) is the predominant factor which is corresponding to the surface area of fibers. Nevertheless, further study to investigate the impact on surface area is suggested.

Table 4.5 BET surface area of products from the carbothermal reduction and nitridation of silica/carbon black composite fibers with carbon-to-silica rato 2:1 using various aging time.

Sample description	BET surface area (m^2/g)
As-spun fibers (no aging)	1.677
Nitrided fibers (no aging)	85.840
Nitrided fibers (3-day aging)	116.648

Table 4.6 BET surface area of products from the carbothermal reduction and nitridation of silica/carbon black composite fibers with various carbon-to-silica ratios and aged for 3 days.

Sample description	BET surface area (m^2/g)
Nitrided fibers ($C:SiO_2=2:1$)	116.648
Nitrided fibers ($C:SiO_2=4:1$)	80.357

4.4.3 Effect of flow rate of reactant gas mixture

In this section, effect of flow rate of ractant gas mixture for the carbothermal reduction and nitridation was investigated by varying the overall flow rate of the reactant gas mixture (nitrogen mixed with 10% hydrogen) in the range of 30-70 l/h. The silica/carbon black composite fibers used in this experiment had carbon-to-silica ratio of 2:1. They were formed from the spinning solution that was aged for 3 days. The X-ray diffraction analysis of products from the nitridation with different flow rates of reactant gas is shown in Figure 4.36.
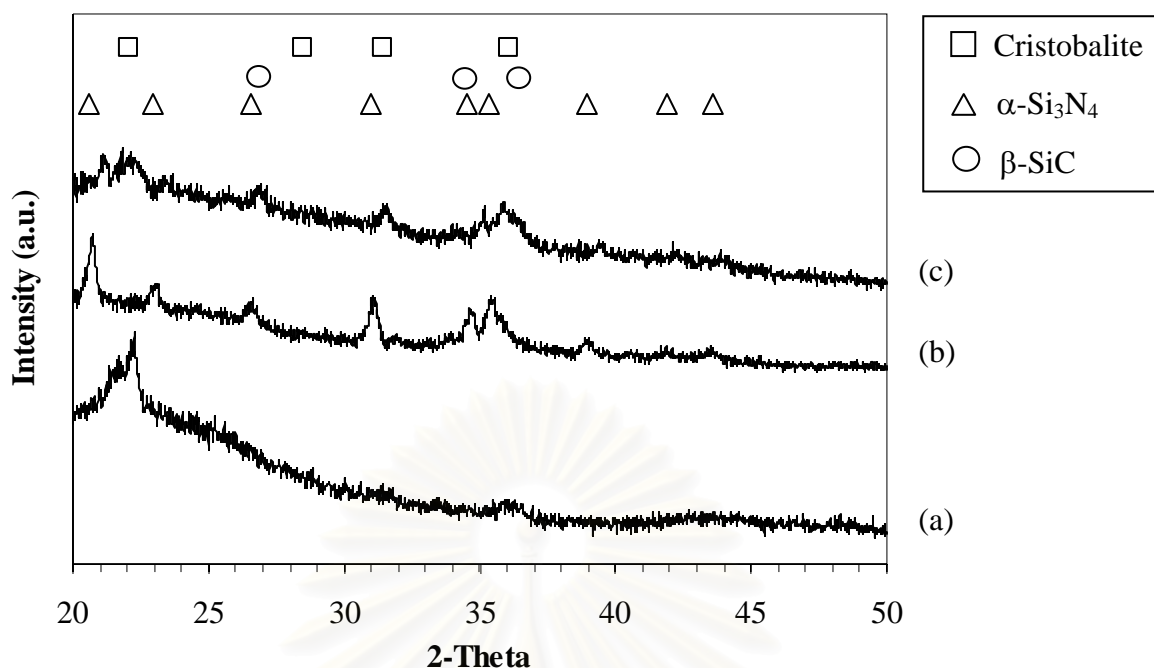
Figure 4.36 XRD patterns of products from the carbothermal reduction and nitridation of silica/carbon black composite fibers under various flow rates of reactant gas mixture: (a) 30 l/h, (b) 50 l/h and (c) 70 l/h.

From this result, it can be found that the nitrided products using the overall flow rate of 50/h and 70 l/h are silicon nitride, while the nitrided product using overall flow rate 30 l/h is cristobalite. It indicates that the overall flow rate of 30 l/h is not adequate for significant amount of SiO vapor to diffuse through the gas film mass transfer resistance to react according to the carbothermal reduction and nitridation process. The increased flow rate reduces the gas film mass transfer resistance for the diffusion of SiO vapor, generated at the surface of fibers, to bulk gas stream. Greater amount of SiO results in higher growth of silicon nitride according to vapor-solid (VS) mechanism. Moreover, since the vapor pressure of silicon monoxide vapor at temperature of system is very low, silicon monoxide vapor generated must be continuously removed by the flow of gas in the reactor, in order to sustain its production [Wotting et al.,]. Ekelund and Forslund (1992) have reported that small amounts of CO (~1%) produced from the system would obstruct the formation of silicon nitride. Hence, a higher flow rate of reactant gas would be favorable in maintaining low CO concentration and also provides more efficient reaction of SiO with N_2 to form silicon nitride.

CHAPTER V

CONCLUSIONS AND RECOMMENDATION

5.1   Conclusions

In this work, preparation of silica/carbon composite gel or electrospun fibers and the reaction to convert the composite into silicon nitride were investigated. The conclusions of the present research are the following:

1. Aging time of the starting composite materials is essential for silicon nitride formation.

2. Free carbon content in the composite is the important factor for converting pyrolyzed silica/PVP composite in form of fiber into silicon nitride.

3. Silicon nitride was successfully synthesized from electrospun silica/carbon black composite fibers via the carbothermal reduction and nitridation.

4. The carbothermal reduction and nitridation mechanism depends upon carbon-to-silica ratio in the composite.

5.2   Recommendations for Future Work

For synthesis of silicon nitride from electrospun silica/poly vinylpyrolidone and silica/carbon black composite nanofibers via the carbothermal reduction and nitridation process, effects of various factors, such as type of silica precursor, composition and aging time of silica in the composite, as well as conditions for the carbothermal reduction and nitridation, on yield of silicon nitride were investigated in this work. Some recommendations for future work are listed as follows:

(1) The type of carbon source should be further investigated. The other polymers besides PVP may be the appropriate carbon source for converting pyrolyzed silica/polymer composite fibers into silicon nitride.

(2) For the reaction to convert the composite into silicon nitride, the additional parameters including reaction time and reaction temperature should be investigated.

REFERENCES

Aelion, R., A. Loebel and F. Eirich. (1950). Journal of the American Chemical Society 72: 5705-5712

Alcala, M. D., J. M. Criado and C. Real. (2001). Infulence of the Experimental Conditions and the Grinding of the Starting Materials on the Structure of Silicon Nitride Synthesised by Carbothermal Reduction. Solid State Ionics 141-142: 657-661.

Arik, H. (2003). Systhesis of Si_3N_4 by the Carbothermal Reduction and Nitridation of Diatomite. Journal of the European Ceramic Society 23: 2005-2014.

Barbosa-Coutinho, E., V. M. M. Salim and C. P. Borges. (2003). Preparation of Carbon Hollow Fiber Membranes by Pyrolysis of Polyetherimide. Carbon 41 1707-1714.

Bergshoef, M. M. and G. J. Vancso. (1999). Transparent Nanocomposites with Ultrathin, Electrospun Nylon-4,6 Fiber Reinforcement. Advanced Materials 11(16): 1362-1365.

Bognitzki, M., W. Czado, T. Frese, A. Schaper, M. Hellwig, M. Steinhart, A. Greiner and J. H. Wendorff. (2001). Nanostructured Fibers via Electrospinning. Advanced Materials 13(1): 70-75.

Chandradass, J. and M. Balasubramanian. (2005). Sol-gel Based Extrusion of Alumina-Zirconia Fibres. Materials Science and Engineering A-Structural Materials Properties Microstructure and Processing 408(1-2): 165-168.

Charoenpinijkarn, W., M. Suwankruhasn, B. Kesapabutr, S. Wongkasemjit and A. M. Jamieson. (2001). Sol-Gel Processing of Silatranes. European Polymer Journal 37(7): 1441-1448.

Choi, J. Y., C. H. Kim and D. K. Kim. (1999). Carbothermic Synthesis of Monodispersed Spherical Si_3N_4/SiC Nanocomposite Powder. <u>Journal of the American Ceramic Society</u> 82(10): 2665-2671.

Choi, J. Y., Y. T. Moon, D. K. Kim and C. H. Kim. (1998). Pyrolytic Conversion of Spherical Organo-Silica Powder to Silicon Nitride under Nitrogen. <u>Journal of the American Ceramic Society</u> 81(9): 2294-2300.

Choi, S. S., S. G. Lee, S. S. Im, S. H. Kim and Y. L. Joo. (2003). Silica Nanofibers from Electrospinning/Sol-Gel Process. <u>Journal of Materials Science Letters</u> 22(12): 891-893.

Chroenpinijkarn, W., M. Suwankruhasn, B. Kesapabutr, S. Wongkasemjit and A. M. Jamieson. (2001). Sol-gel Processing of Silatranes. <u>European Polymer Journal</u> 37: 1441-1448.

Datton, J. (1986). Structure and Sodium Migration in Silicon Nitride Films. <u>Journal of the Electrochemical Society</u> 115: 865-868.

Deitzel, J. M., J. Kleinmeyer, D. Harris and N. C. B. Tan. (2001). The Effect of Processing Variables on the Morphology of Electrospun Nanofibers and Textiles. <u>Polymer</u> 42: 261-272.

Dieudonné, P., A. H. Alaoui, P. Delord and J. Phalippou. (2000). Transformation of Nanostructure of Silica Gels during Drying. <u>Journal of Non-Crystalline Solids</u> 262(1-3): 155-161.

Durham, S. J. P., K. Shanker and R. A. L. Drew. (1991). Carbothermal Synthesis of Silicon Nitride: Effect of Reaction Conditions. <u>Journal of the American Ceramic Society</u> 74(1): 31-37.

Ercin, D. and Y. Yurum. (2003). Carbonisation of Fir (Abies Bornmulleriana) Wood in an Open Pyrolysis System at 50–300 ∘C. <u>Journal of Analytical and Applied Pyrolysis</u> 67: 11-22.

Ertl, G., J. Weitkamp and H. Knèozinger. (1999). <u>Preparation of Solid Catalysts</u>. Weinheim ; Chichester, Wiley-VCH.

Frenot, A. and I. S. Chronakis. (2003). Polymer Nanofibers Assembled by Electrospinning. <u>Current Opinion in Colloid & Interface Science</u> 8(1): 64-75.

Fu, Z. P., J. Q. Ning, B. F. Yang, W. Wu, H. B. Pan and P. S. Xu. (2003). Stable Ultraviolet Photoluminescence from Sol-Gel Silica Containing Nano-Sized SiC/C Powder. <u>Materials Letters</u> 57(13-14): 1910-1914.

Hajji, P., L. David, J. F. Gerard, J. P. Pascault and G. Vigier. (1999). Synthesis, Structure, and Morphology of Polymer-Silica Hybrid Nanocomposites Based on Hydroxyethyl Methacrylate. <u>Journal of Polymer Science Part B-Polymer Physics</u> 37(22): 3172-3187.

Hatakeyama, F. and F. Kanzaki. (1990). Synthesis of Monodispersed Spherical B-Silicon Carbide Powder by a Sol-Gel Process <u>Journal of the American Ceramic Society</u> 73(7): 2107-2110.

Jayesh, D. and D. H. Reneker. (1995). Electrospinning Process and Applications of Electrospun Fibers. <u>Journal of Electrostatics</u> 35: 151-160.

K. Kamiya, T. Y. T. S., and K. Tanaka. (1990). Distribution of Carbon Particles in Carbon/SiO_2 Glass Composites Made from $CH_3Si(OC_2H_5)_3$ by the Sol-Gel Method. <u>Journal of Non-Crystalline Solids</u> 119: 14-20.

Kamiya, K., T. Y. T. Sano and K. Tanaka. (1990). Distribution of Carbon Particles in Carbon/SiO_2 Glass COmposites Made from $CH_3Si(OC_2H_5)_3$ by the Sol-Gel Method. <u>journal of Non-Crystalline Solids</u> 119: 14-20.

Kawai, C. and A. Yamakawa. (1998). Crystal Growth of Silicon Nitridfe Whiskers Through a VLS Mechanism Using SiO_2-Al_2O_3-Y_2O_3 Oxides as Liquid Phase. <u>Ceramic International</u> 24: 136-138.

Konjhodzic, D., H. Bretinger, U. Wilczok, A. Dreier, A. Ladenburger, M. Schmidt, M. Eich and F. Marlow. (2005). Low-n Mesoporous Silica Films: Structure and Properties. Applied Physics a-Materials Science & Processing 81(2): 425-432.

Li, D., Y. L. Wang and Y. N. Xia. (2004). Electrospinning Nanofibers as Uniaxially Aligned Arrays and Layer-by-Layer Stacked Films. Advanced Materials 16(4): 361-366.

Li, Y., L. Q. Liu and S. X. Dou. (1991). Kinetic of Si_3N_4 formation from rice hull. Journal Inorganic Material 6(1): 45.

Liou, T. H. and F. W. Chang. (1995). Kinetics of Carbothermal Reduction and Nitridation of Silicon Dioxide Carbon Mixture. Industrial & Engineering Chemistry Research 34(1): 118-127.

Martos, C., F. Rubio, J. Rubio and J. L. Oteo. (2003). Infiltration of SiO_2/SiOC Nanocomposites by a Multiple Sol Infiltration-Pyrolysis Process. Journal of Sol-Gel Science and Technology. 26: 511-516.

Nicolaon, G. A. and S. J. Teichner. (1968). Bulletin de la Societe Chimique de France.: 1906.

Rao, A. V. and S. D. Bhagat. (2004). Synthesis and Physical Properties of TEOS-Based Silica Aerogel Prepared by Two step (Acid-Base) Sol-Gel Process. Solid State Sciences 6: 945-952.

Reneker, D. H., A. L. Yarin, H. Fong and S. Koombhongse. (2000). Bending Instability of Electrically Charged Liquid Jets of Polymer Solutions in Electrospinning. Journal of Applied Physics 87(9): 4531-4547.

Riley, F. L. (2000). Silicon nitride and related materials. Journal of the American Ceramic Society 83(2): 245-265.

Segal, D. L. (1985). Developments in the Synthesis of Silicon Nitride. <u>Chemistry and Industry</u> 16: 544-545.

Shao, C. L., H. Y. Kim, J. Gong, B. Ding, D. R. Lee and S. J. Park. (2003). Fiber Mats of Poly(Vinyl Alcohol)/Silica Composite via Electrospinning. <u>Materials Letters</u> 57(9-10): 1579-1584.

Soeg, I. S. and C. H. Kim. (1993). Preparation of Monodispersed Spherical Silicon Carbide by the Sol-Gel Method. <u>Journal of Materials Science</u> 28: 3277-3282.

Tamon, H., T. Kitamura and M. Okazaki. (1998). Preparation of Silica Aerogel from TEOS. <u>Journal of Colloid and Interface Science</u> 197(2): 353-359.

Tongpool, R. and S. Jindasuwan. (2005). Sol-Gel Processed Iron Oxide-Silica Nanocomposite Films as Room-Temperature Humidity Sensors. <u>Sensors and Actuators B-Chemical</u> 106(2): 523-528.

Wang, H. and Y. N. Dai. (1996). The Charactor of Reaction Kinetics for Producing Ultrafine Si_3N_4 Powder with Rice Husks. <u>Refractories</u> 30(2): 77.

Watthanaarun, J., V. Pavarajarn and P. Supaphol. (2005). Titanium (IV) Oxide Nanofibers by Combined Sol-Gel and Electrospinning Techniques: Preliminary Report on Effects of Preparation Conditions and Secondary Metal Dopant. <u>Science and Technology of Advanced Materials</u> 6(3-4): 240-245.

Weimer, A. W., G. A. Eisman, D. W. Susnitzky, D. R. Beaman and J. W. McCoy. (1997). Mechanism and Kinetics of the Carbothermal Nitridation Synthesis of Alpha-Silicon Nitride. <u>Journal of the American Ceramic Society</u> 80(11): 2853-2863.

White, D. A., S. M. Oleff, R. D. Boyer, P. A. Budinger and J. R. Fox. (1987). Preparation of Silicon Carbide from Organosilicon Gels: I, Synthesis and Characterization of Precursors Gels. <u>Advanced Ceramic Material</u> 2: 45-52.

Wotting, G., H. A. Linder. and E. Gugel. (1996). Silicon Nitride Valves for Automotive Engines. <u>Advanced Ceramic Material, Key Eng, Mater</u> 122-124: 283-293.

Zhang, G., W. Kataphinan, R. Teye-Mensah, P. Katta, L. Khatri, E. A. Evans, G. G. Chase, R. D. Ramsier and D. H. Reneker. (2004). Electrospun Nanofibers for Potential Space-Based Applications. <u>Materials Science and Engineering B</u> 116: 353-358.
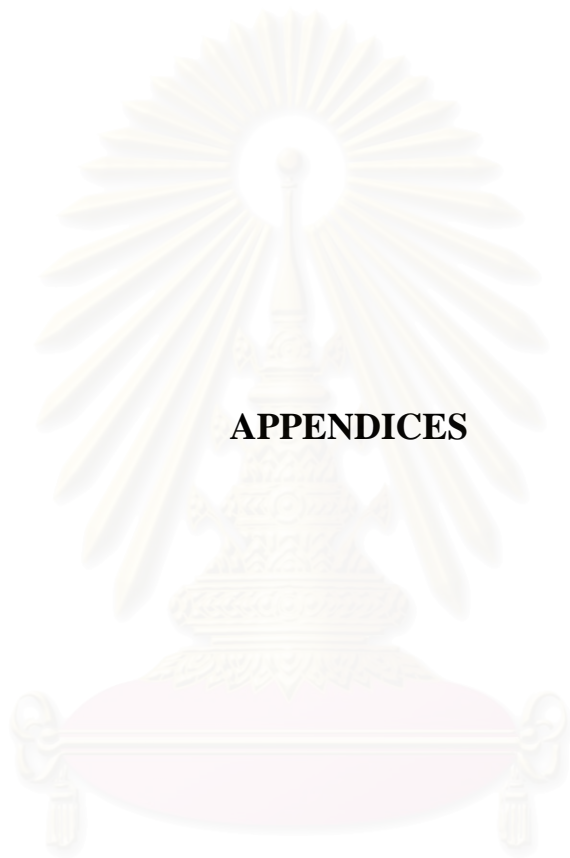
APPENDICES

APPENDIX A

CALCULATION OF AMOUNT OF CARBON FOR
SILICA/CARBON COMPOSITE

For calculation method, carbon source, i.e. l-PVP, h-PVP and carbon black were employed for preparation of silica/carbon composite

A1 Silica/PVP composite using APTMS as silica precursor

5 g of APTMS

$\downarrow$ ÷ 179 (M_w of TEOS)

0.0279 mol of APTMS

$\downarrow$

0.0279 mol of Si

$\downarrow$ Assume 1mol of Si = 1 mol of SiO_2

0.0279 mol of SiO_2

$\downarrow$ Carbon-to-SiO_2 ratio = 4:1

0.112 mol of carbon

$\downarrow$

For l-PVP (Mw 10,000), (C_6H_9No)$_n$, n~100	For h-PVP (Mw 1,300,000), (C_6H_9No)$_n$, n~11,711
$\downarrow$ 540 mol of carbon = 1 mol of l-PVP	$\downarrow$ 70,266 mol of carbon = 1 mol of h-PVP
0.000207 mol of l-PVP	1.593×10^{-6} mol of h-PVP
$\downarrow$ x 10,000 (Mw of l-PVP)	$\downarrow$ x 1,300,000 (Mw of h-PVP)
2.07 g of l-PVP[*]	2.07 g of h-PVP[*]

\
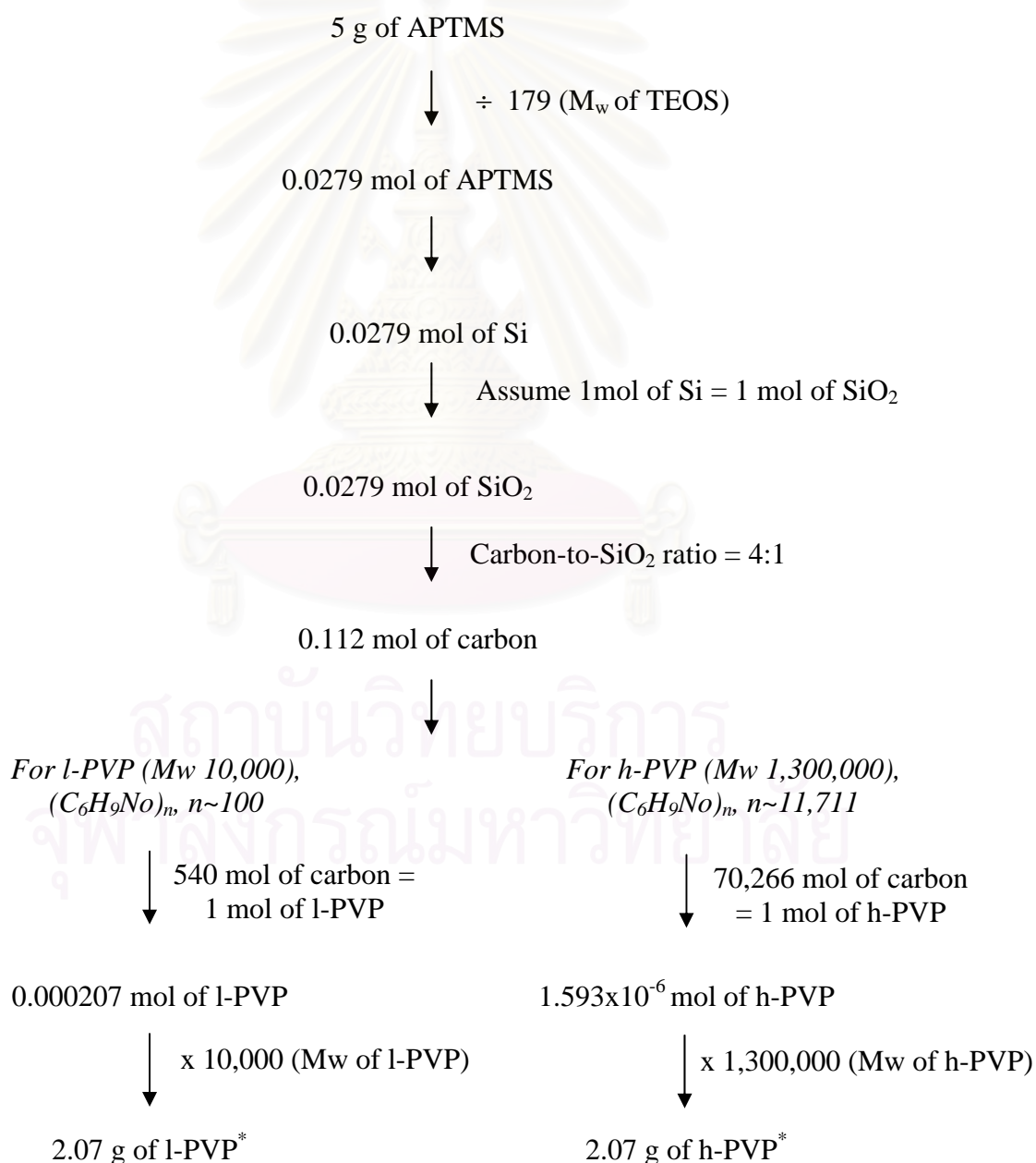
For mixed PVP (l-PVP and h-PVP in the ratio of 1:5) = 2.07 + (0.2)(2.07) = 2.484 g of mixed PVP[*]

A2 Silica/carbon black composite using APTMS as silica precursor

5 g of APTMS

↓ ÷ 179 (M_w of TEOS)

0.0279 mol of APTMS

↓ 1 mol of Si = 1 mol of APTMS

0.0279 mol of Si

↓ Assume 1mol of Si = 1 mol of SiO$_2$

0.0279 mol of SiO$_2$

↓ Carbon-to-SiO$_2$ ratio = 4:1

0.112 mol of carbon

↓ x 12 (Mw of carbon)

1.344 g of carbon black[*]

\
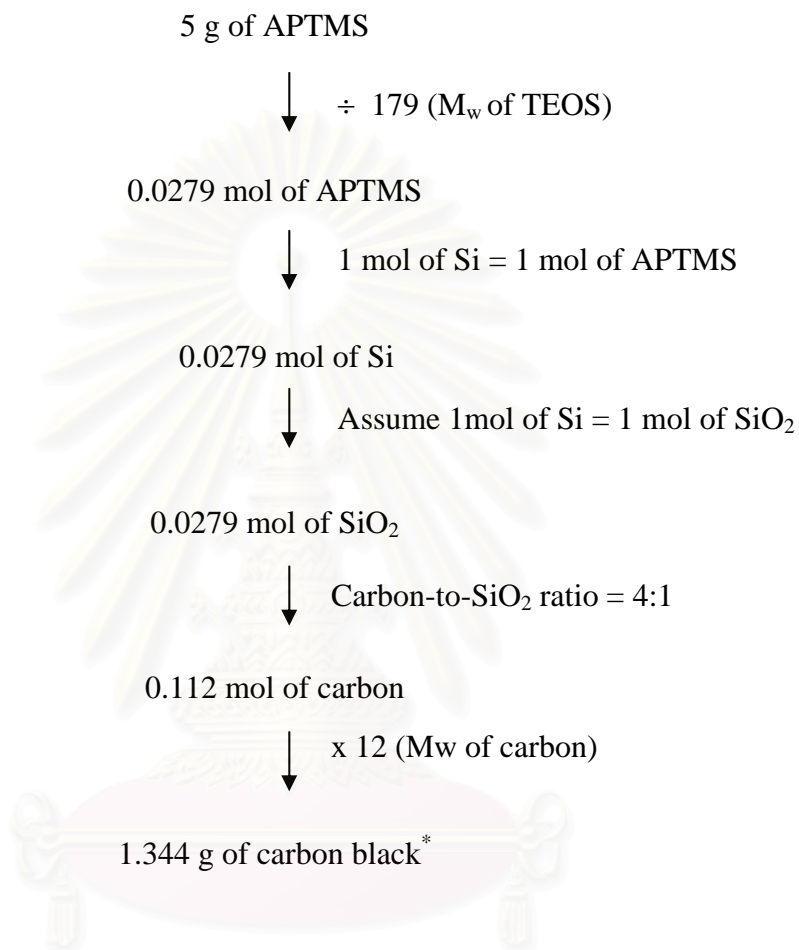
APPENDIX B

EDX MAPPING OF PYROLYZED-NITRIDED SILICA/CARBON COMPOSITE
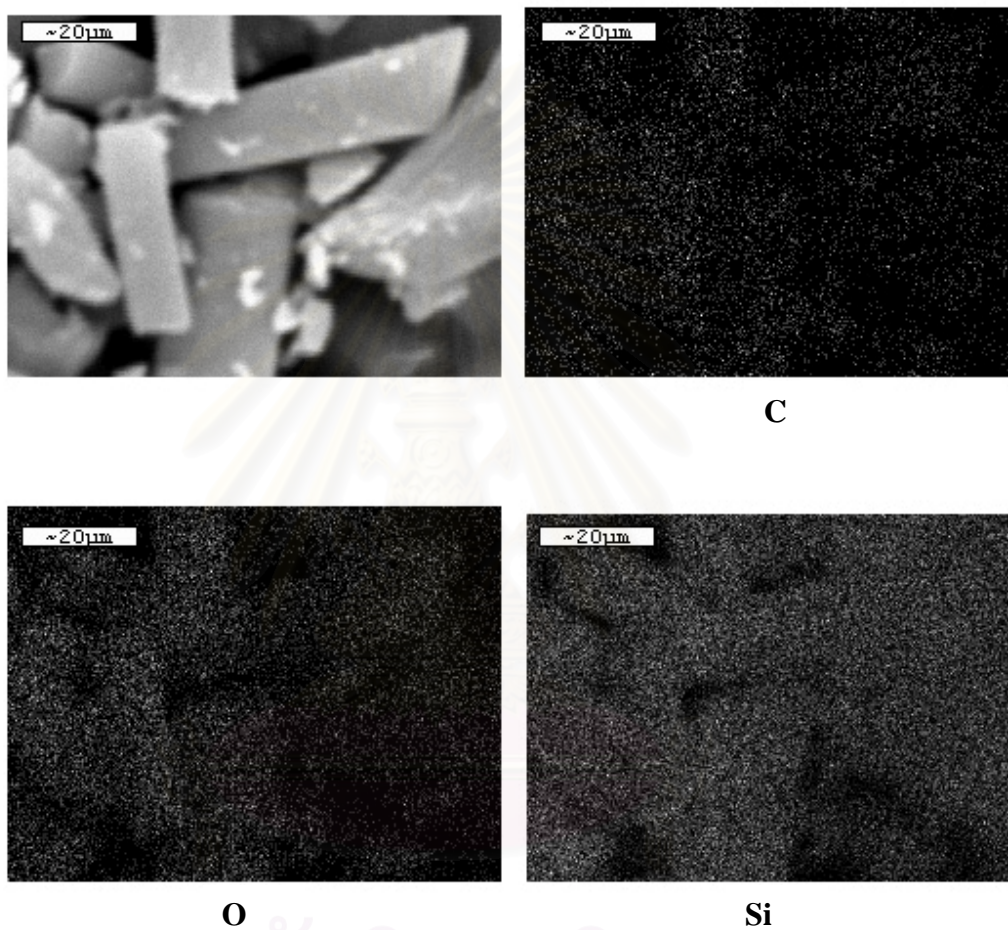
Figure B1 EDX mapping of pyrolyzed silica/mixed PVP composite gel from pyrolysis at 600°C for 6h without aging time as the starting material.
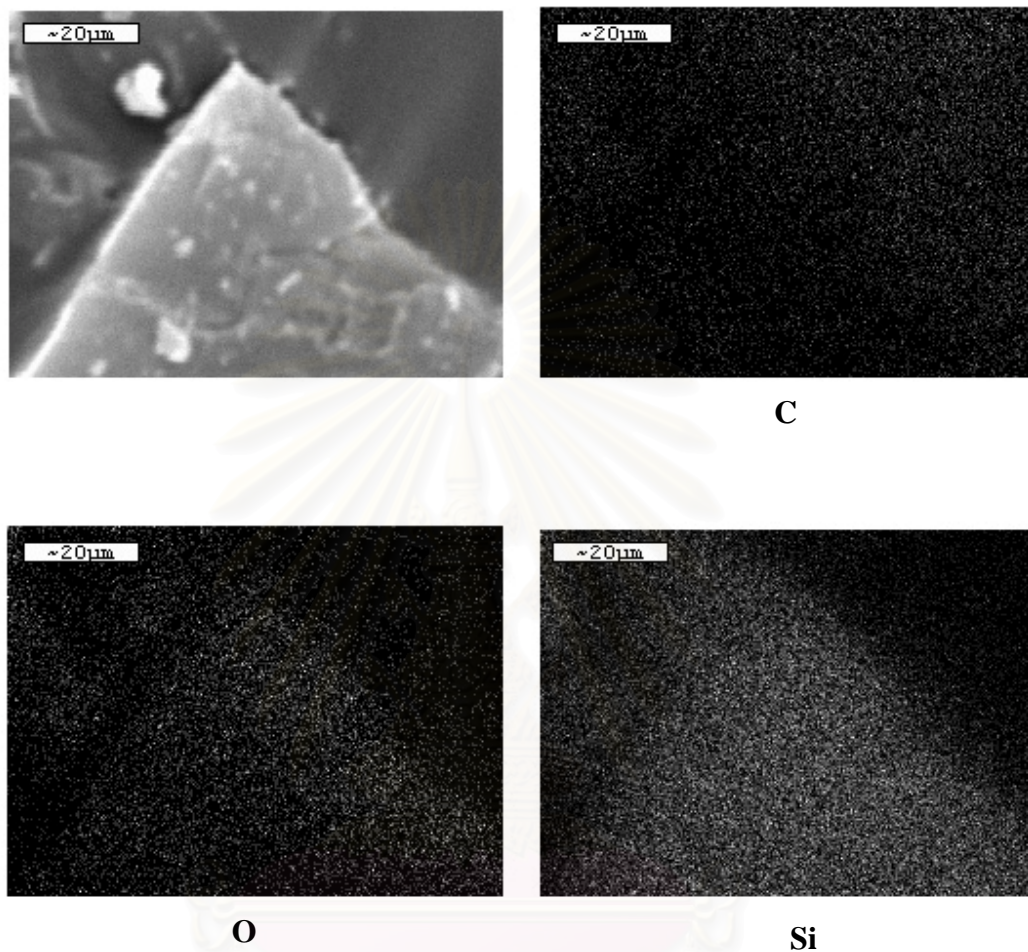
Figure B2 EDX mapping of pyrolyzed silica/mixed PVP composite fibers from pyrolysis at 600°C for 6h with 3-day aging time as the starting material.
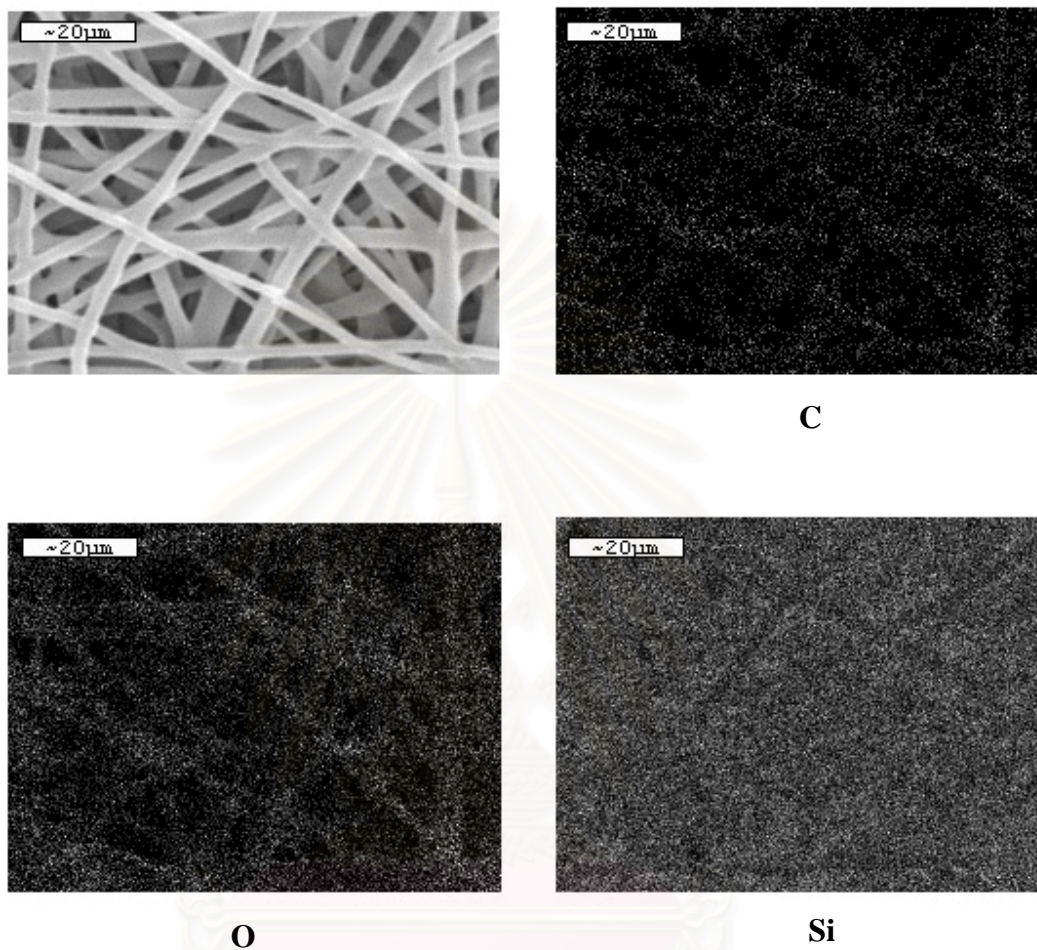
Figure B3 EDX mapping of product from nitridation at $1,450^{o}C$ for 6h using pyrolyzed silica/mixed PVP composite fibers with aging 3days as the starting material.

C

N

Si
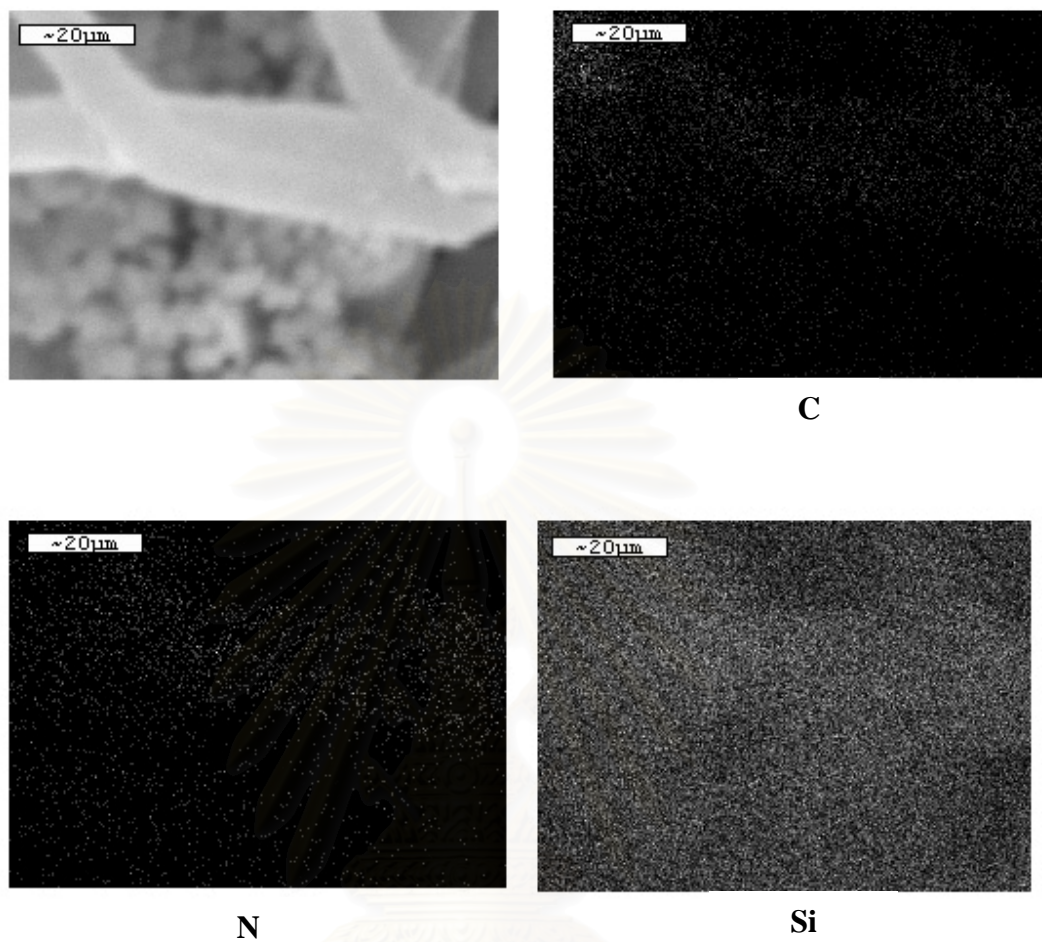
Figure B4 EDX mapping of product from nitridation at 1,450°C for 6h using silica/carbon black composite fibers, carbon-to-silica ratio 2:1 without aging time as the starting material.
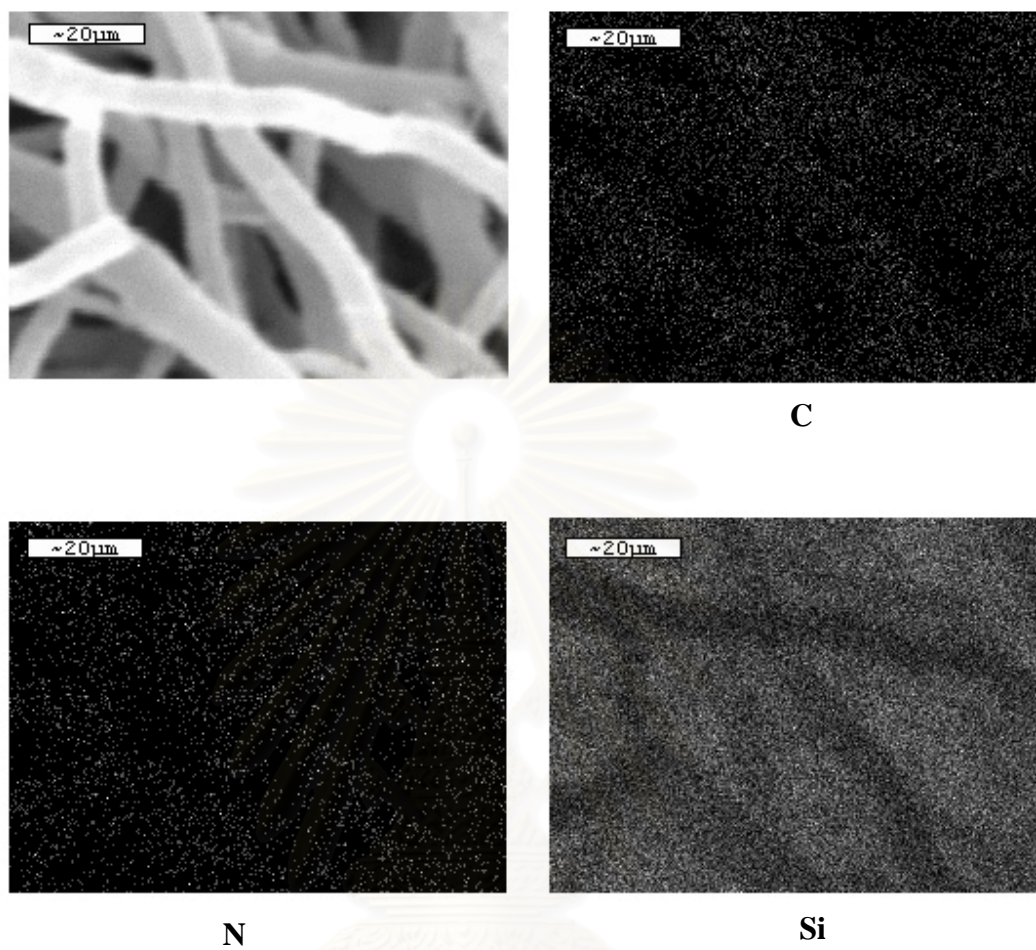
Figure B5 EDX mapping of product from nitridation at 1,450°C for 6h using silica/carbon black composite fibers, carbon-to-silica ratio 2:1 with aging 3 days as the starting material.

APPENDIX C

FT-IR SPECTRA OF AS-SPUN-NITRIDED SILICA/CARBON BLACK COMPOSITE FIBERS
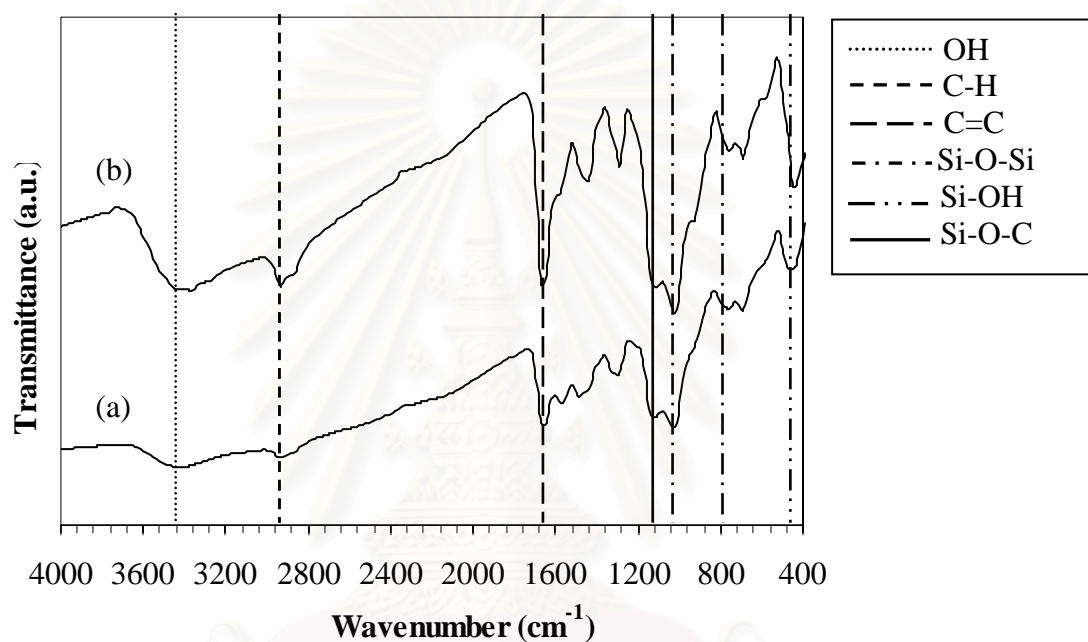
Figure C1 FT-IR spectra of as-spun silica/carbon black composite fibers using carbon-to-silica ratio 2:1 with various aging time: (a) no aging, (b) aging for 3 days.
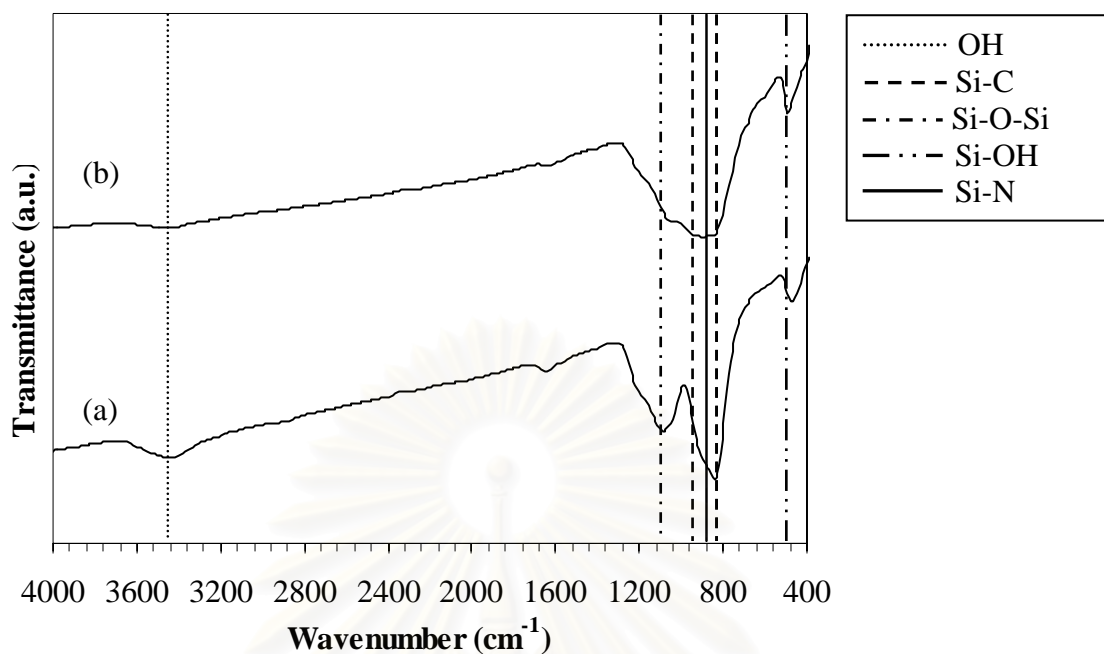
Figure C2 FT-IR spectra of products from the carbothermal reduction and nitridation
of silica/carbon black composite fibers using carbon-to-silica ratio 2:1
with various aging time: (a) no aging, (b) aging for 3 days.
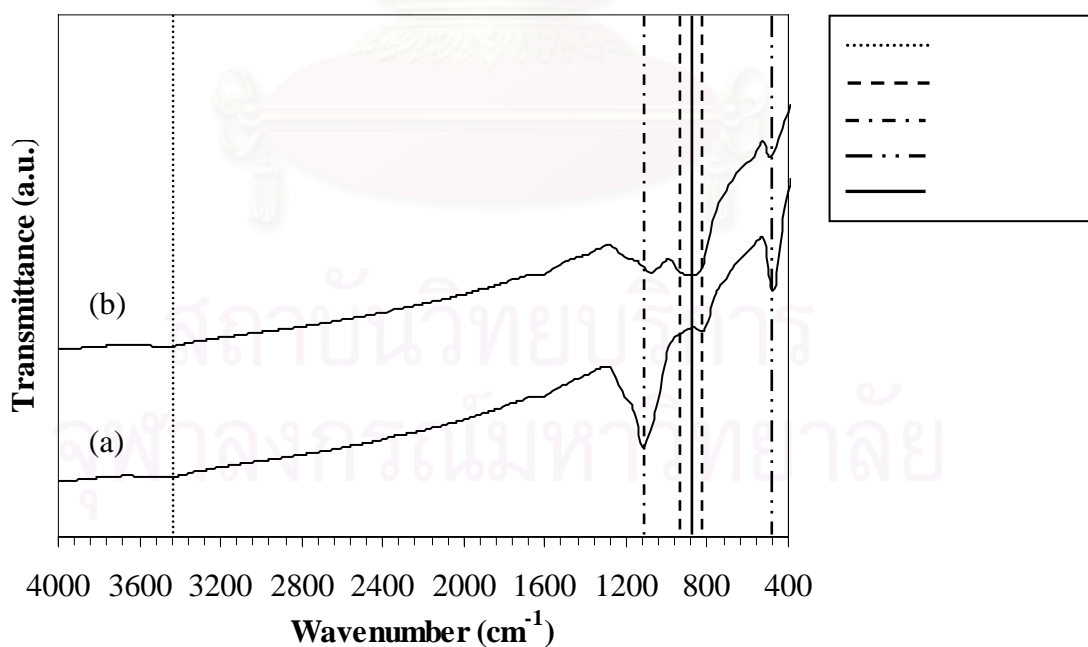
Figure C3 FT-IR spectra of products from the carbothermal reduction and nitridation
of silica/carbon black composite fibers using carbon-to-silica ratio 4:1
with various aging time: (a) no aging, (b) aging for 3 days.

APPENDIX D

TGA ANALYSIS OF PVP
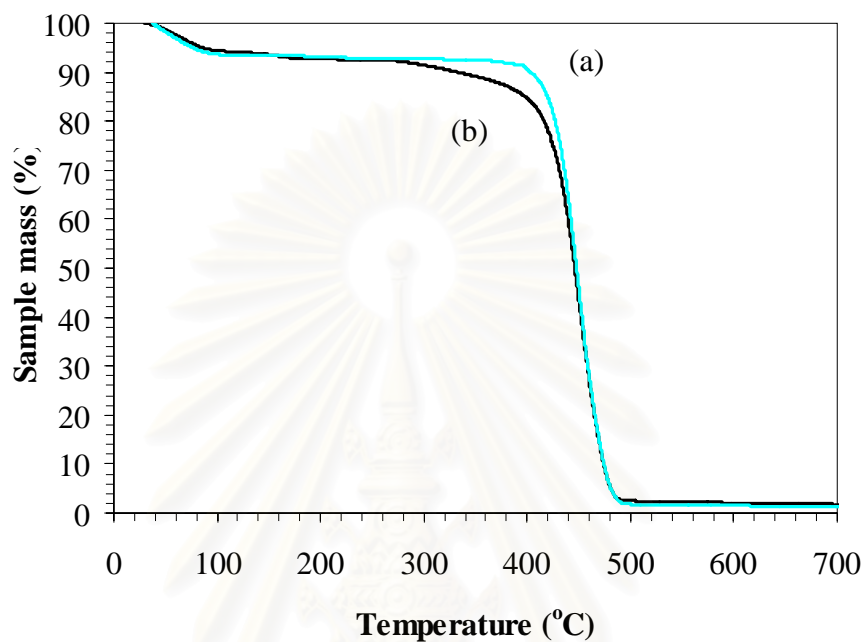
Figure D1 TGA analysis of PVP under N_2 atmosphere using various kinds of PVP:
(a) h-PVP and (b) l-PVP.

APPENDIX E

LIST OF PUBLICATION

1. Rungroj Chanchairoek, Piyasarn Praserthdam, Pitt Supaphol and Varong Pavarajarn, "Effect of Synthesis and Calcination Parameters on Cristobalite Nanofibers by Combined Sol-Gel and Electrospinning Techniques", Proceedings of the Regional Symposium on Chemical Engineering 2005, Hanoi, Vietnam, November 30th-December 2nd, 2005.

\

Effect of Synthesis and Calcination Parameters on Cristobalite Nanofibers by Combined Sol-Gel and Electrospinning Techniques

Rungroj Chanchairoek [a],[*], Piyasan Praserthdam [a], Pitt Supaphol [b],[+] and Varong Pavarajarn[a],[+]

[a] Center of Excellence on Catalysis and Catalytic Reaction Engineering,

Department of Chemical Engineering, Faculty of Engineering, Chulalongkorn University, Bangkok 10330 Thailand.

[b] Technological Center for Electrospun Fibers and the Petroleum and Petrochemical College, Chulalongkorn University, Bangkok 10330, Thailand.

[*] Presenting author

[+] Corresponding author (Tel: +66-02-2186890, Fax: +66-02-2186877)

Email addresses: pitt.s@chula.ac.th (P. Supaphol), fchvpv@eng.chula.ac.th (V. Pavarajarn)

Abstract

Silica/polyvinyl alcohol (PVA) composite nanofibers were prepared from aqueous solution containing PVA and tetraethylorthosilicate (TEOS) via electrospinning technique. Upon the heat treatment at 600°C, the PVA/silica composite fibers were converted into amorphous silica nanofibers having diameter in the range of 200-400 nm. The spun fibers had chemical and thermal stability as well as high specific surface area, suitable for various kinds of application. Further calcination at temperature of 1200°C resulted in phase transformation of amorphous silica to cristobalite, while the shape of the product still remained as fibers. The average diameter of the obtained cristobalite fibers increased to 400-600 nm. and coalescence of fibers was observed. Various techniques such as X-ray diffraction (XRD), infrared spectroscopy (IR), scanning electron microscope (SEM), and thermogravimetric analysis (TGA) were employed to investigated physical and chemical properties of the obtained silica nanofibers. The effects of TEOS concentration, applied electrical potential as well as the calcination conditions on properties of the fibers were also discussed.

Keywords

Silica; Cristobalite; Nanofiber; Electrospinning.

Introduction

Cristobalite is a common crystalline form of silica. It is one of the most stable phase that can be obtained by phase transformation from amorphous silica or quartz at high temperature 1, 2.. Cristobalite has been widely used in several applications such as filler for composite materials 3. and filter 2..

Recently, materials with nanofiber structure have attracted considerable attention because of some novel physical and chemical properties due to the structural and size effects. They are expected to be applicable as reinforcing materials 4., filters 5. and templates for preparation of nanotubes 5.. Fabrication of such structure can be achieved by simple combination of sol-gel method and electrospinning technique.

Electrospinning is a straightforward technique commonly used to produce polymer nanofibers. The technique relies of the fact that a charged jet of polymer solution or polymer melt can be ejected, when electrical force at the surface of liquid droplet overcomes the surface tension. The electrical force greatly elongates the jet to become very thin. Ultimately, the solvent evaporates, or the melt solidifies, resulting in very long ultrathin fibers collected in form of non-woven mat at the collector.

In recent years, electrospinning technique has been adopted to synthesize ceramic nanofibers. Amorphous silica nanofibers with diameter in range of 200 to 400 nm have been prepared from poly (vinyl) alcohol (PVA)/silica composite precursors, using tetraethoxysilane (TEOS) as a source for silicon 6.. Silica ultrafine fibers could also be electrospun directly from silica sol without the aid of

Regional Symposium on Chemical Engineering 2005
*Hanoi Horison Hotel, Hanoi, VIETNAM * November 30th - December 2nd, 2005*

240

polymer or gelator 7.. In this work, synthesis of cristobalite nanofibers from the combined sol-gel and electrospinning techniques was investigated. The effects of spinning conditions as well as the calcination on the obtained fibers were also discussed.

Materials and Methods

The solution used in the electrospinning procedures was prepared by mixing 5 g of TEOS, 0.05 ml of 37% by volume hydrochloric acid and 5 ml of distilled water at room temperature for 3 h. Then, 10 g of PVA aqueous solution, at predetermined concentration of PVA in the range of 10-14 wt.%, was dropped into the mixture and stirrer for 1 h. The resulting solution is referred as the electrospinning solution.

The electrospinning apparatus is consisted of a high-voltage power supply (Gamma High Voltage Research ES30PN), a plastic syringe containing the electrospinning solution equipped with a 20-gauge stainless steel needle, and an aluminum foil used as a collective screen. The needle is connected to the negative electrode of the power supply, while the aluminum collector is attached with the grounding electrode. Upon the application of high electrical potential, in the range of 8 to 20 kV, across the electrodes, the jet of the spinning solution was ejected toward the collector, which was placed 10 cm below the tip of the needle (referred as tip-to-target distance). The collection time was fixed at 30 minutes.

The as-spun fibers collected on the collector plate were calcined in a box furnace at temperature in the range of 600 to 1200°C for 3 h. The morphology and size of the as-spun fibers as well as the calcined fibers were observed on a JEOL JSM 5800 scanning electron microscope (SEM). Crystalline phases of the fibers were identified by a Siemens D5000 X-ray diffractometer (XRD) operated with CuK_α radiation. The products were also analyzed by using Fourier transform infrared spectroscopy (FT-IR) and thermogravimetric analyzer (TGA).
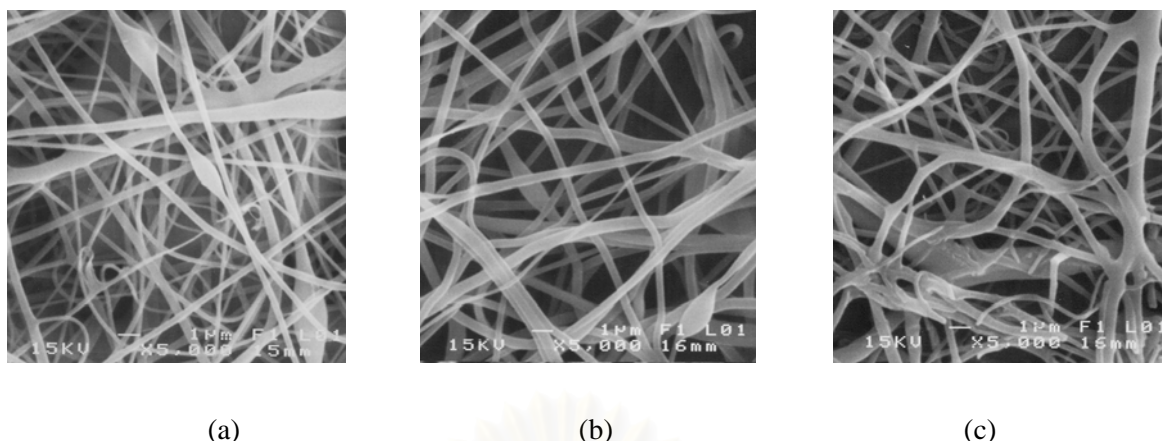
Results and Discussion

Effects of Electrospinning Conditions on Fibers

(a) (b) (c)
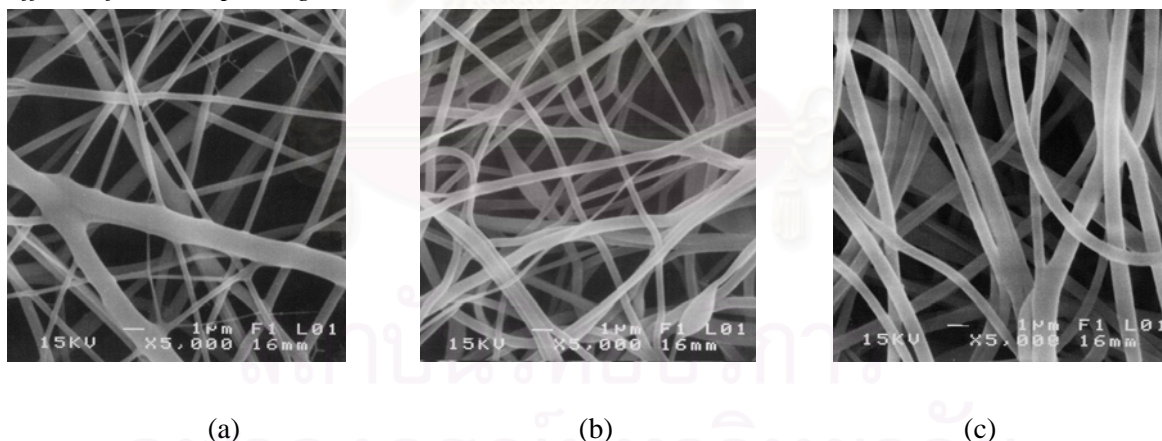
Figure 1- SEM micrographs of the as-spun pre-calcined PVA/silica composite fibers with different PVA contents: (a) 12 wt.%; (b) 14 wt.%; (c) 16 wt.%.

Figure 1 shows SEM images of as-spun PVA/silica composite fibers, using various concentration of PVA. The applied voltage and the tip-to-target distance are fixed at 8 kV and 10 cm, respectively. It can be seen that the obtained fibers generally have diameter in nanometer scale. The diameter of the as-spun composite fibers with 12 wt.% PVA ranges from 200 to 400 nm, while the size of the fibers with 16 wt.% PVA is in the range of 200 nm to 1 μm. The increase in PVA content in the spinning solution results in fibers with broader size distribution. This is in agreement with the findings in our previous report on PVP/titania composite fibers that the increased fraction of polymer in the spinning solution results in changes in viscosity, which subsequently affects the morphology of the spun fibers 8..

Regional Symposium on Chemical Engineering 2005
*Hanoi Horison Hotel, Hanoi, VIETNAM * November 30th - December 2nd, 2005*

241

(a) (b) (c)

Figure 2- SEM micrographs of the as-spun pre-calcined PVA/silica composite fibers produced by different applied voltages: (a) 8 kV; (b) 12 kV; (c) 20 kV.

The effect of applied voltage on the fiber structure is shown in Figure 2, whereas the concentration of PVA is kept at 12 wt.%. It was found that the fibers are less uniform when the applied voltage was increased. More junction and bead formation was observed at applied voltage of 20 kV. This result is in contrast with the observation from the electrospinning of PVP/titania nanofibers 8.. It is suggested that the increasing applied voltage associated with the viscosity of the spinning solution may cause instability of the jet. Moreover, since water employed as solvent in this work is less volatile than ethanol used in our previous work, the spun fibers require longer time to solidify. Therefore, it is possible that the rearrangement and fusing of crossing fibers can take place, especially when diameter of the spun fiber is small.

Properties of the Calcined Fibers

(a) (b)

(c) (d)
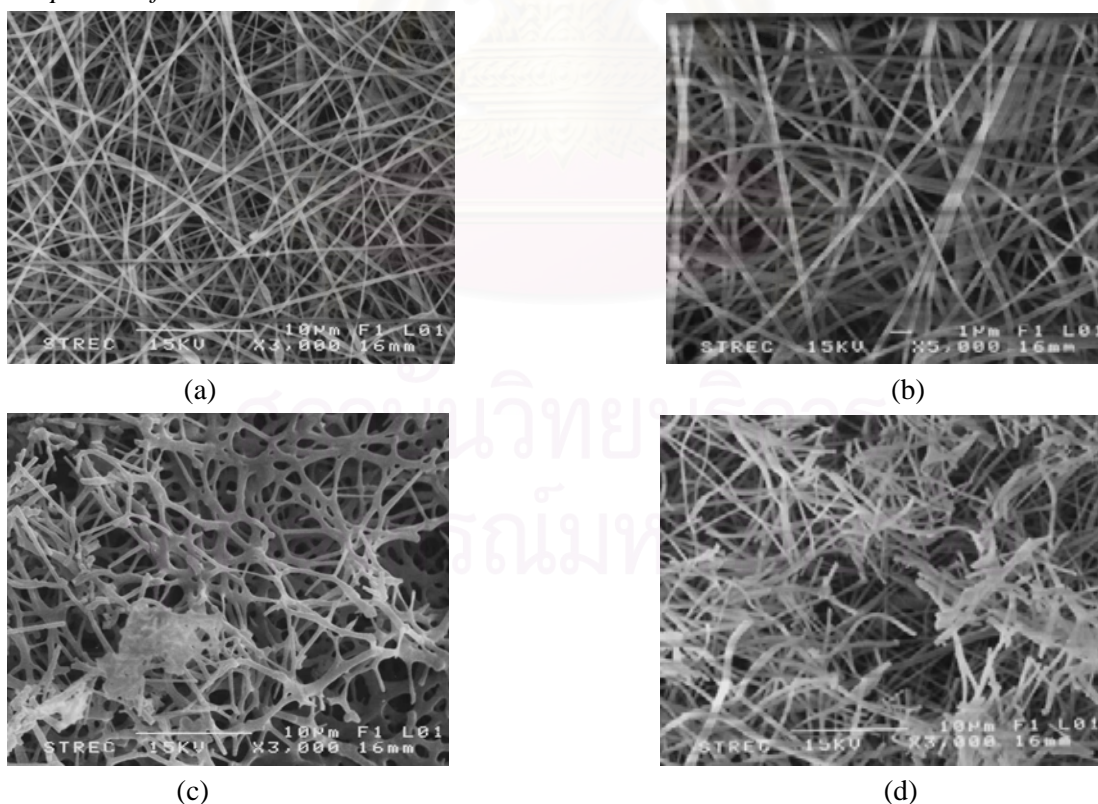
Figure 3- SEM micrographs of the fibers calcined at different temperatures:
(a) 600°C; (b) 800°C; (c) 1000°C; (d) 1200°C.

Regional Symposium on Chemical Engineering 2005
*Hanoi Horison Hotel, Hanoi, VIETNAM * November 30th - December 2nd, 2005*

242

Figure 3 shows SEM micrographs of fibers calcined at various temperatures. The fibers used to investigate the effect of calcination was spun by using applied voltage of 8 kV, the tip-to-target distance of 10 cm and the PVA concentration of 12 wt.% (as-spun fibers shown in Figure 1a). It can be found that the morphology of fibers remains the same as the pre-calcined fibers, although the calcination takes place at 800°C. However, the average diameter of the calcined fibers increases to 400-600 nm. At the calcination of 1000°C, some parts of the obtained fibers are broken off and the fibers appear distorted (Figure 3c). Finally, the coalescence of fibers is observed when the calcination takes place at 1200°C (Figure 3d).
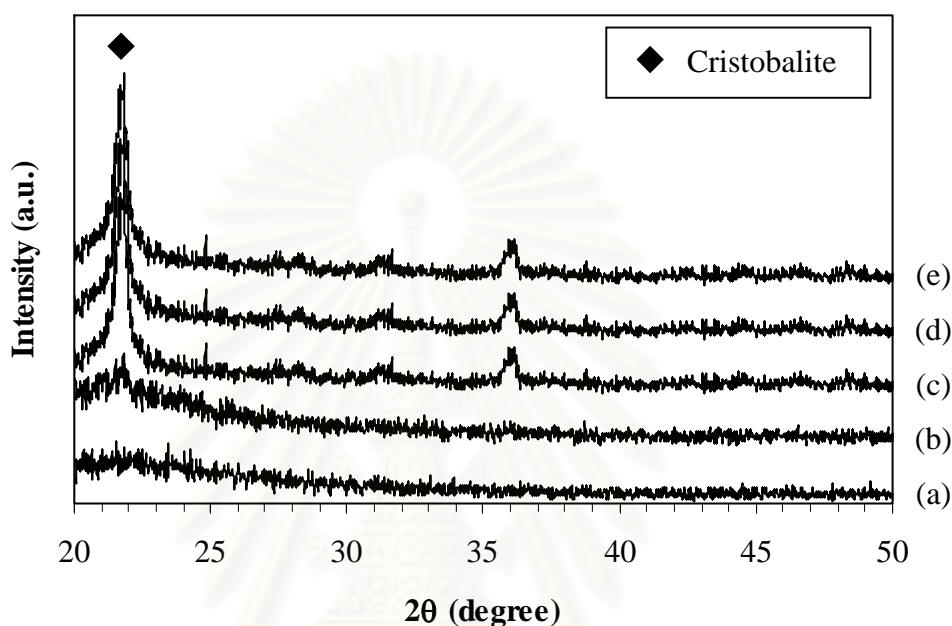
Figure 4- XRD patterns of: (a) as-spun fibers; fibers calcined at (b) 600°C, (c) 800°C,
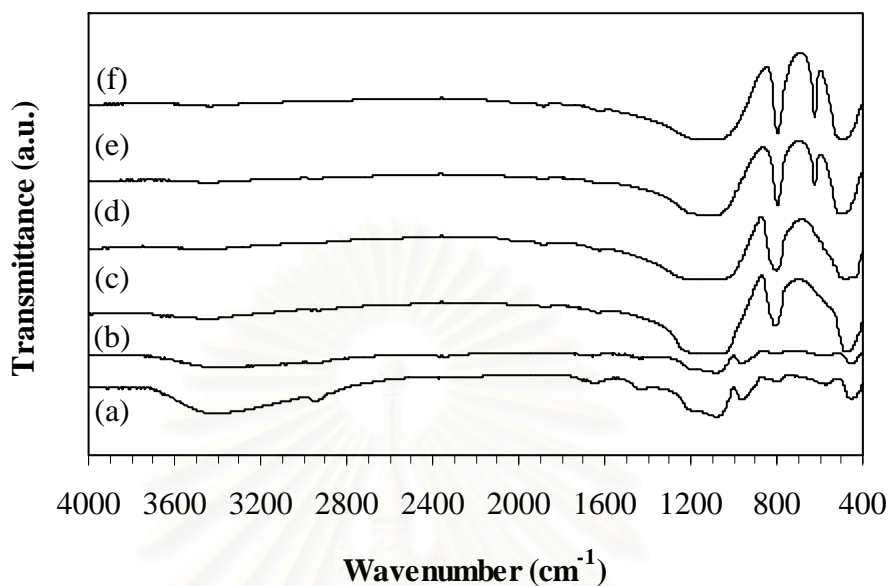(d) 1000°C, and (e) 1200°C.

The crystal structure of the product was investigated by XRD analysis, as shown in Figure 4. It is confirmed that the pre-calcined PVA/silica composite fibers are amorphous. Upon the heat treatment, formation of cristobalite is developed. The amorphous fibers directly transform into cristobalite at temperature approximately 1000°C. No other crystalline phase of silica, such as quartz or tridymite, was detected during phase transformation process.

The FT-IR spectra of the calcined products are shown in Figure 5. It is shown that the as-spun pre-calcined PVA/silica composite fibers have absorption bands at wave number of 1100 and 3400 cm^{-1}, which is corresponding to Si-O-Si and O-H bonding 9., respectively. It is implied that TEOS in the composite fibers is hydrolyzed and condensed to form Si-O-Si bonding according to sol-gel process.

For the calcined fibers, the absorption band according to Si-O-Si vibration is found in all samples. However, the O-H group is significantly decreased, indicating that organic compounds are removed during the calcination. The absorption bands at 623 cm^{-1} corresponding to pseudolattice vibrations of β-cristobalite 10. is clearly visible in the FT-IR spectra from fibers calcined at temperature higher than 1000°C. The result confirms the phase transformation observed from XRD analysis.

The results from the thermogravimetric analysis are shown in Figure 6. It is shown that pure PVA is fully decomposed at temperature lower than 600°C. Mass loss due to the decomposition of PVA matrix can also be observed from the thermodiagram of the as-spun PVA/silica composite fibers (Figure 6b). In fact, three mass loss steps at temperature in the range of 100-300°C, 300-400°C and

Regional Symposium on Chemical Engineering 2005
*Hanoi Horison Hotel, Hanoi, VIETNAM * November 30th - December 2nd, 2005*

243

400-600°C are shown. These steps are corresponding to the loss of absorbed moisture and solvent, the decomposition of side chain (T-ds) of PVA, and the decomposition of main chain (T-dm) of PVA, respectively 11.. The TGA analysis suggested that there was approximately 44 wt.% of silica in the as-spun composite fibers.

Figure 5- FT-IR spectra of (a) pure PVA; (b) as-spun fibers; fibers calcined at (c) 600°C, (d) 800°C, (e) 1000°C, and (f) 1200°C.
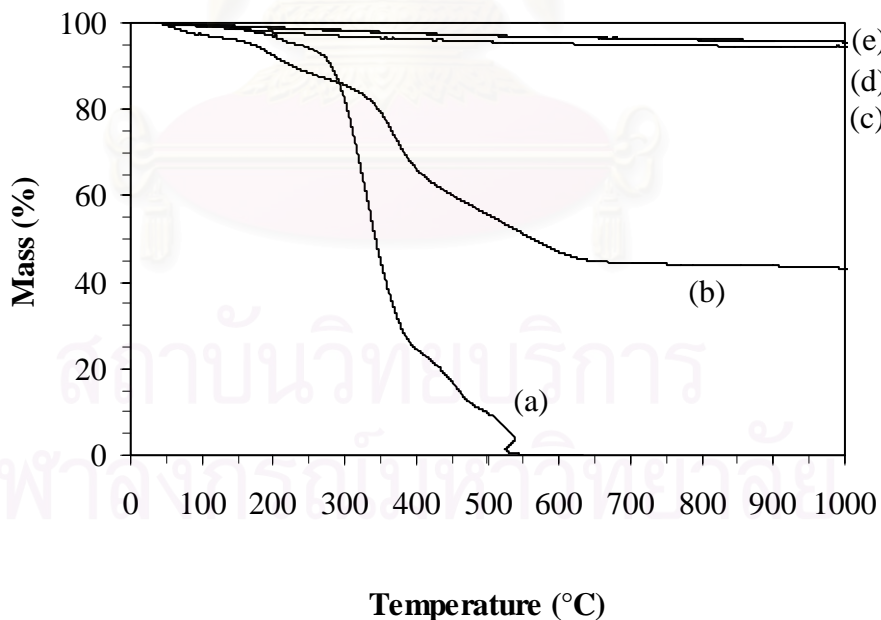
Figure 6- Thermodiagram of (a) pure PVA; (b) as-spun fibers; fibers calcined at (c) 600°C, (d) 800°C, and (e) 1000°C.

Regional Symposium on Chemical Engineering 2005
Hanoi Horison Hotel, Hanoi, VIETNAM * November 30th - December 2nd, 2005

244

On the other hands, for the samples calcined at 600, 800 and 1000°C (Figure 6c, 6d and 6e, respectively), the analysis by TGA indicates that the mass loss is only approximately 4 wt.%, which can be accounted by the evaporation of physical absorption of moisture. It is good indication that all polymer matrix has been removed during the calcination and pure cristobalite is obtained.

Conclusion

Cristobalite nanofibers were successfully synthesized by calcination of the PVA/silica composite fibers produced by the combined sol-gel and electrospinning techniques. The size and size distribution of the spun fibers are influenced by the concentration of PVA in the spinning solution and the applied voltage for the electrospinning process. The morphology and crystal structure of the fibers depend upon the calcination temperature. Pure cristobalite is achievable from the calcination at temperature higher than 1000°C. Higher calcination temperature can result in coalescence of the fibers.

Acknowledgements

References

1. Lee J.E., Kim J.W., Jung Y.G., Jo C.Y. and Palk U., **Effects of Precursor pH and Sintering Temperature on Synthesizing and Morphology of Sol-Gel Processed Mullite**, *Ceramics International 2002; 28: 935-40.*

2. San O., Abali S. and Hosten C., **Fabrication of Microporous Ceramics from Ceramic Powders of Quartz-Natural Zeolite Mixtures**, *Ceramics International 2003; 29: 927-31.*

3. Martinelli J.R. and Sene F.F., **Electrical Resistivity of Ceramic-Metal Composite Materials: Application in Crucibles for Induction Furnace**s, *Ceramics International 2000; 26: 325-35.*

4. Bergshoef M.M. and Vancso G.J., **Transparent Nanocomposites with Ultrathin, Electrospun Nylon-4,6 Fiber Reinforcement**, *Advanced Materials 1999; 11: 1362-5.*

5. Bognitzki M., Czado W., Frese T., Schaper A., Hellwig M., **Steinhart M., Greiner A. and Wendorff J.H., Nanostructured Fibers Via Electrospinnin**g, *Advanced Materials 2001; 13: 70-2.*

6. Shao C.L., Kim H.Y., Gong J., Ding B., Lee D.R. and Park S.J., **Fiber Mats of Poly(Vinyl Alcohol)/Silica Composite via Electrospinning**, *Materials Letters 2003; 57: 1579-84.*

7. Choi S.S., Lee S.G., Im S.S., Kim S.H. and Joo Y.L., **Silica Nanofibers from Electrospinning/Sol-Gel Process**, *Journal of Materials Science Letters 2003; 22: 891-3.*

8. Watthanaarun J., Pavarajarn V. and Supaphol P., T**itanium (IV) Oxide Nanofibers by Combined Sol–Gel and Electrospinning Techniques: Preliminary Report on Effects of Preparation Conditions and Secondary Metal Dopant**, *Science and Technology of Advanced Materials 2005; 6: 240-5.*

9. Hajji P., David L., Gerard J.F., Pascault J.P. and Vigier G., **Synthesis, Structure, and Morphology of Polymer-Silica Hybrid Nanocomposites Based on Hydroxyethyl Methacrylate**, *Journal of Polymer Science Part B-Polymer Physics 1999; 37: 3172-87.*

10. Sitarz M., Handke M. and Mozgawa W., **Identification of Silicooxygen Rings in SiO₂ Based on IR Spectra**, *Spectrochimica Acta Part A-Molecular and Biomolecular Spectroscopy 2000; 56: 1819-23.*

11. Nakajima C., Saito T., Yamaya T. and Shimoda M., **The Effects of Chromium Compounds on PVA-Coated AN and GAP Binder Pyrolysis, and PVA-Coated AN/GAP Propellant Combustion**, *Fuel 1998; 77: 321-6.*

Regional Symposium on Chemical Engineering 2005
Hanoi Horison Hotel, Hanoi, VIETNAM * November 30ᵗʰ - December 2ⁿᵈ, 2005

245

VITA

Mr. Rungroj Chanchairoek was born on 7th September, 1982, in Bangkok, Thailand. He received his Bachelor degree of Science with a major in Chemical Technology from Chulalongkorn University, Bangkok, Thailand in March 2004. He continued his Master study in the major in Chemical Engineering at Chulalongkorn University, Bangkok, Thailand in June 2004.